SEPARATION MECHANISMS IN THE BARBADOS LIGHT AND POWER COMPANY POWER SYSTEM

By

Birat Gyawali

Bachelor of Engineering in Electrical and Electronics Engineering,

Kathmandu University, Nepal, 2014

A Thesis Submitted in Partial Fulfilment
of the Requirements for the Degree of

Master of Science in Engineering

In the Graduate Academic Unit of Electrical and Computer Engineering

Supervisor(s): Chris Diduch, Ph. D., Electrical and Computer Engineering
Eugene Hill, Ph. D., Electrical and Computer Engineering

Examining Board: Bo Cao, Ph. D., Electrical and Computer Engineering
Suprio Ray, Ph. D., Computer Science

This thesis is accepted by the
Dean of Graduate Studies

THE UNIVERSITY OF NEW BRUNSWICK

June 2022

ABSTRACT

Reliability is a major concern for any electric utility and is made more complex in BLPC because it has no supporting interconnections. Additionally, the integration of a large amount of renewable energy in the system presents even more challenges. Historically reliability of the overall power system has been accomplished by better maintenance practices and the continual upgrading of the power system. Recently many papers have proposed that instead of a system wide failure, reliability would be improved by the retention of critical areas of the grid through selection and formation of partial grids or microgrids. The literature shows that significant work has been done on the automatic selection of the parts of the system to be retained in any microgrid.

BLPC is interested in improving the reliability of their power system by avoiding island-wide blackouts through possible formation of electrical islands or isolated power system areas, also called microgrids. It has a natural separation point due to the fact the northern part of the island can be isolated by simply opening two transmission lines serving a major bus in the lower part of the northern section of the island. While historically all the rotational generation has been in the southern area, the northern section of the island now has rotational generation, a large solar farm, and a utility grade battery. The historical record of island-wide power failures appears to show that in many cases there has been some sort of cascading effect.

The major questions then become what is the likely mechanism for causing separation, and what are the best measurement types and locations which would reliably allow a correct decision to be made to separate?

This thesis examines different approaches for analysing the electrical mechanisms, which can be used to decide on separation into two microgrids. The classical instability mechanism of angular separation between the rotor angles of generators during the time of disturbance on the BLPC system is one possible mechanism. Voltage instability in the areas of low voltage deals with the necessity of a sufficient supply of reactive power supply to maintain the required voltage at each load bus. Based on available records, the analysis of blackout events due to cascading effects gives a clear picture of the issues faced in the past. Optimum measurements used to detect the state of the power system by installation of PMUs can assist with the decision of determining the system conditions and time to separate in order to avoid island wide blackouts. Finally, utilizing all the approaches mentioned above, the concept of stability indices has been developed to indicate the relative strength of each local load bus. Ultimately it will be necessary for BLPC to use all the elements of the thesis to develop logical statements allowing them to arrive at a decision to separate the BLPC system into northern and southern microgrids therefore avoiding island wide blackouts.

ACKNOWLEDGEMENT

I would like to express my sincere gratitude to my supervisor, Dr. Eugene Hill for his valuable guidance, comments, and suggestions throughout the development of the research. His approach of teaching from the fundamentals and demonstrating simple example to get us more in-depth understanding helped me to figure out complex concepts. He brings learning into real world problem and shares his immense knowledge and experiences in power system areas to explain key ideas on a fundamental level. I also would like to thank him for his accessibility and prompt reply to emails as well as availability for meeting in any situations. I would also like to convey my deepest appreciation to Dr. Chrish Diduch for giving me the opportunity to conduct my research under his supervision.

It's a matter of great fortune to carry my master's study together with my wife Shyamala Nepal. She has been a great inspiration during the time of intense despair. She helped me to ease my workload and didn't let me to get tensed in stressed situations. Her encouragement to do better throughout my research helped me to gain huge confidence and supported me in every way possible. I am very thankful to my parents, brother and in- laws for their love, support, and motivation to follow my aspirations.

Finally, I would like to thank EMERA and UNB for allowing me to be a part of research in BLPC system as well as funding to support my studies.

TABLE OF CONTENTS

LIST OF TABLES

LIST OF FIGURES

LIST OF ABBREVIATION

AC	Alternating Current
AVR	Automatic Voltage Regulator
B	Steady State Stability Limit
BA	Banks Substation
BC	British Columbia
BE	Belmont Substation
BF	Before Fault
BLPC	Barbados Light and Power Company
CA	Carlton Substation
CASI	Centre of Angle Stability Index
CCT	Critical Clearing time
CE	Central Substation
CEB	Clean Energy Bridge
CIGRE	International Council on Large Electric Systems
CLR	Fault Clearing time
CoA	Centre of Angle
CR	Critical
DES	Desalination Substation
DF	During Fault
DG	Distributed generation
E	Supply Voltage
ETAP	Electrical Transient Analyzer Program

GA	Garrison Substation
GPS	Global Positioning System
HA	Hampton Substation
IEEE	Institute of Electrical and Electronics Engineers
KE	Kinetic Energy
kV	Kilo Volt
kVAR	Kilovolt Ampere of Reactive Power
kW	Kilo Watt
KWh	Kilo Watt hour
MATLAB	Matrix Laboratory
MS	Marhill Street Substation
MVA	Megavolt Ampere
MVAR	Megavolt Ampere of Reactive Power
MW	Mega Watt
MWh	Mega Watt hour
NERC	North American Electric Reliability Corporation
NO	North Substation
OEL	Over Excitation Limiter
OL	Old Works Substation
P	Active Power
PCC	Point of Common Coupling
PE	Potential Energy
PF	Post Fault

PMU	Phasor Measurement Unit
PV	Photo-voltaic
Q	Reactive power
QV	Reactive power-voltage
R	Resistance
RP	Regency Park Substation
RPR	Reactive Power Reserve
SCC	Short Circuit Current
SEP	Stable Equilibrium Point
SP	Spring Garden Substation
ST	Saint Thomas Substation
SW	Seawell Substation
TR	Trent Substation
TSI	Transient Stability Index
TY	Temple Yard Substation
UBC	University of British Columbia
UEP	Unstable Equilibrium Point
V	Terminal/Operating voltage
WA	Warrens Substation
WIL	Wildley Substation
WO	Wotton Substation
WP	Whitepark Substation
X	Reactance

X_{TH}	Thevenin reactance
Z_{TH}	Thevenin equivalent impedance

CHAPTER 1

1. INTRODUCTION

1.1 General

Reliability is one of the major concerns in electric power systems. The inclusion of renewable energy sources has caused an additional level of complexity. While the capacity factors of renewable energy sources are well known, the stochastic nature of renewable sources requires another level of analysis. The daily pattern of wind generation is highly variable from day to day, and during any day. Solar PV has a known pattern since solar power is produced only during hours of sunshine, which also corresponds to the time of peak loads on the system. However, cloud cover can move in and out many times during the day, often reducing PV capacity by as much as 80% in a matter of 10-30 seconds.

More and more, storage systems are appearing in power systems. Occasionally this takes the form of pumped hydro storage, but more frequently this is becoming grid level battery storage. This has proven very effective in island power systems, which by definition are isolated without any interconnections. However, when there is a disturbance with a greater effect, the system may reach a vulnerable state. This leaves power system planners and operators with two alternatives: suffer an island wide blackout or try to increase the power system reliability by planned system separation into smaller islanded power systems, which might be termed microgrids.

Barbados Light and Power Company (BLPC) does not have the concern of flexible formation of multiple microgrids for a very specific reason. It has 239 MW of original rotational generation in the southwest and 33 MW of new rotational generation at the Clean

Energy Bridge (CEB) in the north. The north is also the location of a 10 MW PV solar farm and a 5 MW, 21 MWh battery. From a transmission perspective, there is a major bus between these two areas at a location called St. Thomas, and this bus has two transmission lines connecting it to the south and southwest areas. Consequently, those two transmission lines become a natural separation point allowing the formation of a northern microgrid and a southern microgrid.

Therefore, the major concern is to analyse the electrical mechanisms by which separation might take place, and to consider which measurements might be useful in arriving at a decision to separate. The island is only about 50 km north-south and 25 km east-west. From a typical stability perspective, the rotor angular separation across the grid is not large. On the other hand, most of the transmission system is at 24.9 kV, and there are conditions which result in low voltage so voltage instability may be a concern. As well, transmission lines at 24.9 kV have X/R ratios, which are much lower than the high voltage lines of geographically large power systems, may negate some of the assumptions of the classical voltage instability analysis. Finally, the historical record of island-wide blackouts seems to suggest that there is some form of cascading process that has taken place in the past.

Phasor Measurement Units (PMUs) can be used to extract real time quantities from time domain signals which include phasor amplitude, phase angle, frequency, and rate of change of frequency. The observations made from the application of PMUs on voltage magnitudes can be used to monitor dynamic performance of the power system in real time operation.

1.2 Problem Statement

The premise of the formation of microgrids is that overall system reliability can be improved following a severe disturbance, if part of the customer base can continue to be

served rather than suffering an island-wide blackout. As noted above, if it becomes necessary for separation to take place the natural transmission configuration has led to a decision that there will be a southern microgrid and a northern microgrid. Therefore, the major problem addressed by this thesis is to determine the system condition, or conditions, which will require separation to take place. This can also be stated as identifying and understanding the mechanisms by which separation might occur. Historically all the rotational generation has been in the southern part of the island. With the addition CEB 33 MW medium speed diesel plant at Trents St. Lucy the northern part of the island now has rotational generation. It is proposed that separation might be initiated in one of three ways. The first way is the classical instability mechanism of angular separation between the rotors of the generators during disturbances. At first glance this might seem unlikely because of the short distances involved on the island. However, this is possibly countered by the low transmission design voltage of 24.9 kV. The second way is through poor voltage conditions, and possible voltage instability. Simulations do show areas of low voltage. Additionally, there is a need to develop better analysis capabilities in this area since in general theoretical voltage instability studies have only been done for high voltage power systems where the transmission line X/R ratios are higher by an order of magnitude than for 24.9 kV transmission lines. The third way that separation might occur is through cascading effects. This is one of the mechanisms showing up in the record and analysis of island-wide blackouts which have occurred in the past.

The second problem addressed by this thesis is an analysis of the optimum measurements, which might be used to detect power system conditions that clearly indicate that separation

should be initiated to avoid a full system blackout. BLPC is presently installing PMU which should assist in the identification of these conditions.

The third problem addressed by this thesis is the identification and development of appropriate stability indices for the unique circumstances of an island power system. The intent of these stability indices is not to indicate the health of the power system at any point in time, but rather to indicate the relative strength of each local bus, to assist with recommendations for the placement of measurement units, and to provide information to develop logical statements, which might lead to a separation decision.

1.3 Literature Review

Separating the power system into segments in a controlled manner is the final resort against a full blackout event. The major concern for a separation event is where to separate (point of separation), when to separate (time of separation) and what to do after separation (control action in the new islands)? Controlled separation determines what hardware device should operate for executing separation [2][3]. For a sustainable islanding separation, numerous restrictions should be met. This includes load-generation balance and coherence among generator of individual islands, voltage and angular stability, controllability of circuit breakers and thermal limitations of transmission lines [4]. Prioritizing and allocating a centroid of load clusters considering power balance as well as finding out ways for sustainable operation in case of fluctuation in distributed generation is required [5].

Renewable energy from wind and solar introduces uncertainties and non-controllability production challenges, which may result in power imbalances. Implementation of conventional generators helps in relieving power deviations in divided subsystems by supplying energy with a speedy response. This can contribute significantly toward

mitigating imbalance of generation and load [5][6]. To ensure there is sufficient energy margin, energy storage systems should be available in the distribution system. Storage also has the benefit of controllable generation units to overcome the decreased generation due to capacity limitations and ramp rate [7]. Furthermore, load can also provide great potential to offer regulation service with fast ramping. The regulation cost in this provision can be lower than traditional energy storage devices [5].

According to IEEE/CIGRE," Power system stability is the ability of a power system for a given initial condition to regain a state of equilibrium after being subjected to a disturbance". It is necessary to evaluate the impact of a disturbance on the electromechanical dynamic behaviour of the power system [8]. Rotor angle stability is a study of electromechanical oscillations, that is how the power exchanges take place between synchronous machines when the rotors oscillate [9]. The equal area criterion can be used to analyze stability with an energy function method (amount of critical energy stored in the power system during a fault) for a single machine, infinite bus configuration [10]. Generator protection such as out of step protection, loss of field protection, and distance protection can be simulated with stability studies. This will help ensure that the system will regain a new state of equilibrium after being subjected to a disturbance [11].

Power system stability focuses on modelling synchronous machines including their excitation and governor systems. As well, stability studies focus on simulations under abnormal operating and fault conditions to identify machine rotor angle oscillations, system frequency, voltage variations and to suggest a possible solution to ensure stable operation in severe disturbances [12]. The electrical quantities such as current, bus voltage, active and reactive power are functions of power angle. All these quantities swing

periodically with a change of power angle [13]. Power angles can be calculated from generator terminal conditions and synchronous machine reactance [14]. The angle difference of internal voltages of generators, or phase difference of two busbar voltages, are strong indicators of power system status. This can be found through measurements in two substations of tie-line flows and other data at remote terminals gathered through communication systems [13][15]. Energy functions can be used to determine how close the power system is to voltage collapse through voltage security measures [16]. When oscillations occur on the system stability boundary, the potential energy difference between the Unstable Equilibrium Point (UEP) and Stable Equilibrium Point (SEP) becomes zero which can be used to compute voltage stability [17]. For a given contingency, transient stability can be determined by comparing the total system energy gained in the faulted period with a certain critical potential energy at the unstable equilibrium point which is closest to a stable equilibrium point [18][19]. Critical energy absorbed by a disturbed system when the fault is cleared corresponds to the critical clearing time [20]. Calculation of indices based on Centre of Angle (CoA) for two power systems can be used for controlled separation. This separation should be initiated before undergoing unstable system conditions [21].

With the growing concern of electric power quality, supporting voltage locally can be achieved through Distributed Generation (DG) [22]. However, DG being a fluctuating power source causes deviation of the voltage at the point of common coupling (PCC) with the grid [23]. To limit the voltage change, the generally adopted technique is by compensation with reactive power and sometimes a reduction in active power transferred to the grid in a manner similar to that of a synchronous generator [22]. Adding sufficient

reactive power sources makes the system less vulnerable to voltage collapse and enhances the possibility of being able to restore system voltage to acceptable levels [24]. Voltage instability is generally caused by a disturbance such as an increase in load or change in bus voltage away from the normal operating range [25].

The reactive power margin for each bus can be obtained from the Q-V curve method. This helps in identifying critical buses where reactive power injection is required for ensuring voltage security [26]. In the phenomenon of voltage insecurity, the receiving end voltage of a transmission line may drop to a significantly lower value and may continue to oscillate in an undamped manner [27][28]. Steady state voltage stability analysis provides physical interpretation and determines system voltage margins on a real time basis. It helps in estimating the available reserve margin so one can maintain adequate voltage security. Disturbances in the system trigger voltage instability which will affect dynamic load characteristics, protective relay settings, voltage regulations, speed governing, etc. [29][30]. The current and voltage detected from PMU measurements allow calculation of transient impedance seen by the generators. By converting this impedance to a system margin value, one can monitor voltage stability of power system [31].

The North American Electric Reliability Council (NERC) defines cascading outages as," Uncontrolled loss of any system or facilities or load due to thermal overload, voltage collapse, loss of synchronism except those occurring as a result of fault isolation" [32]. Major blackouts involve cascading events i.e., one event triggers another event [33]. Evaluation of cascading events to determine possible actions for reducing the likelihood of a full system blackout is required [34][35]. Identifying typical patterns of these events and analysing them to find out the sequence is very important for assessment of cascading

failure [36][37]. With increasing criticality of security issues related to the power industry, secure operation of the power system to avoid major blackouts resulting in significant social and economic impact is a must [38][39].

Phasor Measurement Units (PMU) can be a very useful tool for developing data for online power system stability studies. Such measurements, because they involve both magnitude and phase, also provide heretofore unavailable information about what the generator rotor angles are doing in real time. The values and measurements which they provide are often called synchro phasors [40][41]. This estimation is based on a measurement synchronization process between the Global Positioning System (GPS) satellites and the sinusoidal component of the AC waveform in the power system. Hence, magnitudes and phase angles between signals at a given time can be reported [42]. By providing accurate real-time measurements to determine where the power system is heading (either as a stable or an unstable condition) according to prevailing system conditions, it is possible that such information can play a significant role in power system separation decisions [43].

Regular monitoring and control of the power system is required to identify the maximum load the system can withstand before collapsing [44]. To operate the system with maximum reliability, an accurate indicator to evaluate the voltage security of the system is required. Ensuring a good voltage stability margin [45], estimating maximum allowable loading of buses considering reactive power load, identifying source locations and network topology, are major considerations [46]. Using system voltage stability indices such as admittance matrix elements of line and buses, it is possible to estimate the stability margin which is the distance of the actual state of the system to the stability limits [47][48].

1.4 Thesis Objective

The major objective of this research is to develop analytical tools to understand the possible separation processes which might occur on the BLPC power system. These processes are:

- Angular instability
- Voltage instability
- Cascading effects

Separation decisions require good information about the status of the power system at any instant in time.

- Help to develop a strategy for optimal placement of Phase Measurement Units on the BLPC power system,

Placement of measurement units, and logical statements determining the decision to separate, depend on an understanding of the electrical strength of the power system at any bus in the system.

- Develop a stability index for each bus based on an analysis of the separation processes.

1.5 Thesis Outline

The thesis is comprised of six chapters, and they are:

Chapter 2: Methodology

Chapter 3: Angular Stability Analysis, Energy Function

Chapter 4: Voltage Stability Analysis, Voltage-Reactive power curves

Chapter 5: Cascading Effect, Analysis of historical blackout events

Chapter 6: Relating Angular and Voltage Stability

Chapter 7: Conclusion and Recommendation

CHAPTER 2

2. METHODOLOGY

2.1 Introduction

Power systems come in all sizes. The largest power system of familiarity is the eastern two-thirds of the North American continent (excluding the province of Quebec). A small power system is the Barbados system where the island is about 50 km north to south and 28 km east to west. It is the objective of every power system to continually operate as the intended integrated unit. That does not always happen. In the case of the eastern two-thirds of the North American continent, due to faults on the 345 kV interconnection the provinces of Maritime Canada have separated or islanded from the continent, generally continuing to operate in local synchronism.

Barbados is a very different circumstance as an island utility with an original rotational generation capacity of 239 MW. It has suffered island wide blackouts in the past, the records of which are available. Two of these island wide blackouts have been in the recent past. For all its history, the majority of its generation has been located at one large station in the southwest, with two other smaller generating stations in the south of the island. Recently four medium speed diesel generators each with a capacity of 8.25 MW have been installed in the north of the island. Based on the concept that maintaining part of the island in operation during major disturbances would improve customer satisfaction and improve the system reliability indices, the utility has initiated an investigation of the separation of the utility system into a northern section and a southern section. Furthermore, this option

is greatly enhanced by the fact that the island grid has a natural separation point. However, the decision to separate into grids is one which should never be taken unnecessarily.

This initiative has provided the genesis for this thesis work. It is an examination of:

- The electrical manner or electrical mechanisms by which separation into smaller grids might take place.
- The conditions evident from these mechanisms which would indicate, or determine, or demand, that separation into smaller grids should take place.

Briefly stated at this point, the electrical mechanisms by which separation might take place are based on an angular stability analysis, a voltage stability analysis, and cascading effects observed. The conditions which might indicate that separation should take place are developed equations, fundamental understanding of the power system, results of system studies, and instantaneous measurements taken on the system.

Power system stability is the study of disturbances on the power system during the transient period before a new steady-state condition is reached. The objective is to remain in operating equilibrium under normal operating condition and to gain a new equilibrium condition after being subjected to the disturbance [49]. To satisfactorily operate a power system, it is necessary to operate and maintain synchronism among the synchronous machines. For a given fault, a synchronously stable system settles down to a new steady state value as time increases. But to ensure system security against abnormal conditions, simulation of these contingencies should be done in advance so that preventive control action could be taken if required [20]. NERC quotes," Security is the ability of the bulk electric system to withstand sudden disturbances such as electric short circuits or unanticipated loss of system components".

Successful operation of the power system with continuous electrical service can be obtained by retaining a reliable system i.e., the synchronous generators must be kept in parallel so that they generate enough power to meet the load demand. Another important need is to maintain integrity between the transmission systems, generating stations and load centres so that there is no interruption of power flow to the loads [50]. Stability is mainly concerned with the behaviour of synchronous machine after disturbances. If the disturbance results in no change in power, then the state of the machine before and after disturbance should not change but when there is unbalance of power post disturbance then the machine should regain a new operating condition to assure a stable system [50]. Some of the machines which experience severe disturbances may swing away from equilibrium and lose synchronism. This depends on the fault location such as how close or far away the generator is located compared to the fault. When a machine accelerates and decelerates for a longer time, this oscillation can separate that machine from the rest of the system causing instability [51]. For a transient, if the oscillation is damped and settles out to a new operating condition post disturbance, it is called a stable system. Often this will eventually result in fluctuations in the power flow over the transmission lines [50].

2.2 Classification of Stability

The classification of power system stability is based on various factors which contribute to instability and can be categorized as follows [9].

- Nature of disturbance
- Size of disturbance
- Time span of disturbance
- Best approach in calculation of stability

A diagram clearly illustrates the elements of the approach to establishing a structure for analysing stability [9].

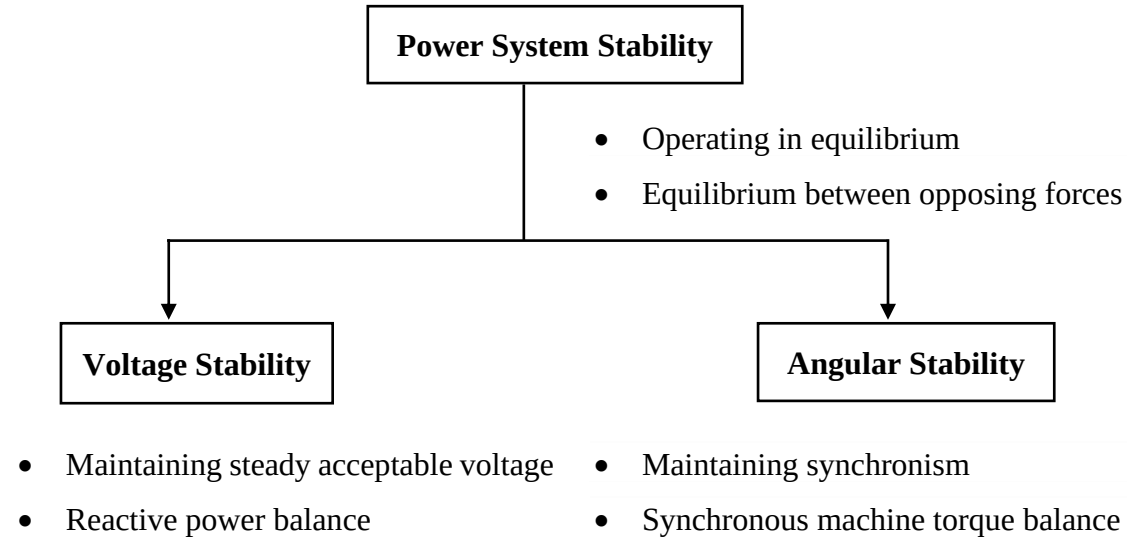

Figure 2-1: Approach for power system stability study

2.3 Categorizing disturbances

The ability of a system to survive a disturbance depends on its operating conditions and time of occurrence, and this disturbance can be categorized as either small or large. A disturbance is considered small if the linearization of the system of equations describing dynamic behaviour of power system can be justified for analysis purposes. The stability concern for small disturbances is in the steady-state stability. The system should operate successfully and maintain the balance between the load and generation under numerous circumstances [9]. If the linearization of the dynamic behaviour of system equation cannot be justified, then the disturbance is said to be large, and the stability concern is transient stability [49]. Faults in transmission lines, abrupt changes in load, and loss of generation are some major examples of larger disturbances.

With the different types of disturbance mentioned above, not all transient events need system separation to sustain the power system as a single entity. Controlled separation is required in order to restrict a disturbance from propagating into the remaining part of the power system. This can be initiated by opening appropriate transmission lines before cascading outages can occur [9]. System separation depends on the energy of certain critical groups of critical machines, and the time required to clear a fault must always be less than the critical duration of a fault [51]. Factors such as voltage and rotor angle of synchronous machines are very important in maintaining controlled power system stability. Voltage is directly affected by the reactive power imbalances and rotor angle is dependent on stability and synchronism in the whole system. If voltage and angular instability is addressed, most times it is possible to avoid undesired collapse or blackout events [52].

2.4 Flow chart

It is useful to apply the flowchart of Figure 2-2 for each fault so that it can be determined in advance whether there is a requirement to separate the system. Consideration is given to using angular stability, voltage stability and cascading effects as possible separation mechanisms. Once these three elements are fully understood, one main objective would be creating a quality vector for buses. This is based on indices from the energy function, from the relationship of voltage and angular stability, from the QV curve method, and from trends in historical blackout events.

This quality vector will help in identifying PMU locations, the number of PMU placements required, and it will also help in proposing an algorithm such that separation should be triggered and formation of the northern and southern microgrids should take place.

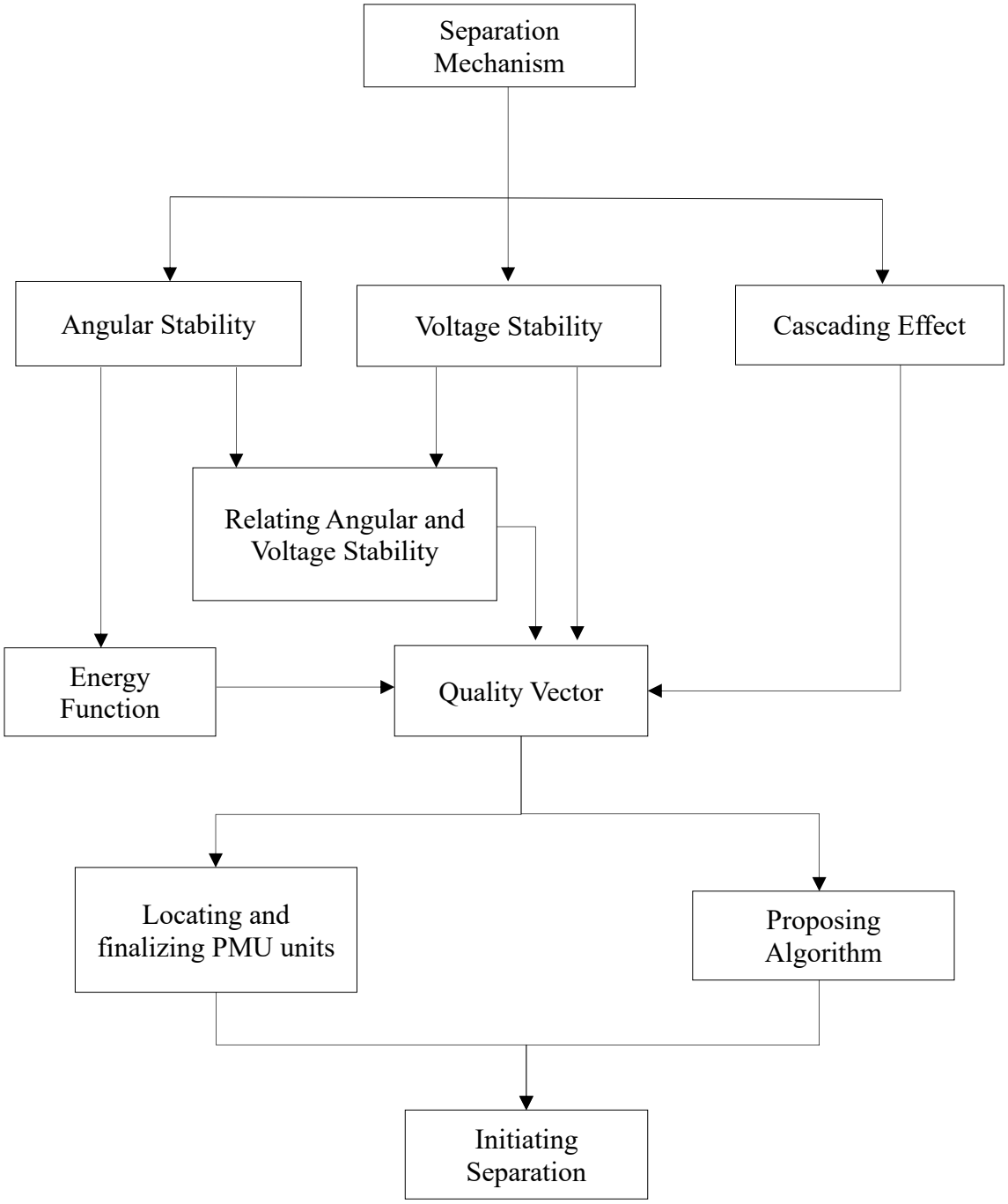

Figure 2-2: Flow chart of overall methodology

2.5 Equation of motion for angular stability

As it pertains to angular stability, the representation of the dynamics of a synchronous machine is based on the rotational inertia equation of balance between the mechanical

power input and the electromagnetic power generated and delivered by synchronous machine. The equation is called the swing equation and given by [9],

$$M * \frac{d^2\delta}{dt^2} = P_m - P_e \qquad 2.1$$

Here M is the inertia constant of the generator, δ is angular position of the rotor, P_m is mechanical power input to the generator and P_e is electrical power output of the generator.

2.6 Angular stability analysis

There is an inherent tendency for synchronous generators to stay in synchronism due to the synchronizing torques present in synchronous machines, and it is common for large power system to operate with thousands of generators synchronized together. The first approach in analysing angular stability is based on the classical method of doing large numbers of transient stability simulations generally for extreme cases, and through that process identifying potential loading and potential critical outage circumstances on the power system. It can be used to identify initial rates of change of frequency following disturbances, it can indicate how well oscillations are damped, and it can indicate the stability margin present in the system.

2.6.1 Deriving single machine Infinite Bus

When a power system become unstable, it often divides the synchronous machines into two groups: critical machines and remaining machines. To represent all these critical machines into one single equivalent machine and the rest of the machines into another group is termed as a single machine infinite bus system. There is a direct way to determine whether a system is stable or unstable by computing a Transient Stability Index (TSI). It helps in determining the margin of stability by calculating the difference between the

critical clearing time of a circuit breaker to clear a fault and the actual time set to clear it. For an unstable machine due to loss of synchronism, its angular velocity rises very high compared to the rest of the machines [20]. A disturbance in any power system can be described in a set of three differential equations in three-time frames i.e., before the fault, during the fault and post fault.

$$\dot{x(t)} = f^{BF}\big(x(t)\big) \qquad -\infty < t \leq 0$$

$$\dot{x(t)} = f^{DF}\big(x(t)\big) \qquad 0 < t \leq t_{clr}$$

$$\dot{x(t)} = f^{PF}\big(x(t)\big) \qquad t_{clr} < t < \infty$$

Here the fault occurs at $t = 0$ and this state remains until the fault is cleared at $t = t_{clr}$ and during that time it is represented by f^{DF}. There is a change in the dynamics of the system before and after $t = 0$ and $t = t_{clr}$. Before the fault, the system follows f^{BF} and after the fault it behaves as f^{PF}. $x(t)$ is the vector of the state variables at time t.

To successfully remove a fault in a large disturbance in transient stability studies, it is necessary to calculate the critical clearing time of the circuit breaker. This can be used in interpreting the maximum amount of energy transferred in the fault state [53].

2.6.2 Energy Function

The energy function is used to compute the critical energy absorbed by a disturbed system before clearing a fault and restoring the system to a stable state. The energy function is the integral sum of the kinetic and potential energy which determines the stability status of the power system [20]. To avoid instability, the system must be capable of absorbing during the post disturbance state the kinetic energy created by the fault.

The energy function $V_{(\delta,\omega)}$ is the sum of the kinetic and potential energy of the machine. Whenever there is a disturbance in the power system, there is a change in kinetic energy of

the system which must be countered by the potential energy of the system. In the swing equation 2.1, the electrical power can be replaced by $P_e = P_e max * sin\,\delta$ where $P_e max$ is the maximum electrical power output.

$$M * \frac{d^2\delta}{dt^2} = P_m - P_e max * sin\,\delta \qquad 2.2$$

The post fault stable point is:

$$\delta^s = \sin^{-1}\frac{P_m}{P_e max}$$

This is also called the stable equilibrium point (SEP).

The unstable equilibrium points (δ^μ) can be defined.

$$\delta_1^\mu = \pi - \delta^s$$

$$\delta_2^\mu = -\pi - \delta^s$$

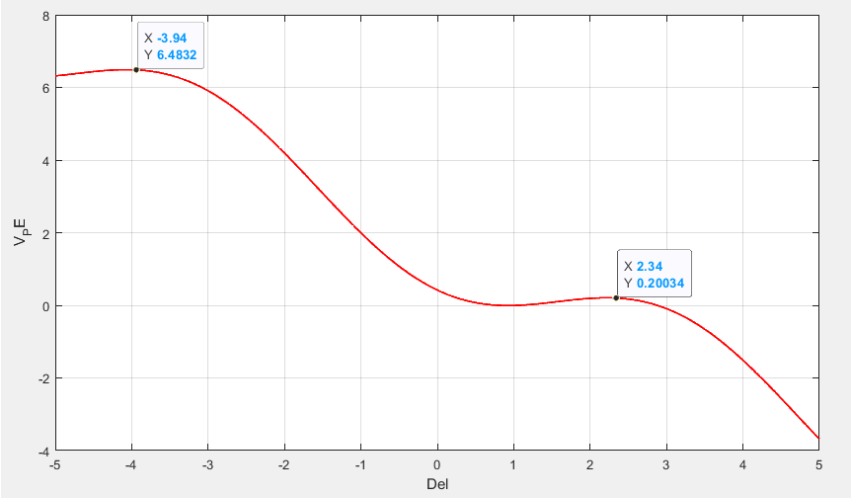

Figure 2-3: Variation of potential energy of a system during a fault

VpE is the potential energy and Del is the rotor angle of generator. The stable equilibrium point (δ^s) is surrounded by two unstable equilibrium points (δ^μ). Those are the two peaks shown in Figure 2-3.

The energy function is given by equation 2.3

$$V_{(\delta,\omega)} = \frac{1}{2}M\omega^2 - P_m(\delta - \delta^s) - P_e\, max(\cos\delta - \cos\delta^s) \quad 2.3$$

Here, $V_{KE} = \frac{1}{2}M\omega^2$ is the transient kinetic energy and,

$V_{PE} = -P_m(\delta - \delta^s) - P_e\, max(\cos\delta - \cos\delta^s)$ is the transient potential energy.

The sum will always remain a constant value after clearing the fault. The value of $V_{(\delta,\omega)}$ calculated at $t = t_{clr}$ gives the energy available in the system and as per the conservation of energy principle accumulated kinetic energy must be absorbed by the system after clearance of the fault.

Two conditions must be satisfied for stability [53]:

1. The function $V_{(\delta,\omega)}$ must be ≥ 0.
2. Any track of ω and δ on the surface of V must decrease with time

2.6.3 Equal area criteria:

For a system to be stable in terms of energy, the total energy $V_{(\delta,\omega)}$ must be less than the critical energy which is represented by V_{cr}. It is also called the region of attraction in the energy function. Similarly, the critical clearing time (t_{cct}) can be calculated from the instant when $V_{(\delta,\omega)} = V_{cr}$ on the faulted trajectory.

V_{cr} is obtained by letting $\omega = 0$ and $\delta = \delta^{\mu}$ in $V_{(\delta,\omega)}$.

$$V_{cr} = -P_m(\pi - 2\delta^s) - 2P_e max\cos\delta^s \quad 2.4$$

For a system to be stable, $V_{(\delta,\omega)} < V_{cr}$ for a faulted trajectory, and at $t = t_{clr}$, $V_{(\delta,\omega)} = V_{cr}$ for the faulted trajectory.

If we let $\delta = \delta^s$, and $\omega = 0$ then $V_{(\delta,\omega)}$ in equation 2.3 becomes

$$V_{(\delta^s,0)} = \frac{1}{2}M0^2 - P_m(\delta^s - \delta^s) - P_e\, max(\cos\delta^s - \cos\delta^s) = 0$$

For a fault, the machine will accelerate or decelerate such that $\omega \neq 0$. So, ω must be the incremental speed.

In the general energy function $V_{(\delta,\omega)}$, the KE term must be kinetic energy "added" during the fault. If speed changes by an increment, then the stored rotational energy at any speed changes by an increment relative to M x [Actual per unit speed (squared) - 1 (squared)].

2.6.4 Stability index

A transformation used for transient stability analysis results in a concept referred to as the centre-of-inertia, often called the centre of angles (CoA). It represents a single machine equivalent to all generators in a defined area [54]. This CoA represents the mean motion of the system and is used as a new reference angle rather than referencing each angle to a specific machine. The CoA reference transformation defines the CoA angle and speeds as

$$\delta_0 \triangleq \frac{1}{M_T}\sum_{i=0}^{m} M_i \delta_i \qquad 2.5$$

$$\omega_0 \triangleq \frac{1}{M_T}\sum_{i=0}^{m} M_i \omega_i \qquad 2.6$$

Where,

$$M_T \triangleq \sum_{i=0}^{m} M_i$$

To evaluate synchronous stability, angles are referenced to the CoA replacing the usual relative rotor angle. It transforms the variables δ_i , ω_i to the CoA.

Hence θ_i is a new term representing the change in rotor angle compared to the CoA angle.

$$\theta_i = \delta_i - \delta_0$$

$$\widetilde{\omega_i} \triangleq \omega_i - \omega_0$$

Then the derivative gives:

$$\dot{\theta}_i = \dot{\delta}_i - \dot{\delta}_0 = \omega_i - \omega_0 \triangleq \widetilde{\omega_i}$$

With the calculation of CoA, the literature further applies this concept to develop an index used to determine whether the system will be stable or unstable following a disturbance. The index is the Centre of Angle Stability Index (CASI) which is:

$$CASI = \left| \frac{\delta_{01}^{AD} - \delta_{02}^{AD}}{\delta_{01}^{BD} + \delta_{02}^{BD}} \right| * 100 \qquad 2.7$$

Here, 01 and 02 refer to two systems, and the BD and AD refer to before and after disturbance conditions. The disturbance may be an electrical fault, but it could also be the loss of a major transmission line.

2.7 Voltage stability analysis

A power system is considered stable from a voltage point of view if, when subjected to a disturbance, it settles at an equilibrium voltage within the region of attraction. A voltage stability study is used to observe the overall behaviour of the system, its stress level, the point of instability and the effect of a gradual change in load. The ability of a system to transfer reactive power from a generation source to a load area is a major aspect of voltage stability. Logically, voltage instability is the absence of voltage stability. This happens when the receiving end voltage drops below a normal operating range and cannot be restored by any compensating phenomenon. This means it is the inability of the power system to meet the reactive power demand.

The major criteria for a system to be voltage stable are that the voltage magnitude at a bus must increase with the injection of reactive power at the same bus. If the voltage magnitude decreases with reactive power injection at that bus, then the system is unstable. A sequence

of events leading to voltage instability can lead to voltage collapse which can be described as an unacceptable voltage profile for a significant part of the power system [9].

The first approach in analysing voltage stability is the experimentally based classical method of doing a large numbers of load flow simulations generally for extreme cases, and through that process identifying the weak or potentially problem buses.

The Q-V (MVAR - voltage) method is the approach chosen in this thesis to analyse the Barbados power system. It does not require the power system to be represented as a two-bus equivalent. At any critical bus at any point in the system, reactive power required at that bus is plotted against the bus voltage. This is experimentally accomplished by placing a fictious generator with zero MW at a critical bus and running a load flow to determine the reactive power required under the specified conditions of load power and voltage.

2.7.1 Q-V Curve

Voltage stability in a power system is dependent on the change in reactive power and its effect on voltage at the receiving or load end. The of Q-V (MVAR- voltage) method is widely used to analyse voltage performance at a bus. It does not require the power system to be represented as a two-bus equivalent. However, it requires a preliminary judgement to determine the critical buses in the power system, otherwise the process must be carried out for each load bus (which can be done for smaller systems such as the BLPC power system). The base case operating point can be found at the zero reactive power output of the fictitious generator. The point where dQ/dV becomes zero is a critical point or voltage instability point on the curve. If this occurs when the fictious generator is putting out MVAR, the power system is MVAR deficient at that bus. Similarly, if this occurs when the fictious generator is taking in MVAR, the power system has reactive power reserve at

that bus. The part of the Q-V curve to the right of the critical point represents a stable operating point and to the left represents an unstable operating point. With the help of Q-V curve, it is possible to accurately determine the value of reactive power shunt compensation to maintain voltage within an acceptable limit.

2.7.2 Q-V for a lossless system

As is typically done, the initial focus is on only the reactance model for a transmission line (no resistance, no capacitance). For a two-bus system, the power transfer from one bus to another can be expressed as [55].

$$P = \frac{EV}{X} \sin \delta \qquad 2.8$$

Here, E is the supply voltage $E = E \angle \delta$, and V is the voltage at that bus $V = V \angle 0$. δ is the rotor angle for the supply voltage.

It is possible to calculate the initial steady state angle from the equation 2.8 above,

$$\delta = \sin^{-1} \frac{PX}{EV}$$

Similarly using the initial angle from the above equation, the reactive power delivered by the transmission line can be given by:

$$Q = -\frac{V^2}{X} + \frac{EV}{X} \cos \delta \qquad 2.9$$

Assuming Q_{load} such that the power factor at that bus is a typical value of 90%,

$$\theta = 25.84°$$

$$\tan \theta = \frac{Q}{P} \cong 0.5$$

$$Q_{load} = 0.5 * P_{load}$$

Hence the difference between the value of Q_{load} and the Q able to be supplied by the transmission line at the specified condition can be used to determine $Q_{required}$ locally

$$Q_{required} = (0.5 * P) + \frac{V^2}{X} - \frac{EV}{X} \cos\delta \qquad 2.10$$

Given that the supply system has a reactance X and a voltage E, to deliver power P to the load bus at voltage V the system can only supply the value Q of equation 2.9 to the load bus. To supply a different Q load under the above conditions of X, E, P, V, some MVAR have to be supplied locally. This is called $Q_{required}$ as expressed in equation 2.10. Plotting this $Q_{required}$ versus the desired operating voltage V for different values of P in per unit on the same graph gives the Q-V plot as shown in Figure 2-4.

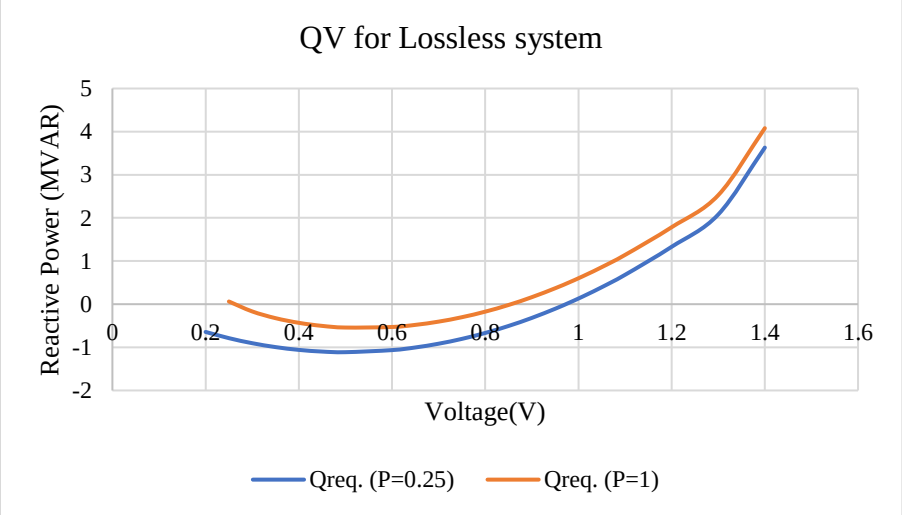

Figure 2-4: QV plot for lossless system with E=1 and X=0.2

It is useful to review the conditions which must be satisfied for any solution.

2.7.3 Q-V for a lossy system

For a transmission line with low operating voltage, typically the line shunt capacitance/line charging is essentially non-existent. However, for lower voltage systems, the

reactance/resistance X/R ratios are not nearly as high as in high voltage transmission lines. For low voltage transmission line, $X/R < 10$ is observed.

The fundamental equation is: $P + jQ = V_T * I^*$

For a transmission line with both inductance X_T and resistance R_T, the current flowing in the transmission line is:

$$I = \frac{(E\llcorner\delta - V_T) * (R_T - jX_T)}{(R_T^2 + X_T^2)}$$

Then the equations for P and Q become:

$$P = \frac{E * V_T}{R_T^2 + X_T^2}(R_T \cos\delta + X_T \sin\delta) - \frac{V_T^2 * R_T}{R_T^2 + X_T^2} \qquad 2.11$$

$$Q = \frac{E * V_T}{R_T^2 + X_T^2}(X_T \cos\delta - R_T \sin\delta) - \frac{V_T^2 * X_T}{R_T^2 + X_T^2} \qquad 2.12$$

To make the equation 2.11 and 2.12 simpler, assume:

$$A = \frac{E * V_T}{R_T^2 + X_T^2};\ B = \frac{V_T^2 * R_T}{R_T^2 + X_T^2};\ C = \frac{V_T^2 * X_T}{R_T^2 + X_T^2}$$

Then,

$$P = A * Z_T \cos(\gamma - \delta) - B \qquad 2.13$$

Here γ is the angle between the resistance and reactance, that is the angle of the transmission line impedance. Finding the angle from

$$\gamma - \delta = \cos^{-1}\left(\frac{P + B}{A * Z_T}\right) \qquad 2.14$$

Hence the reactive power delivered can be obtained from

$$Q = A * Z_T \sin(\gamma - \delta) - C \qquad 2.15$$

Similar to the lossless system in equation 2.10, the difference between Q_{load} and the supply from transmission line Q at specified condition is used to determine $Q_{required}$

$$Q_{required} = 0.5 * P - A * Z_T \sin(\gamma - \delta) + C \qquad 2.16$$

There are some conditions imposed on E so that the $\sin(\gamma - \delta)$ term is not greater than 1.0. The transmission lines for smaller power systems might be at the 24.9 kV level, and at this voltage level resistance is significant and cannot be neglected. The QV plots for a sample system are shown in Figure 2-5 and plots of other lossy transmission systems are demonstrated in Appendix B, pages 91-92.

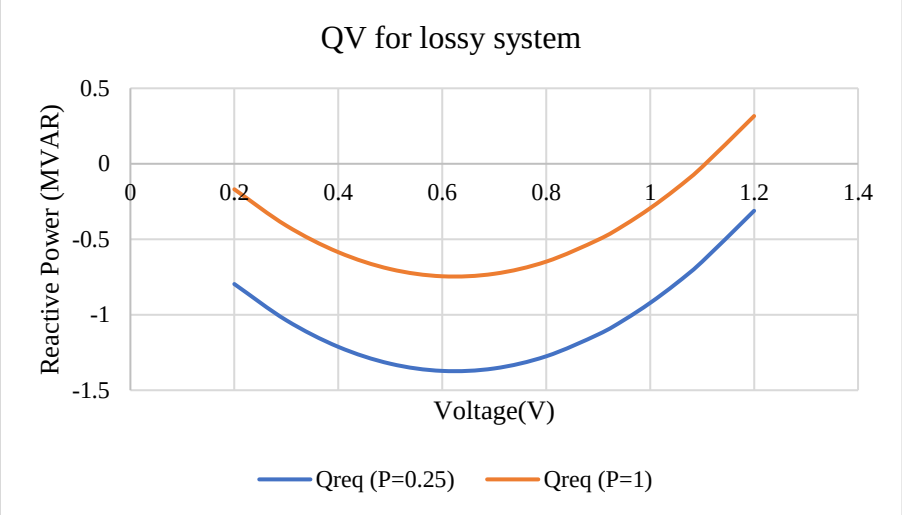

Figure 2-5: QV plot for lossy system with E=1, X=0.2 and R=0.15

2.8 Cascading effects mechanism.

BLPC had provided the historical record and time-line analysis of island-wide blackouts on their power system over several years. In two or three instances, the record shows that auxiliary equipment such as turbine-generator governors tripped due to low voltage. This indicates that compressor motors maintaining hydraulic fluid pressure tripped due to low voltage. Since electrical supplies for such auxiliary equipment is taken from sources close to the respective generator terminals, this suggests generators came up against an excitation limiter and could no longer control their terminal voltage. This indicates measurements should sense intermediate events and initiate separation creating the northern microgrid.

2.9 Relating Angular and Voltage Stability

There is no one quantity which will fully represent angular stability, and there is no one quantity which will fully represent voltage stability. This thesis chooses to use steady state stability limit B as an indication of angular strength. It also chooses to represent the voltage strength at a bus as the reactive power injection required at that bus to maintain the specified/desired voltage condition at the given value of load. The thesis derives a relationship between angular and voltage stability based on these two quantities. It is tested in both the theoretical and operating power systems (as illustrated later).

2.9.1 Deriving the relationship

With steady state stability limit (B) being a measure of angular stability, and MVAR Q needed for adequate bus voltage support being a measure of voltage stability, the following unique/original relationship has been developed.

From power system stability analysis, equation 2.8 shows the electrical power transfer capability across a lossless transmission line. The term EV/X which multiplies the sin δ term is called Steady State Stability Limit (SSSL). For ease of notation, it will be called B.

$$B = \frac{EV}{X}$$

The equation in terms of B becomes: $P = B * \sin\delta$

Referring to equation 2.10, it is necessary to get rid of the $\cos\delta$ term as follows.

$$\sin\delta = \frac{P}{B}$$

Using right angle triangle where $\sin\delta$ is the opposite side, $\cos\delta$ is the base and 1 is the hypotenuse, $\sin^2\delta + \cos^2\delta = 1$

$$\cos\delta = \sqrt{1-\sin^2\delta} = \sqrt{1-\left(\frac{P}{B}\right)^2}$$

Hence the equation 2.10 become,

$$Q_{required} = (0.5 * P) + \frac{V^2}{X} - B\sqrt{1-\left(\frac{P}{B}\right)^2} \qquad 2.17$$

Again, assuming $E = KV$

$$\frac{V^2}{X} = \frac{B}{K}$$

Then the equation become:

$$Q_{required} = 0.5P + B\left[\frac{1}{K} - \sqrt{1-\left(\frac{P}{B}\right)^2}\right] \qquad 2.18$$

Hence the above equation 2.18 gives the relation between reactive power required to maintain a specified voltage at a given loading P for any steady state stability limit B.

2.10 Locating and finalizing PMU units

PMUs can be used to extract real time quantities from time domain signals which include phasor amplitude, phase angle, frequency, and rate of change of frequency. Hence with the installation of PMUs in the BLPC system, they will be very important measuring devices in transmission line monitoring and control. Finalizing the location and number of PMUs required would provide adequate data for further development of algorithms analysing separation mechanisms.

CHAPTER 3

3. ANGULAR STABILITY ANALYSIS

3.1 Simulating the Energy Function

There are several references that present the use of direct stability methods based on stability energy functions. While it does not appear that such direct methods have been commercially programmed, it could be useful to consider their application on a small power system consisting of a single machine and an infinite bus. The pattern of the trajectory in the region of attraction of rotor angle and velocity can be seen in Appendix A, page 80-81. The plan is to study possibility of energy functions for stability of an island power system. A simulation has been carried out using MATLAB Simulink to justify the relation of the energy function $V_{(\delta,\omega)}$ with the critical energy V_{cr} The fault was cleared at different times to get the critical clearing time $t_{cct} = 0.315\ s$ as calculated from the instant when $V_{(\delta,\omega)} = V_{cr}$ on the faulted trajectory.

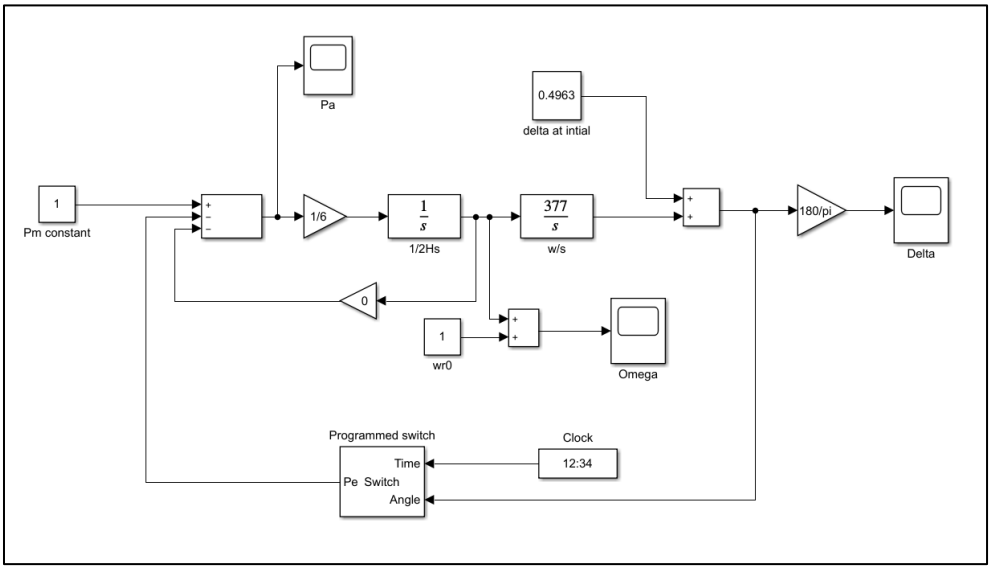

Figure 3-1: Model representing single machine infinite bus

Figure 3-1 is the model of a single machine operating into an infinite bus. The model is designed to observe the changes in acceleration, angular velocity, and rotor angle when the system is subjected to a disturbance. The mechanical power input has been taken as a constant and a disturbance in electrical power has been fed through the programmed switch in the feedback loop. While the pre-fault represents the initial steady state, the fault and post-fault conditions have been set in programmed switch to occur at 0.313 s and 0.317 s.

3.1.1 Analysis of the results

The energy function is simulated in Appendix A, page 81-84 for various fault clearing times, and the results for each clearing time are shown as one row in a table. From the results of simulating the energy function it can be observed that:

1. The system is stable if $V_{(\delta,\omega)}$ is less than V_{cr} along the faulted trajectory and the fault clearing time (t_{clr}) is less than the critical clearing time t_{cct}. The first six rows of the table in Appendix A, page 84 represent stable operating points, and last five rows represent unstable points.
2. The region of attraction of $(\delta^S, 0)$ is defined by the inequality constraint, $V_{(\delta,\omega)}$ is less than V_{cr}, for all points in the stable cases, but this is not true for unstable cases.
3. The value of $V_{(\delta,\omega)}$ at the critical clearing time $t_{cct} = 0.315\ s$ is very close to V_{cr} (i.e., $V_{(\delta,\omega)} = 0.55245$ and $V_{cr} = 0.55393$) but not exactly equal.

Hence, with the use of the energy function and critical energy, it has been possible to find the critical clearing time which ultimately is useful in determining in advance whether the system will be stable or unstable for a given fault condition.

3.2 The Centre of Angle Stability Index

While many quantities are important descriptors in power system stability studies, the load or power or torque angle δ of each generator is the most significant one because it describes the motion of the actual rotors of the synchronous machines. The individual rotor angles are stand-alone quantities. On the other hand, it is often useful to have a "collective indication" of what is happening in a power system especially as it may relate to what is happening in an adjacent interconnected power system, or even what is happening in another area of the same power system. The Centre of Angle gives the "mean acceleration" of all machines in the system [20]. From Chapter 2 the CoA δ_0 is defined in equation 2.5.

$$\delta_0 \triangleq \frac{1}{M_T}\sum_{i=1}^{m} M_i\delta_i$$

In this expression M_i is the inertia constant of turbine-generator i and M_T is the sum of the inertia constants of all turbine-generators in the system. The CoA is in fact the weighted average of all rotor angles in the system, weighted according to their inertia constants [20]. This can be carried one step further by considering the CoA of two areas in a power system, or more importantly the CoA of two power systems connected through an interconnection transmission line or lines. A comparison of the CoA of each system with the other gives an indication of the "mean angular motion" of the rotors of the two systems relative to each other. This has resulted in the definition of a stability index called the Centre of Angle Stability Index, CASI [21] is defined in equation 2.7. The CASI in a smaller reference system, the IEEE 9-Bus system, is demonstrated in Appendix A, page 84-87.

The CASI is an interesting system index. A search of the literature has not revealed where it was initially defined and used. In other words, there is no "first" statement and use of it.

A literature search shows that it has been used in University of British Columbia (UBC) research on two occasions. The first application was on the interconnection tie-line between Alberta Power and British Columbia Hydro in Canada. Initially they had a system separation criterion for the two systems based on voltage conditions in the areas adjacent to the interconnection. It appears that the voltage criteria sometimes gave false separation signals, so there was an investigation of an angular criteria. A UBC thesis shows the application of the CASI to the Alberta – British Columbia interconnection [21]. The second application was in the northern interior of British Columbia where an investor-owned mining company also produced electrical power and sold it into the BC Hydropower system. The CASI was also demonstrated as a separation index for that power plant [56].

One other interesting feature of the CASI is that the literature shows no derivation for a threshold value. The separation threshold in the two UBC examples is intuitive, based on the calculation of the CASI for a very significant number of stability runs. For the applications shown, a CASI in the 100 range was suggested as an appropriate value [21].

3.3 CoA and CASI in the BLPC system

After installation of the four CEB 8.25 MW units in the northern section of the BLPC system, it becomes possible to consider formation of a northern microgrid and a southern microgrid. Also, there is a 5 MW 21 MWh Battery Energy Storage System at Trent in the north to control frequency during a disturbance. To establish a “separation criteria” upon which a decision could be made to separate, a determination of the CoA behaviour in the BLPC northern and southern microgrid is required. This allows determination of the CASI. It is useful to again describe the “natural separation configuration” for the BLPC system. In the top one-third of the island grid there is a major terminal called the St. Thomas bus.

The St. Thomas bus has two transmission lines coming from the south. One is from the major generating station at Spring Garden and the other is from a major terminal station called Central. Two major disturbances were considered.

Disturbance 1 - Opening Saint Thomas to Spring Garden transmission line

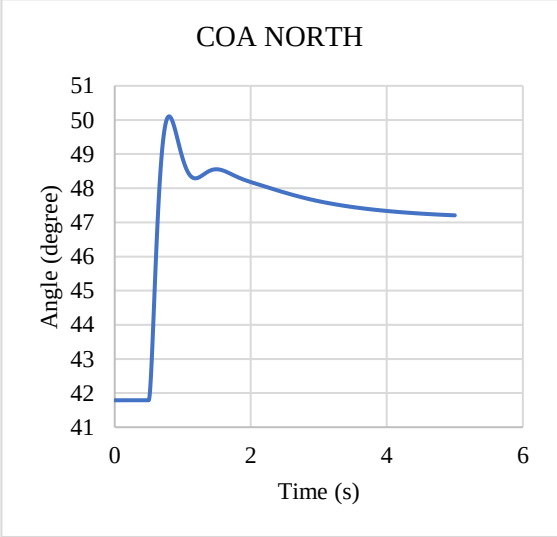

Figure 3-2: Centre of angle for northern microgrid on Disturbance 1

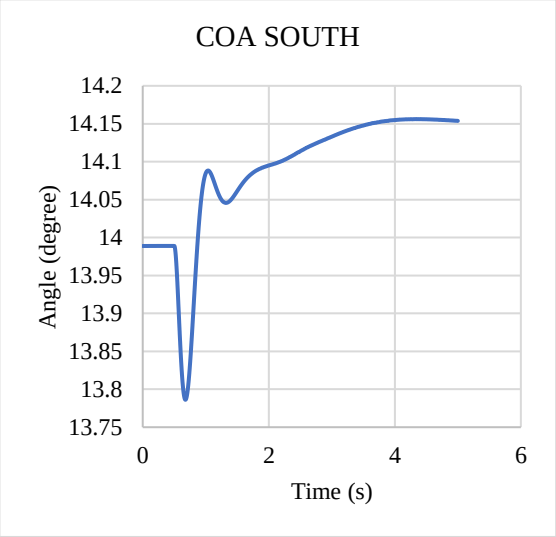

Figure 3-3: Centre of angle for southern microgrid on Disturbance 1

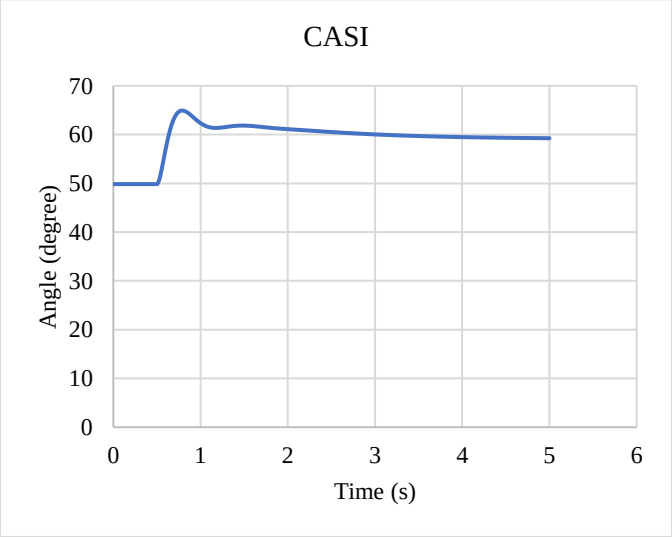

Figure 3-4: Centre of Angle Stability Index for Disturbance 1

Disturbance 2 - Opening St. Thomas to Spring Garden line and tripping a Spring Garden generator of 11 MW in the south and one CEB generator of 8.25 MW in the north.

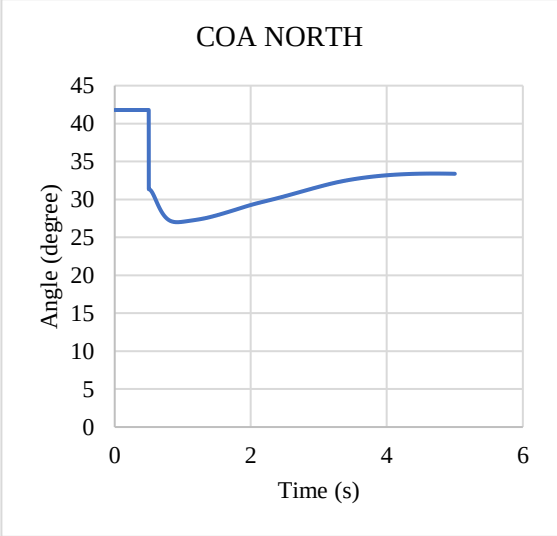

Figure 3-5: Centre of angle for northern microgrid on Disturbance 2

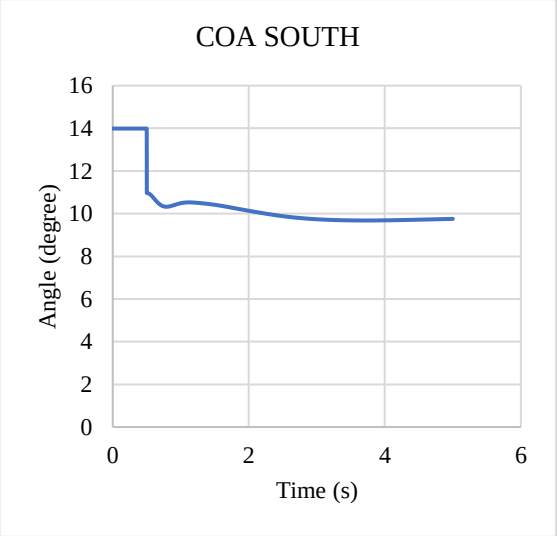

Figure 3-6: Centre of angle for southern microgrid on Disturbance 2

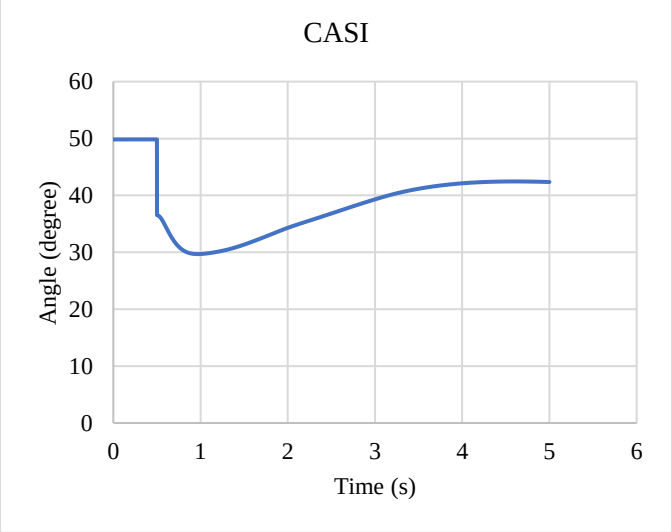

Figure 3-7: Centre of Angle Stability Index for Disturbance 2

Another disturbance of opening the Saint Thomas to Spring Garden line and tripping a Spring Garden Generator is shown in Appendix A on pages 84-86.

Discussion of Results:

Disturbance 2 is the worst disturbance which could occur on the BLPC system. Despite the significance of the disturbances, none of them caused any results that would suggest the necessity to separate the two systems according to the criteria implicitly used in the CASI. From a mechanical power point of view, it does not matter at which bus, or in which system, the load change/increase occurs. All generator governors move down their droop characteristics and put out more power. The only thing that can happen is a "small change" in power system losses but that will only impact mechanical power in a negligible way.

As a note of clarification, the BC Hydro results show the CASI value as always having an initial value of nearly zero. This can always be accomplished by means of an offset. In the simulation of the BLPC system in this thesis, there was always power flow between the north and the south, so the CASI always has an initial value. No attempt was made to introduce an offset.

The CASI threshold for the two BC Hydro circumstances appears to be an incremental value of about 100 [21]. However, every power system is different and the BLPC system is significantly different because of its small size and low voltage transmission.

None of the disturbances resulted in a continually increasing value of CASI. As already noted, the second disturbance of the simultaneous loss of two generators together with the loss of one of the transmission lines to the north must be classified as a major disturbance. Because none of the disturbances resulted in a continually increasing value of CASI, it has not been possible to set a threshold value of CASI for the BLPC system. The fact of a very small and controlled value of CASI suggests that separation into a northern microgrid and a southern microgrid will not be due to angular separation.

CHAPTER 4

4. VOLTAGE STABILITY ANALYSIS

Arising from the discussion of methodologies in Chapter 2, the most widely used approach to voltage stability analysis is in the Q-V method. It considers many aspects of controlling the voltage at a load bus by the injection of reactive power at that bus and observing the results of that injection. It is helpful to start with the simplest transmission model consisting only of a reactance, adding the complexity of including a resistance, and finally looking at an operational power system with multiple lines. QV plots for the four "corner cases" of system voltage and transmission reactance can be seen in Appendix B, page 89-91 (the “corner cases” being min and max extremes of transmission reactance and system voltage).

4.1 Bus Vector Indices

One objective is to describe each load bus by means of a bus vector. This bus vector becomes significant when Q-V method is used to characterize load buses on an operating power system. It is proposed that the bus vector should be made up of six indices as follows.

4.1.1 Thevenin impedance at the load bus

The first bus index is the value of Thevenin impedance/ reactance, at the bus. The process for determining Thevenin impedance at each load bus is defined later in this Chapter.

4.1.2 Reactive power reserve

The second bus index is the reactive power reserve. It is measured as the distance between the lowest MVAR point of Q-V curve and voltage axis. For many load buses the reactive power appears as a negative value on the Q-V plots. This means that additional active

power at a load could be added before more reactive power would have to be supplied locally. Thus, reactive power reserve suggests how much the loading on that bus can be increased before its loading limit is reached without causing voltage collapse on that bus. These margins are based on the reactive reserves in generators and synchronous condensers which can first be used in the process of computing a Q-V curve at any bus [57].

The dots in Figure 4-1 below represent the reactive power deficiency in the power system itself since the value of Q required on the vertical axis must be supplied locally via the fictitious generator. The reactive power reserve (RPR) is the negative of these values. For the top three graphs, there is no inherent system reserve so the reactive power values indicated by the dots must be supplied locally. These would appear as negative values of reactive power reserve as far as the system is concerned.

One final point should be noted. Reactive power reserve values often appear at unacceptably low levels of bus voltage such as 0.5 or 0.6 per unit. This indicates that there is much reactive reserve available to bring this low voltage up to the desired operating voltage of 1.0 pe unit.

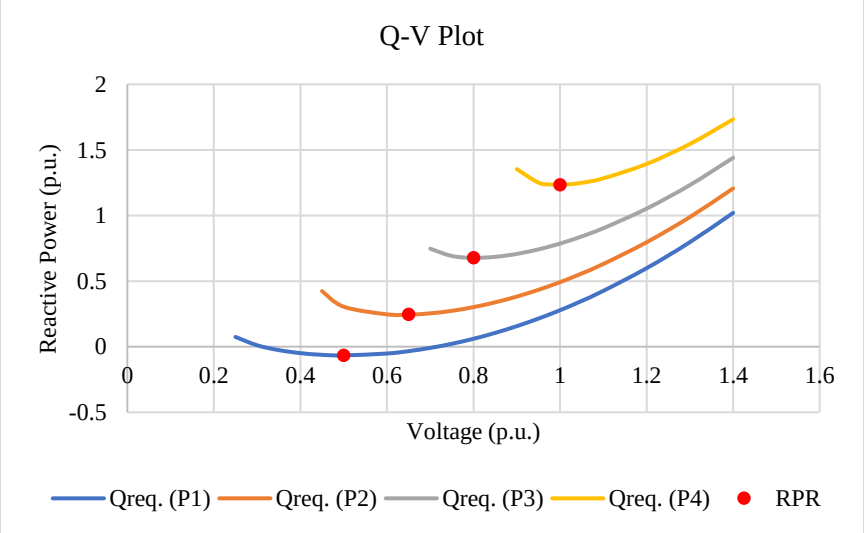

Figure 4-1: QV plot representing reactive power reserve

4.1.3 Reactive power required to maintain rated voltage of 1.0 per unit

The third bus index is the reactive power required maintain rated voltage of 1.0 per unit for a given loading condition. Positive values mean that the initial load voltage was low and reactive power was needed to bring it up to 1.0 per unit voltage. However, negative values represent an initial voltage that is above rated value, and an inductor bank is required to maintain rated voltage. The reactive power values required to maintain rated voltage are shown as the dots on Figure 4-2.

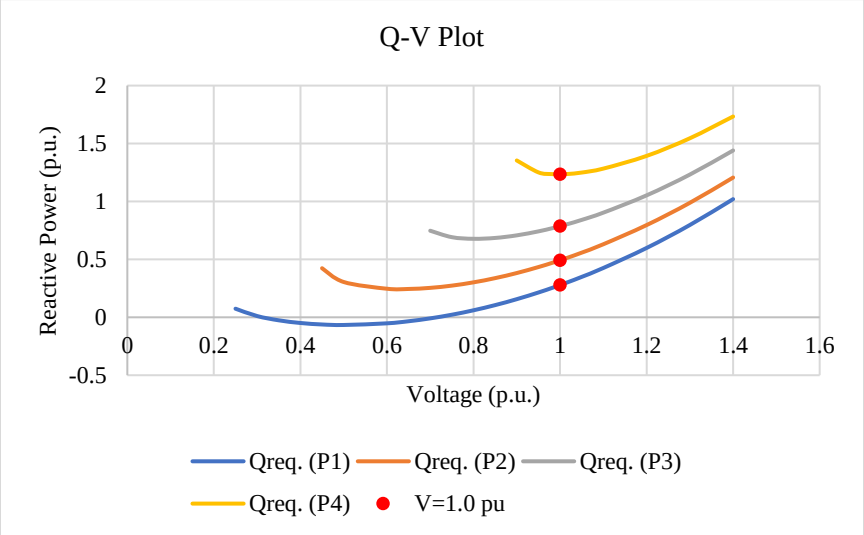

Figure 4-2: QV plot representing reactive power to maintain voltage

4.1.4 ΔQ/ΔV, the slope of the Q-V curve at rated voltage

ΔQ/ΔV is the fourth bus index. It tells the increment of reactive power required to improve the voltage by a specified increment ΔV at rated voltage. Since reactive power is often provided by installing capacitor banks, and since the cost of capacitor banks is expressed in dollars per kVAR, the ΔQ/ΔV represents the cost of improving the voltage at a load bus. On Figure 4-3 two consecutive points are shown on each graph by which it is possible to visualize the ΔQ/ΔV at each load level.

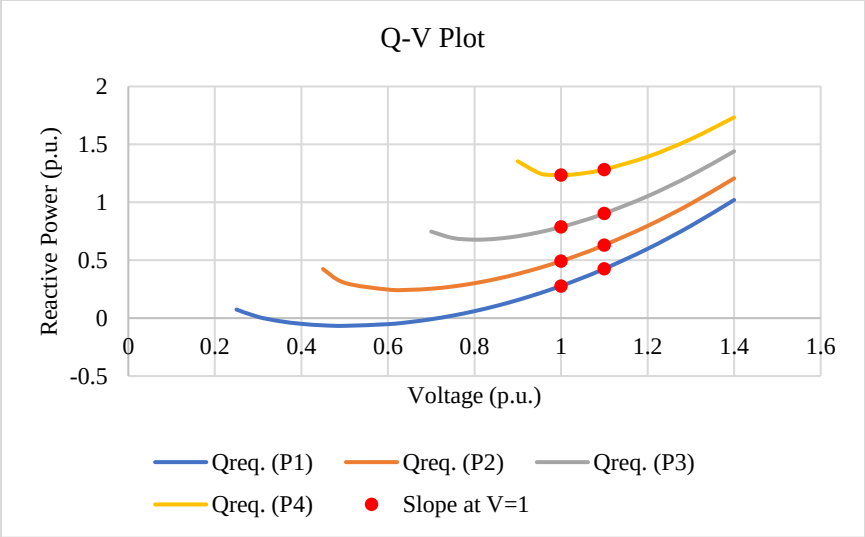

Figure 4-3: QV plot representing slope at rated voltage

4.1.5 Closeness of voltage instability point

The relative closeness of the voltage instability point is the fifth bus index. All Q-V plots have a point where dQ/dV = 0. To the right of this point, adding reactive power increases the voltage which is desirable. To the left of this point, adding reactive power decreases the voltage, so this is an unstable region. Consequently, the point where dQ/dV = 0 is called a voltage instability point. Typically, at most buses this voltage instability point is very far below rated voltage, but that is not always the case. This bus index can help in determining how vulnerable the bus is with respect to voltage collapse.

4.1.6 Reactive power increment due to load changes at rated voltage

The sixth bus index is the change in reactive power needed with a change in the load to maintain the voltage at the rated value of 1.0 per unit. It helps in indicating how much the voltage at a bus is influenced by load change and gives a factor representing load dependency.

4.2 Strength of Buses

The previous analysis was for a single transmission line supplying a load bus. Attention is now given to the BLPC operating power system with many low voltage transmission lines terminating on any one load bus. It is useful for comparative purposes to determine the "equivalent transmission capability" coming to any load bus in an operating power system. The commercial software package ETAP is used for short circuit calculations. For a three-phase fault at a load bus, it determines short circuit current (SCC) level in amperes and in per unit. Assuming that the Thevenin voltage is one per unit, the Thevenin equivalent impedance is 1.0 per unit voltage divided by SCC in per unit. That is, $Z_{Th} = \frac{V}{I_{Short\ Circuit}}$

Thevenin impedance calculated for each load bus in BLPC system is shown in Table 4-1.

Table 4-1: Thevenin equivalent impedance for all 24.9 kV BLPC's buses

S.N.	Buses (24.9 kV)	SCC 3φ (kA)	Angle(deg)	Zth in ohms	Xth in ohms	Xth p.u. (30 MVA base)	X/R ratio
1	North	3.1900	-65.0200	4.5066	4.0850	0.1977	2.1465
2	Trent	3.7070	-64.7000	3.8781	3.5061	0.1696	2.1155
3	Carlton	4.1000	-69.6200	3.5063	3.2869	0.1590	2.6918
4	St. Thomas	5.0070	-76.5300	2.8712	2.7922	0.1351	4.1749
5	Old Works	5.2110	-74.9700	2.7588	2.6644	0.1289	3.7242
6	Banks	6.1920	-74.5300	2.3217	2.2376	0.1083	3.6132
7	Hampton	7.1230	-78.8800	2.0183	1.9804	0.0958	5.0876
8	Wotton	9.5110	-72.6400	1.5115	1.4427	0.0698	3.1988
9	Seawell	9.5440	-71.6300	1.5063	1.4295	0.0692	3.0114
10	Wildey	9.9430	-75.7600	1.4458	1.4014	0.0678	3.9404
11	Garrison	11.6890	-71.9000	1.2299	1.1690	0.0566	3.0595
12	Warrens	12.0570	-69.2300	1.1923	1.1148	0.0539	2.6367
13	Marhill Street	14.0570	-75.0100	1.0227	0.9879	0.0478	3.7347
14	Regency Park	14.6780	-77.5300	0.9794	0.9563	0.0463	4.5219
15	Whitepark	15.1630	-77.0300	0.9481	0.9239	0.0447	4.3418
16	Temple Yard	15.5180	-76.7500	0.9264	0.9017	0.0436	4.2468

17	Belmont	16.2090	-79.6800	0.8869	0.8726	0.0422	5.4917
18	Central	17.6750	-82.6600	0.8134	0.8067	0.0390	7.7632
19	Desalination	18.6340	-80.2000	0.7715	0.7602	0.0368	5.7894
20	Spring Garden	21.4400	-83.7300	0.6705	0.6665	0.0323	9.1016

It is necessary to comment on the significance of the Thevenin impedance at a bus. If the Thevenin impedances is small, the short circuit current is high which requires higher capability circuit breakers to interrupt the fault current. At the same time a small Thevenin impedance means a smaller voltage drop in the equivalent transmission and better voltage regulation at the bus, which is good. Also, a small Thevenin impedance, or reactance, means a higher steady state stability limit, which is also good.

As shown in Table 4-1, the Thevenin impedance can be used to rank the "electrical strength" of a bus, with low values of Thevenin impedance meaning a stronger bus, and high values of Thevenin impedance indicating a weaker bus.

4.3 Q-V characteristics on BLPC system

A load flow study shows the resultant voltage at all load buses in the power system. It is a well understood power system concept that low voltage at a load bus can be improved by adding reactive power (vars/MVARs) at the bus. A trial-and-error process could be carried out by adding reactive power at a load bus and noting the voltage attained, which would ultimately give the Q-V characteristic at that bus.

Power system researchers and planners have devised a more efficient approach. A "fictitious test generator" with zero MW power output is placed at the load bus. Because it is a generator, it has Automatic Voltage Regulator capability and can control the load bus voltage at any specified voltage level by adjusting the rotor field current to cause the generator to either produce reactive power, or to absorb reactive power, to achieve the

desired voltage at that load bus. As noted, the fictitious generator will always have zero MW output, otherwise it just changes the value of load at the load bus. The "fictitious generator" should always have an MVA rating very high compared to the system load. That will give it lots of leeway to supply, or absorb, reactive power.

For the BLPC operating power system, Q-V graphs for all the load buses in the system have been determined by putting a fictitious generator at load buses and observing the voltage and reactive power behaviour. A few representative load bus results are presented.

Weaker Buses

Weaker buses have a high value of Thevenin reactance (i.e., greater than 0.12 on a 30 MVA base). Most of these buses have only few transmission lines coming to them, and most are quite electrically distant from generation. North substation is an example of a weaker bus.

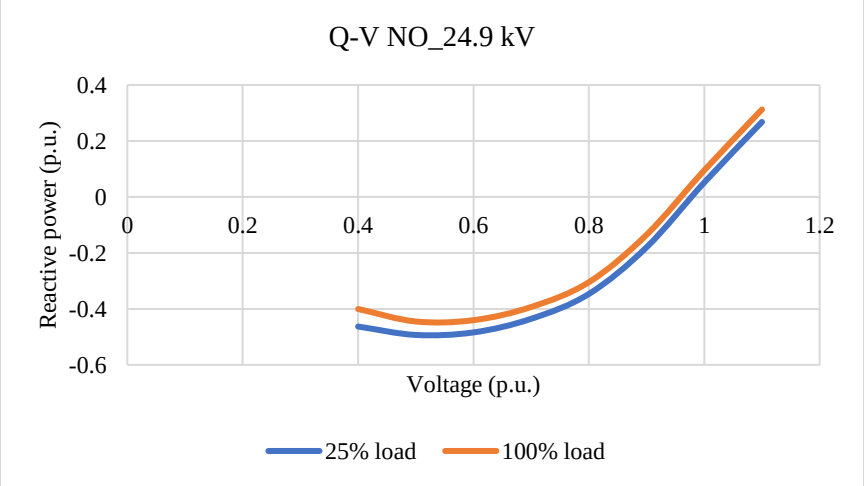

Figure 4-4: QV plot for North 24.9 kV bus

Moderate Buses

These are the buses which have a value of Thevenin reactance in middle range (i.e. less than 0.12 and greater than 0.05 on a 30 MVA base). The Warrens substation is an example of a moderately strong bus.

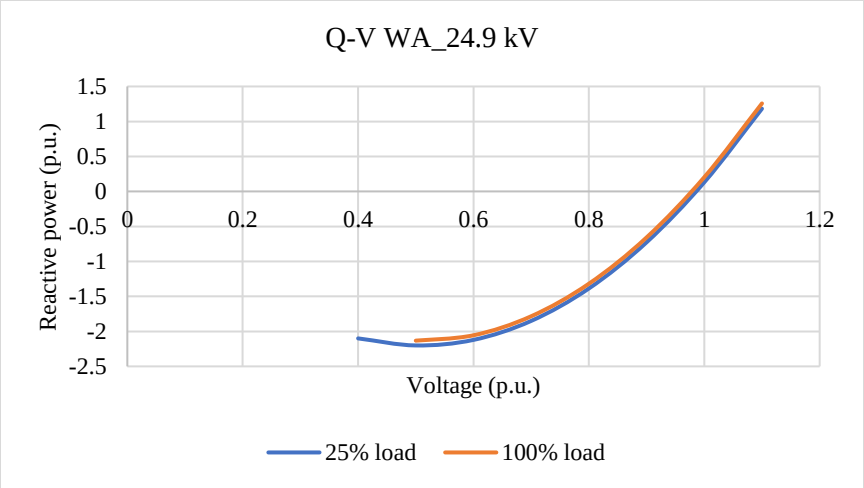

Figure 4-5: QV plot for Warren 24.9 kV bus

Strong Buses

These are the buses which have many transmission lines connected to them, and typically these are short transmission lines so that many other buses are electrically close to them. The result is that changing the voltage on these buses is difficult. These buses have a low value of Thevenin reactance (i.e. less than 0.05 on a 30 MVA base).

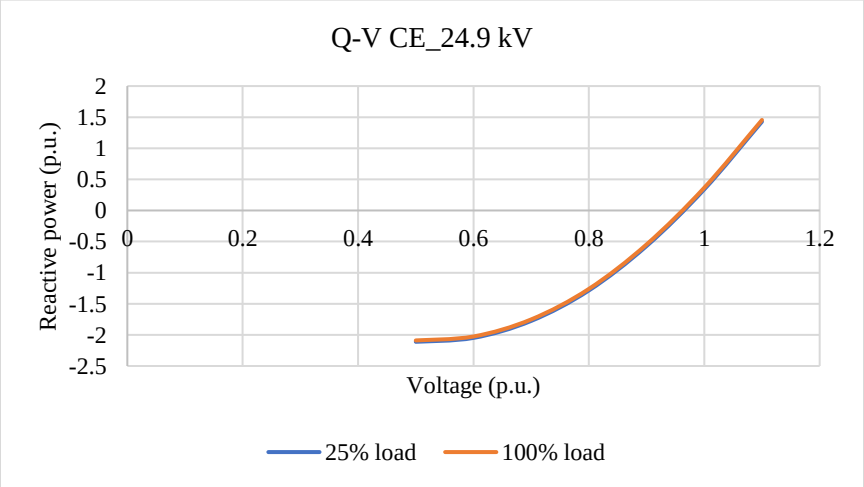

Figure 4-6: QV plot for Central 24.9 kV bus

4.4 Observation from the QV Curves

For entire BLPC power system, six bus indices are shown in the Table 4-2 which follows.

Table 4-2: Bus vector indices for BLPC's 24.9 kV buses

S.N.	Bus ID	Zth (A)	Res. Margin (B)	Qreq (C)	ΔQ/ΔV (D)	V at dQ/dV = 0 (E)	ΔQ at V=1 (F)	V at 100% load	X/R ratio
1	NO	0.218	0.445	0.095	2.170	0.5	0.044	0.954	2.146
2	TR	0.188	0.327	0.001	1.650	0.6		1.000	2.116
3	CA	0.170	0.584	0.110	2.840	0.6	0.048	0.967	2.692
4	ST	0.139	0.733	0.104	3.460	0.6	0.062	0.967	4.175
5	OL	0.133	0.652	0.145	3.450	0.5	0.035	0.952	3.724
6	BA	0.112	1.000	0.186	5.270	0.5	0.040	0.959	3.613
7	HA	0.098	0.601	0.152	3.270	0.5	0.041	0.946	5.088
8	SW	0.073	0.961	0.241	5.270	0.5	0.050	0.947	3.199
9	WO	0.073	1.142	0.281	6.280	0.5	0.066	0.948	3.011
10	WI	0.070	1.741	0.292	8.980	0.5	0.040	0.963	3.940
11	GA	0.060	1.428	0.190	7.080	0.5	0.080	0.956	3.060
12	WA	0.058	2.132	0.203	10.550	0.5	0.070	0.978	2.637
13	MS	0.049	2.368	0.342	12.140	0.5	0.050	0.968	3.735
14	RP	0.047	1.572	0.282	8.210	0.5	0.025	0.960	4.522
15	WP	0.046	2.770	0.367	14.070	0.5	0.060	0.970	4.342
16	TY	0.045	2.840	0.374	14.590	0.5	0.070	0.971	4.247
17	BE	0.043	2.655	0.008	13.700	0.5	0.010	0.967	5.492
18	CE	0.039	2.089	0.366	10.890	0.5	0.026	0.962	7.763
19	DE	0.037	6.195	0.352	29.130	0.5	0.010	0.987	5.789
20	SP	0.032	9.771	0.494	48.720	0.6	0.060	0.989	9.102

Legend:

(A) Thevenin impedance in p.u. on 30 MVA base.

(B) Reactive Reserve Margin expressed in a positive sense on 100 MVA base

(C) Q Required to maintain 1.0 p.u. voltage on 100 MVA base

(D) ΔQ required to adjust/correct voltage ΔV by 1.0 per unit (that is, ΔQ/ΔV at V = 1.0 p.u.)

(E) Voltage at dQ/dV = 0 point, voltage at the lowest point of the curve.

(F) ΔQ necessary over 25% to 100% load levels at V = 1.0 p.u. on 100 MVA base (This indicates how sensitive is the MVAR requirement to load changes)

The first index in the bus voltage vector is the Thevenin impedance given in Table 4-1. The other five indices at all the BLPC load buses are shown in the diagrams which follow.

Reactive Power Reserve (B)

The reactive power reserve is determined from Q-V plots. Figure 4-7 shows reactive power reserve for each bus in BLPC power system in decreasing order of Thevenin impedance.

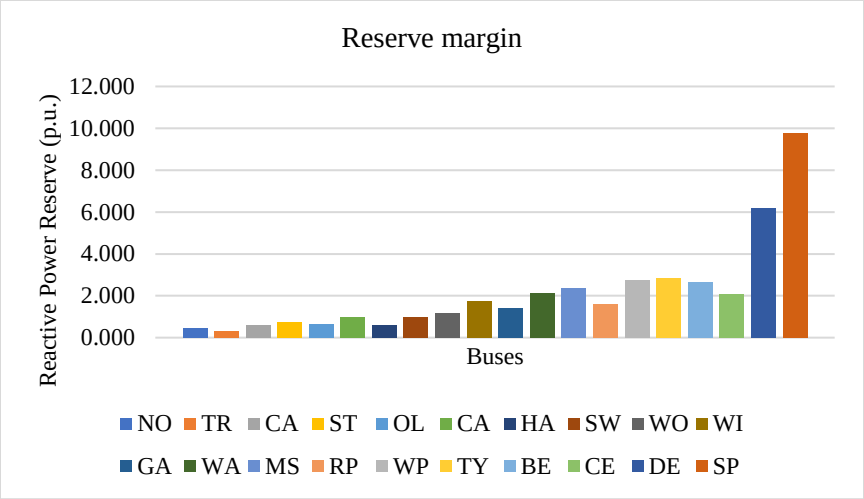

Figure 4-7: Reactive Power Reserve of all buses

Reactive power required to maintain rated voltage (C)

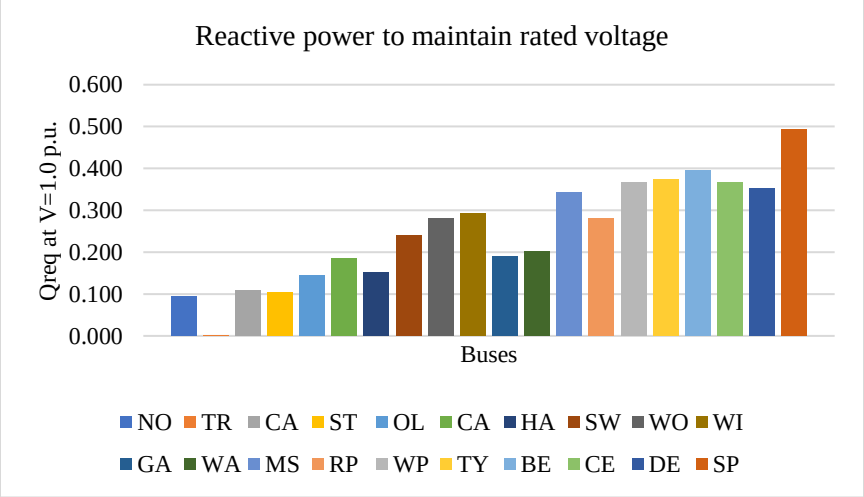

Figure 4-8: Reactive power for rated voltage of all buses

The reactive power required to maintain rated voltage increases with decrease in Thevenin impedance, except for a few buses impacted by a particular configuration. The value can also be impacted by initial loading conditions. The value of reactive power demand is very high compared to the load at that bus. To maintain the voltage at a bus, it is also necessary to move/increases the voltage at adjacent buses. Hence the value ranges from 10 MVAR to 50 MVAR over all the BLPC's buses, with any one load not being more than 14 MVAR.

Slope ΔQ/ΔV of Q-V curve at rated voltage (D)

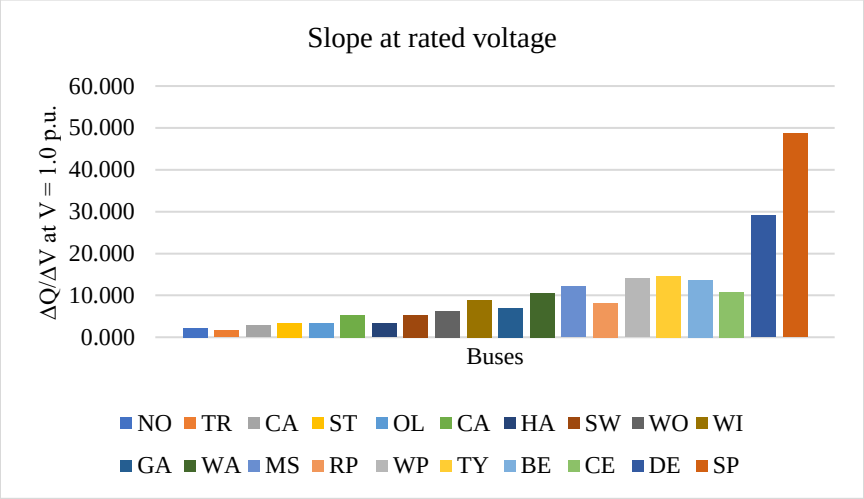

Figure 4-9: Slope of all buses at rated voltage

The slope of the Q-V curve at rated voltage generally increases with an increase in the electrical strength of the bus. However, the results also depend on the power system configuration at a bus, which is the reason that the bar graph shown is not strictly monotonically increasing. Some distortion in the gradual increase in slope is due to the number of transmission line connected to the bus.

Closeness of voltage instability point (E)

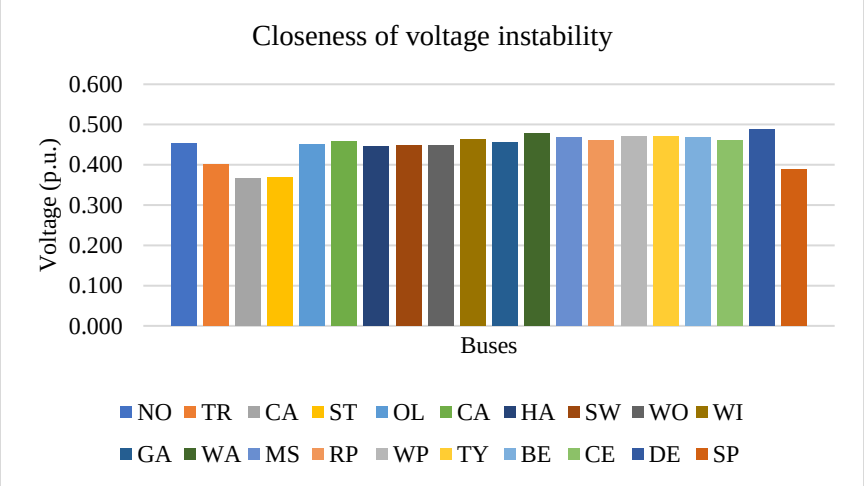

Figure 4-10: Closeness of voltage instability for all buses

All the buses have similar value of voltage at the point of reactive power reserve. Figure 4-10 suggests that with very small distances between the buses on the BLPC system and operating at low voltage level, voltage instability point on all buses does not change much.

Increment of reactive power required at rated voltage for load changes (F)

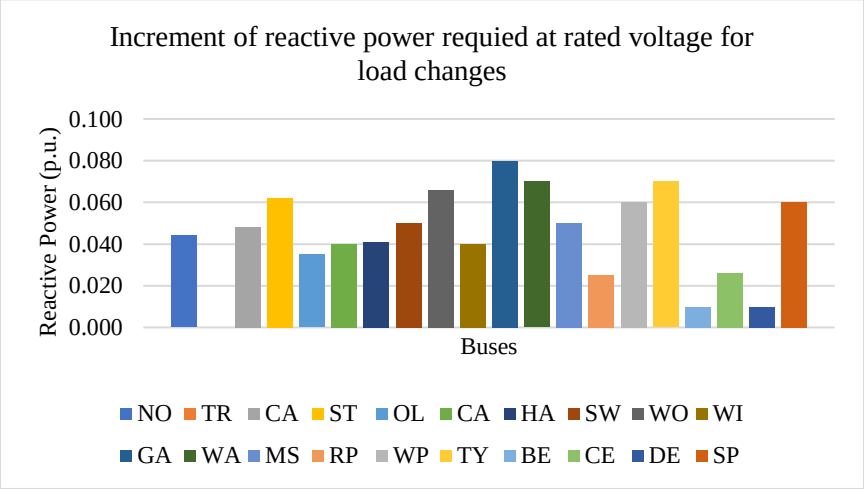

Figure 4-11: Load change increment of reactive power for all buses

The buses are dependent on the variation of load. If a bus has a higher load, the reactive power variation is high and for low load, reactive power change is lower. The requirement of reactive power varies between 1 MVAR to 8 MVAR on a load change within 10 MW.

4.7 Analysing Q-V curves

The Q-V curve is an experiment carried out on behaviour of a load bus to determine its voltage properties. When a load bus is only separated from a generator bus by a transformer, or a short transmission line, there is significant interaction between the two buses. If reactive power is injected at a load bus by the fictitious generator to bring the voltage up to one per unit, that will also tend to increase the voltages at adjacent buses. If the adjacent bus is a generator bus, its synchronous generators will act to absorb reactive power to maintain its terminal voltage at the scheduled value. This means that fictitious

generator and an operating generator end up fighting with each other. The solution is to increase terminal voltage set point at the operating generator by two or three per cent to correct voltage at electrically close load buses. For this reason, Trent and Spring Garden generation buses, and Desalination Plant bus being very close to Spring Garden bus, is eliminated from Q-V study.

The electrical strength of a load bus is very important. It is useful to examine some of the indices of the voltage bus vector to see how they vary with the electrical strength of the load bus. The bus indices are plotted versus $1/Z_{Th}$. For a weak bus the $1/Z_{Th}$ will be a smaller number while for a strong bus it will be a larger number. Also, as pointed out in reference [59] $1/Z_{Th}$ is the short circuit current (SCC) at the bus which number will typically be known by power system personnel from fault studies. The following is a plot of Reactive Power Reserve margin versus $1/Z_{Th}$ for the buses on the BLPC system.

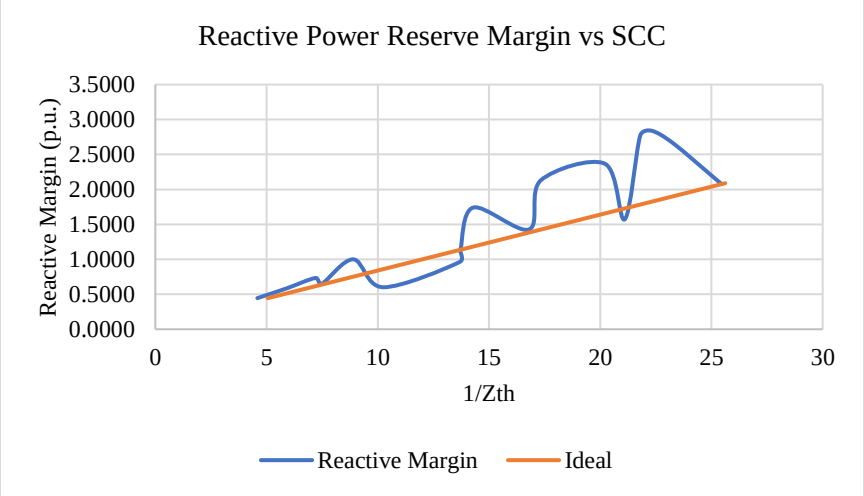

Figure 4-12: Reactive Power Reserve margin versus 1/ZTh for load buses

Starting with the load bus voltages from a load flow study, the same plot was obtained for the reactive power required at the various buses to attain one per unit voltage. The pattern for this bus index is very similar to that of the previous bus index.

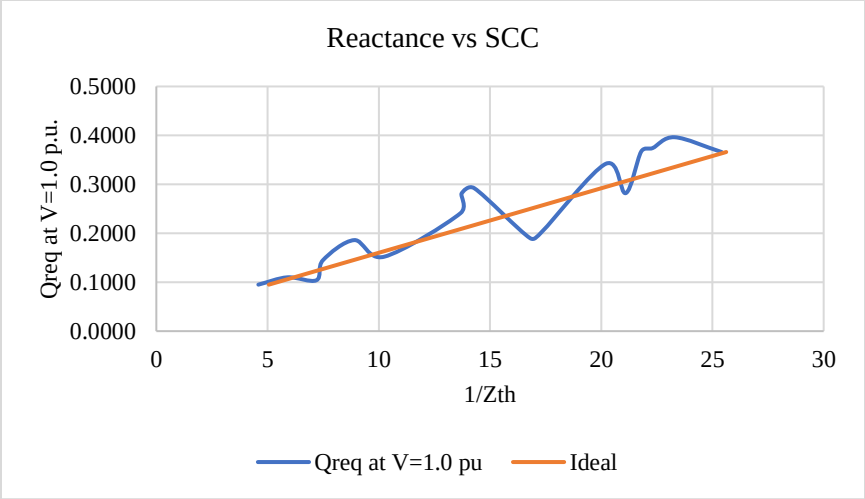

Figure 4-13: Reactive Power at rated voltage versus 1/ZTh for the load buses

The curve of Figure 4-13 follows a pattern and depicts that the reactive power required to maintain rated voltage at a bus is proportional to the inverse of the Thevenin impedance.

Next the ΔQ/ΔV values are examined. This is slope of the Q-V characteristic at 1.0 per unit voltage, and these values is determined for remaining 17 BLPC buses varying from 8.71 MVAR/kV to 58.59 MVAR/kV. Based on electrical strength, they are classified as:

Weak Bus	8.71 – 13.12 MVAR/kV
Moderate Bus	13.13 – 42.35 MVAR/kV
Strong Bus	42.36 – 58.59 MVAR/kV

Three very important conclusions can be arrived at from the ΔQ/ΔV values.

First, static capacitors are often installed to correct bus voltages and the cost in $/kVAR of static capacitors is known. Using these two numbers, it is possible to determine the relative cost of correcting the voltage at any bus.

Second, reference [59] states that a high value of ΔQ/ΔV is in the range of 10 - 15 MVAR/kV. From the results of the Q-V curve, correcting the voltage on the BLPC system is quite expensive. However, a note should be added that reference [59] examples involve 132 and 275 kV cables which themselves have natural high MVAR in cable capacitance.

Third, reference [59] develops an expression which shows that for a lossless transmission system consisting only of reactance in transmission lines, theoretical value of ΔQ/ΔV is:

$$\Delta Q/\Delta V = V/X_{Th} = \text{SCC in per unit}$$

Figure 4-14 shows the actual values of ΔQ/ΔV at the BLPC buses compared to the theoretical values at the buses. There is remarkably good agreement.

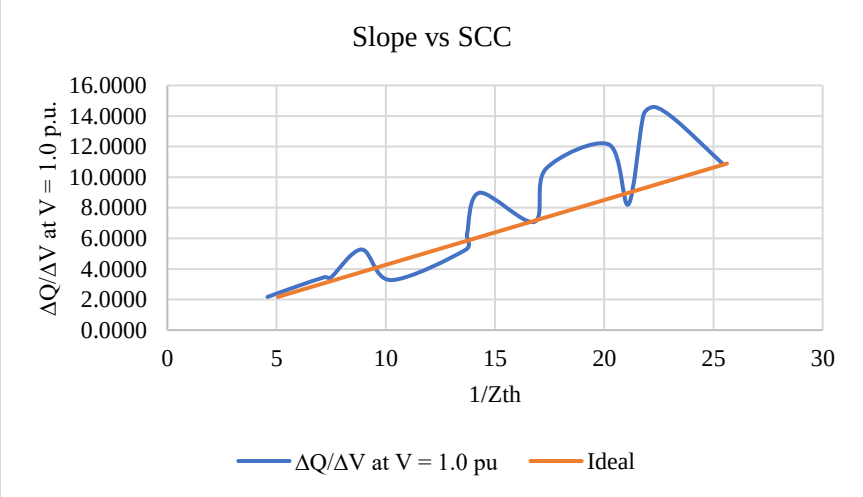

Figure 4-14: Slope at rated voltage versus $1/Z_{Th}$ for load buses

Because both ΔQ/ΔV and Reactive Power Reserve Margin vary generally in proportion to $1/Z_{Th}$, it is useful to plot these two quantities against each other as shown in Appendix B, page 93. While there is not a continuously monotonically increasing relationship between the two bus indices, nevertheless the linearity between the two bus indices is evident.

4.8 Effects of faults on adjacent bus voltage

It is important to know the effects of faults on adjacent bus voltages. This effect could impact the number of measurement units required to sense major voltage disturbances as part of any algorithm which might be developed for deciding on separation into two grids. Six buses from three categories were chosen to observe the voltage variations: North and Old Works, Banks and Warren, and Marhill Street and Central respectively from weaker,

moderate and strong buses. Generator buses Trent and Spring Garden were also included. To observe voltage changes in adjacent buses when a three-phase fault occurs at various locations, simulations were carried out to get the transients. The effect of faults on adjacent buses can be seen in plots in Appendix B, pages 93-96 and results are shown in Table 4-3.

Table 4-3: Summary of voltage change due to fault at different locations

S. N.	Buses (rated 24.9 kV) Impacted	Voltage in kV at 1 sec. when fault occurred at 0.5 sec.					
		Fault at NO	Fault at OL	Fault at BA	Fault at WA	Fault at MS	Fault at CE
1	North	0	15.97	13.66	8.72	7.56	6.92
2	Trent	12.44	19.92	17.76	13.21	12.13	11.53
3	Old Works	16.33	0	9.38	5.02	3.05	0.21
4	Banks	16.67	12.44	0	5.42	2.17	2.4
5	Warrens	17.22	13.89	11.25	0	4.56	4.01
6	Marhill Street	16.92	13.1	9.35	5.6	0	3.17
7	Central	16.45	11.07	9.56	5.03	3.16	0
8	Spring Garden	17.56	14.74	11.8	6.05	4.97	5.09

From the observation of Table 4-3, the following conclusions can be drawn:

1. All three phase faults at a load bus pull the voltage down at adjacent buses. and to a lesser extent at distant buses.
2. Faults at a weak bus pull the voltage at adjacent buses down to about 50% of rated value, but only pull the voltage at distant buses down to about 65-70% of rated value.
3. Faults at a strong bus pull the voltage adjacent buses down to about 20% of rated value, and voltage at distant buses down to about 50% of rated value.

Based on these results:

- A measurement unit placed at a strong bus such as Central would need a logic such as:

Separate if the measurement is Less Than or Equal the Set Point, with Set Point at 17 kV.

- A measurement unit placed at a weak bus such as North would need a logic such as:

Separate if the measurement is Less Than or Equal to Set Point, with Set point at 6 kV.

4.9 Ranking based on Bus vector Indices

Utilizing Bus Vector Indices at the BLPC buses, a position can be obtained for all buses based on these ranking values. The most favourable value is 10 and the least favourable will be valued proportional to the best value. The lowest value of Thevenin impedance (Zth), highest value of Reserve Margin (RM), lowest reactive power to maintain rated voltage (Qreq), lowest slope of QV curve at rated voltage (ΔQ/ΔV), lowest voltage at Reserve margin (V at dQ/dV=0) and lowest increment at rated voltage (ΔQ at V=1) are the best values in the ranking scheme. The sum is the total value of each bus from the six different voltage indices (i.e., out of 60). Spring Garden, Trent and Desalination Plant, have been removed from the study being generation buses and/or too close to generation buses.

Table 4-4: Ranking of BLPC buses based on bus vector indices

Bus ID	Zth	RM	Qreq	ΔQ/ΔV	V at dQ/dV=0	ΔQ at V=1	Sum
NO	2	2	10	10	10	5	38
CA	2	2	9	8	8	4	33
ST	3	3	9	6	8	3	32
OL	3	2	7	6	8	6	32
BA	4	4	5	4	10	5	31
HA	4	2	6	7	10	5	34
SW	5	3	4	4	10	4	31
WO	5	4	3	3	10	3	29
WI	6	6	3	2	10	5	32
GA	7	5	5	3	10	3	32
WA	7	8	5	2	10	3	34
MS	8	8	3	2	10	4	35
RP	8	6	3	3	10	8	38
WP	9	10	3	2	10	3	36
TY	9	10	3	1	10	3	36
BE	9	9	2	2	10	10	43
CE	10	7	3	2	10	8	40

Based on the ranking of voltage indices, the overall voltage performance of a bus can be obtained.

CHAPTER 5

5. CASCADING EFFECT

Island power systems have two characteristics which distinguish them from other power systems. First, they have the specific disadvantage that they do not have interconnections with other utilities which might be able to assist them during disturbances. Second, they often have one or more generating units whose capacity is in the range of 20% of the peak system load. In this case, it become very uneconomical to try to arrange spinning reserve to cover the loss of the largest generating unit. Generally, the reserve is a modest value of megawatts, but not nearly equal to the loss of the largest unit. Island utilities try to compensate for these circumstances by arranging quite sophisticated underfrequency load shedding schemes. Despite all this, island power systems can suffer island wide blackouts, which often involve a cascading process over a period of a few seconds.

5.1 Summary of Blackout Events

BLPC has a record of island wide blackout on their system over the last 10-year time frame. It is impossible to duplicate all the technical details, but it is important to at least highlight those aspects which appear to involve a cascading process. A summary of the blackout events is as follows:

Case 1. Bad weather and high lightning activity around 13:19 on 15th July 2012 caused a fault on the 24.9 kV overhead line between the Marhill St. and Belmont substations. This fault was “electrically close” to the Spring Garden plant in the tight transmission loop involving the short Marhill St.-Belmont line.

- Generators D11, D14, D15 tripped within 527 ms.

- Generator D10 tripped within 1292 ms
- The fault was cleared in 1361 ms.
- Other generators later tripped offline

The objective of power system relaying protection is to remove the faulted equipment as quickly as possible to assure that all generators remain in service and continue to supply the load. It is reasonable to suggest that there was a failure of the primary relaying, and as a result the fault was removed by the secondary relaying which typically has a time delay associated with it.

Case 2. A small truck collided with, and broke, a pole around 18:10 on 16th June 2013 causing a three-phase fault on the 24.9 kV overhead line between Central and Old Works substations. While further away than Case 1, the fault location is still "relatively electrically close" to the Spring Garden plant

- Generators D12, D13, D15, S1 tripped before opening of the Central end of the transmission line at 1339 ms.
- Other generators later tripped offline

Case 3. A flashover on a transformer's 24.9 kV circuit breaker around 05:56 on 1st September 2016 occurred as a fault on the White Park substation. As for Case 1, this fault is "electrically close" to the Spring Garden plant.

- Bus faults are typically protected by remote Zone 2 and Zone 3 distance relays.
- One line coming to White Park tripped in 579 ms.
- A second line to White Park tripped on timed directional overcurrent in 978 ms.
- Generator D11 tripped before the fault was cleared.
- Other generators later tripped offline.

Case 4. Bad weather and high lightning activity resulting from Hurricane Maria in the area at around 15:30 on 18th Sept 2017 caused a fault on the Banks 24.9 kV distribution feeder. The fault was a phase B to phase C flashover with equal and reduced voltage at the nearby Temple Yard substation.

- A Belmont relay started to act through Zone 3 distance relaying, but after 644 ms relay action on the reverse Zone 4 relaying was observed.
- Since the fault was an arcing flashover, it self-cleared in 1248 ms.
- Generators D10, D12 tripped before the fault was cleared.
- Other generators later tripped offline.

Case 5. Flashover on the generator GT04 transformer 24.9 kV circuit breaker occurred around 14:35 on 8th Jan 2018 caused a fault on the 24.9 kV bus in the Seawell substation. Based on that electrical configuration, it was necessary to trip four lines coming to the Seawell bus and to trip the Seawell generators in order to clear the fault. However, the bus does not have bus differential protection, so it was necessary for distance relays to clear the fault.

- Central 1 to Seawell transmission line tripped on Zone 2 in 23 ms (which is typically too fast for Zone 2).
- Hampton to Seawell line tripped on Zone 1 in 680 ms (which is too slow for Zone 1)
- Central 2 to Seawell line tripped on Zone 1 in 798 ms (too slow for Zone 1)
- Wotton to Seawell line tripped on Zone 1 in 823 ms (too slow for Zone 1)
- Generators GT05, GT06 tripped at the Seawell plant.
- Generator D12 tripped at the Spring Garden plant

- Other generators later tripped offline

Case 6. A rodent entered the busbar section of the transformer around 05:42 on 24th April 2020 causing a fault on the 24.9 kV bus at the St. Thomas substation. Two incoming transmission lines from Central and Spring Garden to St. Thomas opened resulting in loss of electrical supply to the north of the island.

- Generators D10 to D13 tripped due to loss of auxiliaries, including loss of governor control due to low voltage.
- Generator D14 tripped due to low frequency experienced because of generators D10 to D13 tripping.
- Generators S1 and GT06 remained synchronized which possibly expedited the restoration of feeders.
- Other generators later tripped offline

5.2 BLPC's network

The first five blackouts were triggered by events in the southern BLPC system, and the last blackout was due to a fault in the north. The BLPC is rich is loops, or alternate flow paths, in the southern one-third of the power system. The White Park- Temple Yard – Marhill Street– Belmont loop is a small tight loop. It is also a loop within other loops. Further, there are essentially six alternate flow paths between the Spring Garden plant and the Central substation. Additionally, there are essentially three loops in the Central-Seawell- Hampton area. This means that the southern one-third of the power system is "electrically strong".

5.3 Activities during fault

This cascading of generators tripping after the fault, but prior to clearing the fault, was common in all blackout cases. Because of the preponderance of generators and control device (AVRs and governors) at the Spring Garden plant location, it is likely necessary to have a complete listing of the protective device settings as well as a complete time tracking of when the devices operated to fully understand what happened. Based on the information provided in Blackouts Summary, it is possible to develop a series of activities:

1. When a fault occurs on the power system, there is normally a reduced voltage at the fault and at many points in the power system.
2. If the bus loads are a function of voltage, then there will be a reduced load and a subsequent reduction in generator output requirements.
3. When the voltage at the faulted location is pulled down to a low level, this reduces the voltage at all buses in the vicinity of the fault.
4. When an AVR hits an Over Excitation Limiter (OEL), it loses the ability to maintain generator terminal voltage.
5. There are many generators, excitation system, AVRs, and limiters at the Spring Garden plant served from the same location at the 24.9 kV buses. This common source can easily lead to a cascading effect.
6. Blackout history record shows that auxiliaries tripped on low voltage during many of the events.

5.4 Simulation of Case 1 blackout event

A power system stability simulation was conducted for the conditions which occurred during the blackout event of Case 1. Assuming a fault halfway between the Belmont and

Marhill Street substations at 0.5 s, it is cleared at 1.861 s (which is equivalent to the historical record of clearing at 1.361 seconds). The effects on various power system variables can be observed from the simulation.

Effect on Generation

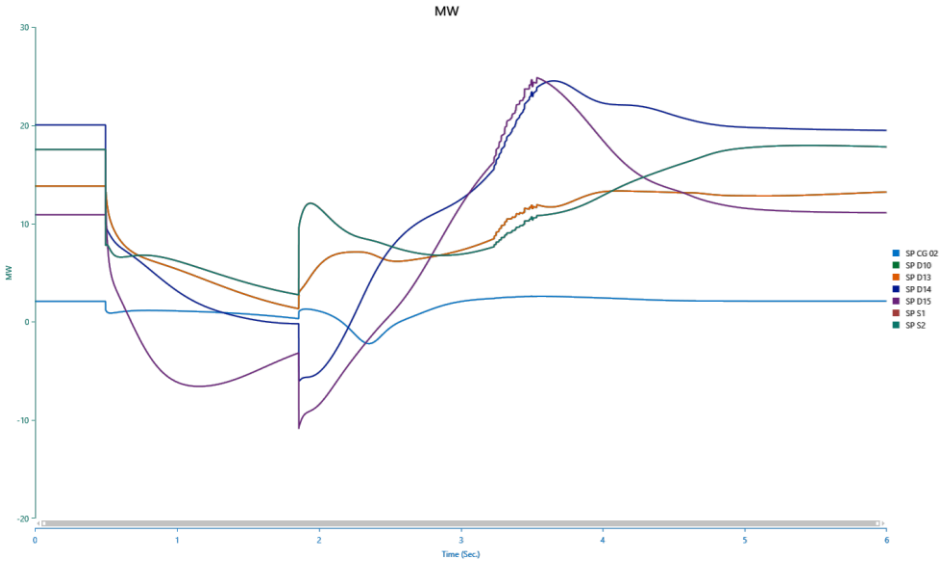

Figure 5-1: Effect on generation when fault occurred between Belmont and Marhill Street

Effect on Bus Voltage

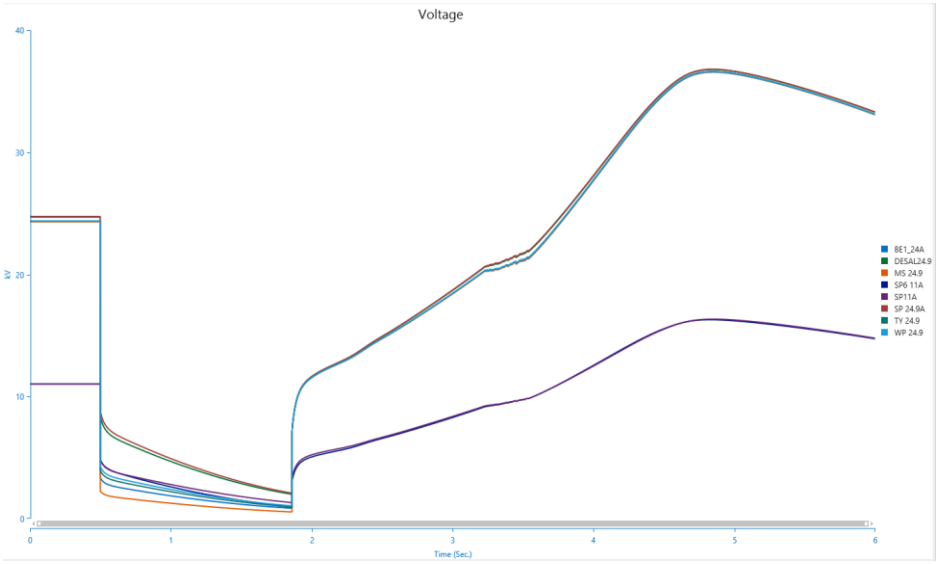

Figure 5-2: Effect on voltage at nearby buses when fault occurred between Belmont and Marhill Street

The local voltage falls below rated voltage for more than 3 seconds which would be more than enough to run down the generator auxiliary equipment. Additionally, the under-voltage protection of the generator itself would cause the generators to trip, normally after a time delay.

Effect on Bus Frequency

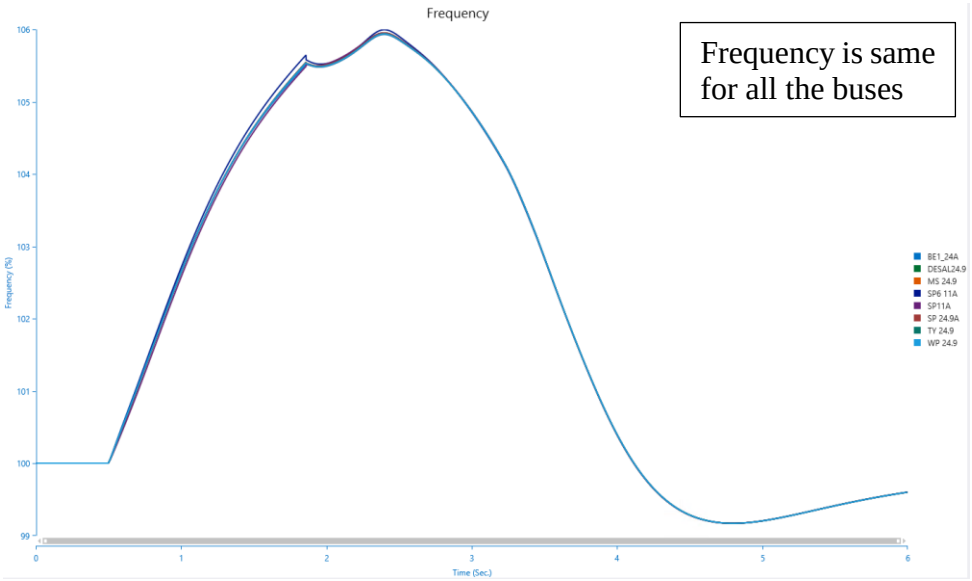

Figure 5-3: Effect on frequency at nearby buses when fault occurred between Belmont and Marhill Street

The above simulation assumed that all generators remained in service., but the historical record shows otherwise. The simulation was run again except Generator Group 1 tripped at 1.027 seconds, Generator Group 2 tripped at 1.796 seconds, and the fault was cleared at 1.862 seconds. The cascading effect for Case 1 including tripping of generators can be observed in results shown in Appendix C, page 117-118.

5.5 Approach to avoid cascading

To avoid cascading effects and a complete blackout of the entire BLPC system, it seems necessary to develop a special protection system triggered by circumstances arising from

a fault event in order to initiate formation of a Northern Microgrid, and potentially also retain the Southern Microgrid in service. While the operating rules have not yet been fully developed, the elements of the special protection system should be developed around fundamental principles.

- Generator tripping is a crisp, identifiable event. It can be used for timing purposes. If any four generators tripped in a time span of 1 second, then cascading is likely. Formation of the Northern Microgrid should be initiated.
- If the fault is not removed by distance relaying Zone 1 protection, then the consequent time delays associated with Zone 2 and Zone 3 relaying would be long resulting in cascading trips.
- If after a fault on a transmission line a Zone 2 or Zone 3 or Timed Directional Over Current relay operates, this would also be cause for formation of a Northern Microgrid.
- Attempt to identify the existence of a fault anywhere on the system by voltage measurement at one single location/bus (which may not be possible).
- Alternatively, identify the initial existence of the fault using measurements of voltage at three selected locations.

CHAPTER 6

6. RELATING ANGULAR AND VOLTAGE STABILITY

Chapter 2 introduced the idea of trying to relate angular stability and voltage stability. There is no one quantity which will fully represent angular stability, and there is no one quantity which will fully represent voltage stability. This thesis choses to use steady state stability limit B as an indication of angular strength. It also represent voltage strength at a bus as the reactive power injection required to maintain specified voltage conditions for a given value of load. A Q-B characteristics based on the derived equation relating reactive power required as a function of steady state stability limit B is presented in Appendix D, page 119-121.

6.1 Relating angular and voltage stability for BLPC

It is desired to investigate the Q-B relationship using data from the operating BLPC power system. Since the calculation of B requires knowledge of equivalent system reactance, it is necessary to determine the Thevenin equivalent reactance at each bus in the BLPC system.

6.1.1 Plotting Q-B based on BLPC data

Based on a transmission model of a Thevenin reactance at each bus from Table 4-1, the Q-B plots for all buses on the BLPC system have been calculated. To see the impact of system voltage, the plots have been done for three voltage conditions.

For Figure 6-1, assuming E=1 p.u. and V=0.926 p.u. so that K = 1.08

For Figure 6-2, assuming E=1.0 p.u. and V=1.0 p.u. so that K = 1.00,

For Figure 6-3, assuming E=1.0 p.u. and V=1.087 p.u. so that K = 0.92

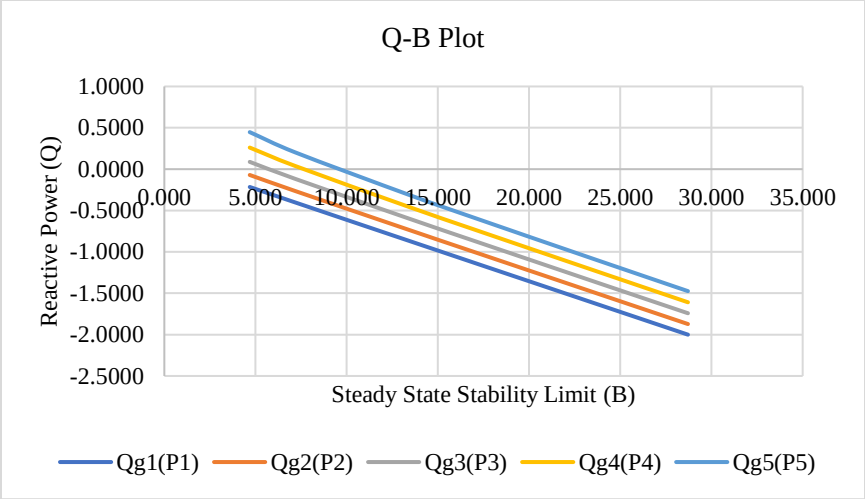

Figure 6-1: QB plot for BLPC buses when supply voltage is 1.08 time the receiving voltage

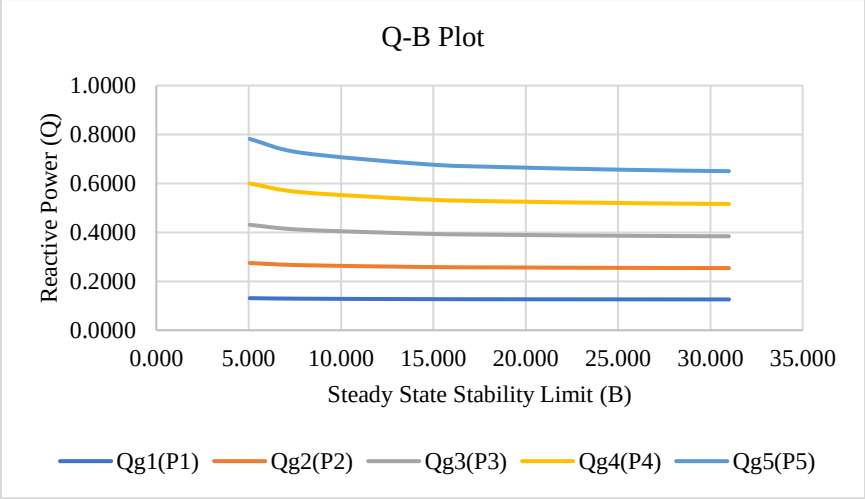

Figure 6-2: QB plot for BLPC buses when supply voltage is equal to receiving voltage

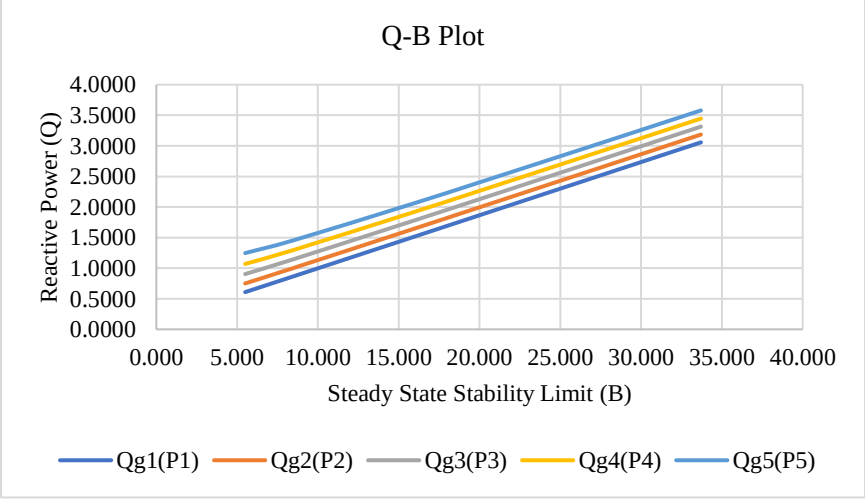

Figure 6-3: QB plot for BLPC buses when supply voltage is 0.92 time the receiving voltage

6.2 Simulating Q-B in actual BLPC system

The next step is to see the behaviour of Q-B plots while retaining the full BLPC power system model rather than representing it by a Thevenin reactance. The 24.9 kV buses selected are North, Old Works, Seawell, Warren, Temple Yard and Central, which means that there are two buses from each of the weak, moderate, and strong bus categories. The fictious generator is moved from load bus to load bus. Fixing the supply voltage to 0.98 p.u. for all generator buses (which represents Eth in the equivalent model), the terminal voltage (V) at each of the load buses is obtained from the load flow data.

Table 6-1: Data representing BLPC buses when supply voltage is 0.98 pu

Buses 24.9 kV	K	Initial Opt. V	Initial Load (MVA)	B
North	1.054	93.01%	7.061	4.958
Old Works	1.055	92.88%	6.350	7.602
Seawell	1.060	92.42%	8.470	14.168
Warrens	1.027	95.47%	11.386	18.167
Temple Yard	1.078	94.58%	11.822	22.460
Central	1.043	93.96%	5.533	25.107

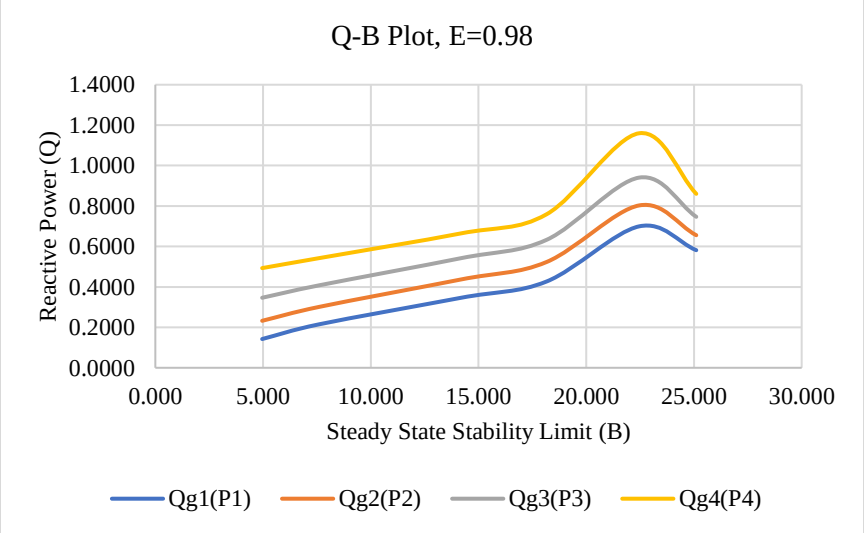

Figure 6-4: QB plot from simulating BLPC buses when supply voltage is 0.98 pu

Fixing the supply voltage (Eth) to 1.0 p.u. for all generator buses, the terminal voltage (V) is obtained from the load flow data.

Table 6-2: Data representing BLPC buses when supply voltage is 1.0 pu

Buses 24.9 kV	K	Initial Opt. V	Initial Load (MVA)	B
North	1.050	95.22%	7.061	5.059
Old Works	1.051	95.16%	6.350	7.757
Seawell	1.056	94.69%	8.470	14.457
Warrens	1.025	97.59%	11.386	18.538
Temple Yard	1.054	96.74%	11.822	22.919
Central	1.040	96.16%	5.533	25.620

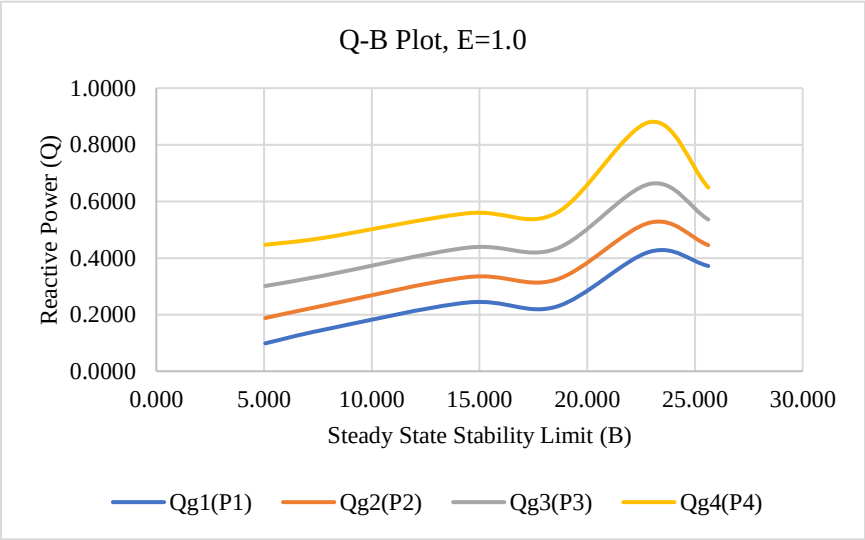

Figure 6-5: QB plot from simulating BLPC buses when supply voltage is 1.0 pu

Fixing the supply voltage (Eth) to 1.02 p.u. for all generator buses, the terminal voltage (V) is obtained from the load flow data.

Table 6-3: Data representing BLPC buses when supply voltage is 1.02 pu

Buses 24.9 kV	K	Initial Opt. V	Initial Load (MVA)	B
North	1.047	97.43%	7.061	5.160
Old Works	1.047	97.42%	6.350	7.912
Seawell	1.052	96.94%	8.470	14.746
Warrens	1.023	99.70%	11.386	18.909
Temple Yard	1.031	98.89%	11.822	23.377
Central	1.037	98.35%	5.533	26.132

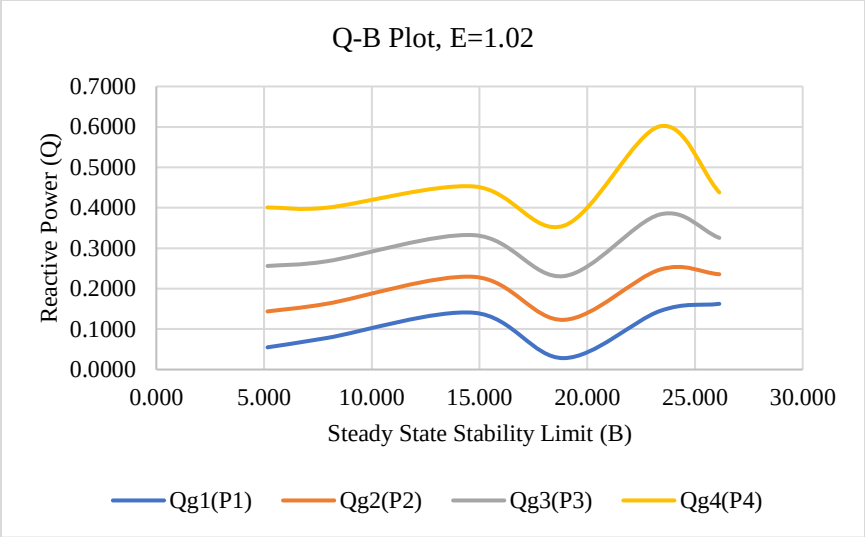

Figure 6-6: QB plot from simulating BLPC buses when supply voltage is 1.02 pu

6.3 Conclusion of the results

The Q-B plots from the simulation results for the operating BLPC power system generally follow the pattern for the Thevenin reactance, or ideal, model. There are two reasons for any variations. First, the load flow results show that each of the six selected buses has different values of initial bus voltages, which is quite normal. This means that each bus has a different value of K = E/V. In contrast, in the ideal case it was possible to assure a consistent value of K at all buses. Second, the results are quite configuration dependent. As an example, a bus might have a small value of Thevenin reactance. Nevertheless, that small value of Thevenin reactance could involve a bus with several strong transmission lines coming to it, but also one weak line in a parallel configuration. If there is a generator on the relatively weak transmission line coming to the selected bus, that local area generator may need MVAR support. In this case the reactive power for a certain steady state stability limit value may increase significantly.

CHAPTER 7

7. CONCLUSION AND RECOMMENDATION

The results of this research work provide technical background as the basis for any decision on the separation of the BLPC system into a northern microgrid and a southern microgrid. The BLPC power system has a natural separation point by opening the transmission lines connecting the Saint Thomas bus to the Spring Garden station and the Central substation.

7.1 Determining System Stability

There are numerous methodologies to determine in advance whether the system will be stable or not. Some of the methodologies applied in this research work are as follows.

- If the energy function faulted trajectory $V_{(\delta,\omega)}$ is less than critical energy V_{cr} with fault clearing at $t = t_{clr}$, then the system is stable.
- Voltage magnitude at a bus should increase with an increase of reactive power injection. If it is decreasing with an increase in reactive power, then the system is unstable.
- The part of Q-V curve to the right of the critical point represents a stable operating condition and to the left represents an unstable operating condition.

7.2 Angular Stability approach

The following conclusion were observed from the angular stability approach:

- Because of the distinct configuration of the BLPC power system, with a group of generators in the south and a group of generators in the north, and with a natural

separation point in between, the Centre of Angle (COA) concept was a natural one to apply in the circumstances.

- The Centre of Angle Stability Index (CASI) was applied between the two groups of generators.
- Based on a comprehensive set of possible fault conditions, it was not possible to obtain a value of CASI which would indicate that the two systems should be separated based on angular conditions. After the fact, it is possible to suggest such a result since the BLPC system has quite small distance between buses, a small size, and low voltage transmission.
- Because it was not possible to attain separation instability based on angular separation, it has not possible to set a threshold value of CASI for the BLPC system.

7.3 Electrical strength calculation

For each load bus on the BLPC system, a short circuit analysis was done to determine the Thevenin equivalent reactance which is an indication of the electrical strength of that bus. It was observed that the X/R ratio of all the buses lies in a range of 2.147 to 9.102 with an average of 4.22. The order of all the buses in terms of electrical strength from the weakest to the strongest is as follows:

North, Trent, Carlton, St. Thomas, Old Works, Banks, Hampton, Wotton, Seawell, Wildey, Garrison, Warrens, Marhill Street, Regency Park, Whitepark, Temple Yard, Belmont, Central, Desalination, Spring Garden

7.4 Analysis from Q-V curves

The electrical strength for a load bus is significant in determining some of the indices in voltage bus vector.

- The reactive power reserve margin for a load bus is directly proportional to the electrical strength of that bus.
- Reactive power required to maintain rated voltage is related to the electrical strength of the bus.
- The slope of the Q-V curve ($\Delta Q/\Delta V$) also depict a proportional relation with strength of bus.
- Given the cost in $/kVAR of static capacitors used to correct bus voltages, the slope of Q-V curve determines the relative expensiveness of correcting the voltage at that bus.

7.5 Relating Voltage and Angular stability

The derivation of the relationship between voltage and angular stability i.e., steady state stability limit (B) and reactive power injection (Q) at a bus, yields some interesting results for an ideal transmission line.

- For a system with higher supply voltage (E) compared to the receiving end voltage (V), the reactive power support to maintain a voltage at a load bus decreases as the transmission gets stronger i.e., increasing steady state stability limit.
- For a system with equal supply voltage (E) compared to the receiving end voltage (V), the reactive power support to maintain a voltage at a load bus is independent of the steady state stability limit.
- For a system with lower supply voltage (E) compared to the receiving end voltage (V), the reactive power support to maintain a voltage at a load bus increases as the transmission get stronger i.e., increasing steady state stability limit.

7.6 Future Work and Recommendation

The research work of this thesis is comprehensive, by intention. In terms of application, one of the first things that must be done is to sift through all the results and identify those aspects of the BLPC system operation which are dominant in any decision on separation into microgrids.

A second area for future work is a critical examination of the operating status of the present power system. This is written specifically in the context of protective relays, because one or more of the island-wide blackouts seems to have occurred because of improper settings or improper operation of protective relays.

Third, ultimately it will be necessary to formulate an algorithm which will make the decision to separate into a northern and a southern microgrid.

7.7 Summary of Contributions

1. During a major disturbance, the separation of a power system into two microgrids is based on the premise that power system reliability is increased if at least part of the customer base can continue to be served rather that suffering a system-wide blackout.
2. A stability index, called the Centre of Angle Stability Index (CASI), has been introduced. The CASI was applied to the BLPC system as a measure to decide if separation into a northern microgrid and a southern microgrid should take place.
3. Analysis and system studies have shown that the BLPC power system has a high level of angular stability. Because of this fact, the thesis shows that it has not been possible to determine a CASI threshold numerical value for a decision to separate into microgrids.

4. The QV method has been used to study voltage stability on a power system. The thesis defines six elements, or indices, of a bus quality vector for each load bus in the power system. The thesis shows most of the indices from the QV analysis depend heavily on the electrical strength of a bus as represented by its Thevenin impedance. This can be used as a major element in deciding on locations for phase measurements units (PMUs) and in the structuring of the separation algorithm itself.
5. A historical record exists of previous island-wide blackouts. An analysis of the blackout events gives a clear picture of generators being removed from service before the fault is cleared from the system. There are strong indications of cascading effects often arising from improper operation of protection relays and the fact of a common point for voltage supply to generator auxiliaries.
6. The thesis makes a unique contribution to the technical literature by proposing and developing the relationship between angular stability and voltage stability in a power system.

LIST OF REFERENCES

[1] Madden Marlon, “Dirty Fuel, Aging Generators Blamed For 13-Hour Blackout”, Barbados Today, November 19, 2019, Page 3, 4 & 5, https://barbadostoday.bb/2019/11/19/dirty-fuel-aging-generators-blamed-for-13-hour-blackout/

[2] K. Sun, K. Hur and P. Zhang, "A New Unified Scheme for Controlled Power System Separation Using Synchronized Phasor Measurements," 2012 IEEE Power and Energy Society General Meeting, 2012, pp. 1-6, doi: 10.1109/PESGM.2012.6345167.

[3] M. Amini, H. Samet, A. R. Seifi and M. Davarpanah, "An Effective Controlled Islanding Method for Power Grid Through a Sequence of Optimization Problems," in CSEE Journal of Power and Energy Systems, doi: 10.17775/CSEEJPES.2020.01010.

[4] M. Amini, H. Samet, A. R. Seifi, M. Al-Dhaifallah and Z. M. Ali, "An Effective Multi-Solution Approach for Power System Islanding," in IEEE Access, vol. 8, pp. 93200-93210, 2020, doi: 10.1109/ACCESS.2020.2995085.

[5] M. Zhang and J. Chen, "Islanding and Scheduling of Power Distribution Systems with Distributed Generation," in IEEE Transactions on Power Systems, vol. 30, no. 6, pp. 3120-3129, Nov. 2015, doi: 10.1109/TPWRS.2014.2382564.

[6] J. Wu, J. Wen, H. Sun, and S. Cheng, “Feasibility Study of Segmenting Large Power System Interconnections with AC Link Using Energy Storage Technology,” IEEE Trans. Power Syst., vol. 27, no. 3, pp. 1245–1252, Aug. 2012.

[7] S. I. Vagropoulos and A. G. Bakirtzis, "Optimal Bidding Strategy for Electric Vehicle Aggregators in Electricity Markets," in IEEE Transactions on Power Systems, vol. 28, no. 4, pp. 4031-4041, Nov. 2013, doi: 10.1109/TPWRS.2013.2274673

[8] J. J. Grainger and W. D. Stevenson, Power System Analysis. McGraw-Hill, 1994

[9] P. Kundur, N. J. Balu, and M. G. Lauby, Power System Stability and Control. McGraw-hill New York, 1994

[10] Lu Fang and Yu Ji-lai, "Transient Stability Analysis with Equal Area Criterion Directly Used to a Non-Equivalent Generator Pair," 2009 International Conference on Power Engineering, Energy and Electrical Drives, 2009, pp. 386-389, doi: 10.1109/POWERENG.2009.4915162.

[11] Prem Kumar, Dale Fredrickson, Koushik Chanda," Stability Studies for System Dependent Generator Protection Functions", INFRASTRUCTURE MINING & METALS NUCLEAR, SECURITY & ENVIRONMENTAL OIL, GAS & CHEMICALS, 2011

[12] J.J. Dai, Richard Dourian, "Standard Approach to Perform Power System Stability Studies in Oil and Gas Plants," PCIC Europe, Paper No. PCIC EUR19_04

[13] Lin Teng, Wanshun Liu, Wei Yang, Tao Zheng, Zhiliang Yin and Tao Zhang, "Study on Power System Separation Based on the Local Electrical Quantities," Proceedings. International Conference on Power System Technology, 2002, pp. 349-354 vol.1, doi: 10.1109/ICPST.2002.1053564.

[14] V. Centeno, J. de la Ree, A. G. Phadke, G. Michel, R. J. Murphy and R. O. Burnett, "Adaptive Out-Of-Step Relaying Using Phasor Measurement Techniques," in IEEE Computer Applications in Power, vol. 6, no. 4, pp. 12-17, Oct. 1993, doi: 10.1109/67.238199.

[15] Y. Ohura et al., "A Predictive Out-Of-Step Protection System Based on Observation of the Phase Difference Between Substations," in IEEE Transactions on Power Delivery, vol. 5, no. 4, pp. 1695-1704, Oct. 1990, doi: 10.1109/61.103664

[16] T. J. Overbye and C. L. DeMarco, "Improved Techniques for Power System Voltage Stability Assessment Using Energy Methods," in IEEE Transactions on Power Systems, vol. 6, no. 4, pp. 1446-1452, Nov. 1991, doi: 10.1109/59.116988

[17] T. J. Overbye, M. A. Pai and P. W. Sauer, "Some Aspects of the Energy Function Approach to Angle and Voltage Stability Analysis in Power Systems," [1992] Proceedings of the 31st IEEE Conference on Decision and Control, 1992, pp. 2941-2946 vol.3, doi: 10.1109/CDC.1992.371273.

[18] T. Athay, R. Podmore and S. Virmani, "A Practical Method for the Direct Analysis of Transient Stability," in IEEE Transactions on Power Apparatus and Systems, vol. PAS-98, no. 2, pp. 573-584, March 1979, doi: 10.1109/TPAS.1979.319407.

[19] C. J. Tavora and O. J. M. Smith, "Stability Analysis of Power Systems," in IEEE Transactions on Power Apparatus and Systems, vol. PAS-91, no. 3, pp. 1138-1144, May 1972, doi: 10.1109/TPAS.1972.293470.

[20] M. A. Pai, “Energy Function Analysis for Power System Stability”, Kluwer Academic Publishers, Chapter 1, pp. 1-19, 1989

[21] M. Rahmatian, W. G. Dunford and A. Moshref, "PMU Based System Protection Scheme," 2014 IEEE Electrical Power and Energy Conference, 2014, pp. 35-40, doi: 10.1109/EPEC.2014.47.

[22] G. Joos, B. T. Ooi, D. McGillis, F. D. Galiana and R. Marceau, "The Potential of Distributed Generation to Provide Ancillary Services," 2000 Power Engineering Society Summer Meeting (Cat. No.00CH37134), 2000, pp. 1762-1767 vol. 3, doi: 10.1109/PESS.2000.868792.

[23] M. Triggianese, J. Morren, S. W. H. de Haan and P. Marino, "Improved and Extended DG Capability in Voltage Regulation by Reactive and Active Power," 2007 International Conference on Power Engineering, Energy and Electrical Drives, 2007, pp. 583-588, doi: 10.1109/POWERENG.2007.4380207.

[24] K. M. Rogers, R. Klump, H. Khurana, A. A. Aquino-Lugo and T. J. Overbye, "An Authenticated Control Framework for Distributed Voltage Support on the Smart Grid," in IEEE Transactions on Smart Grid, vol. 1, no. 1, pp. 40-47, June 2010, doi: 10.1109/TSG.2010.2044816.

[25] T. J. Overbye, I. Dobson and C. L. DeMarco, "Q-V Curve Interpretations of Energy Measures for Voltage Security," in IEEE Transactions on Power Systems, vol. 9, no. 1, pp. 331-340, Feb. 1994, doi: 10.1109/59.317593.

[26] P. Guimarães, U. Fernandez, T. Ocariz, F. W. Mohn and A. C. Z. de Souza, "QV and PV Curves as a Planning Tool of Analysis," 2011 4th International Conference on Electric Utility Deregulation and Restructuring and Power Technologies (DRPT), 2011, pp. 1601-1606, doi: 10.1109/DRPT.2011.5994153.

[27] S. Chakrabarti,” Notes on Power System Voltage Stability” Dept. of EE, IIT, Kanpur

[28] C. W. Taylor, Power System Voltage Stability, McGraw-Hill, 1994

[29] R. K. Gupta, Z. A. Alaywan, R. B. Stuart and T. A. Reece, "Steady State Voltage Instability Operations Perspective," in IEEE Transactions on Power Systems, vol. 5, no. 4, pp. 1345-1354, Nov. 1990, doi: 10.1109/59.99386.

[30] H. Kirkham and R. Das, "Effects of Voltage Control in Utility Interactive Dispersed Storage and Generation Systems," in IEEE Transactions on Power Apparatus and Systems, vol. PAS-103, no. 8, pp. 2277-2282, Aug. 1984, doi: 10.1109/TPAS.1984.318543.

[31] Yunhwan Lee and Sangwook Han, “ Real-Time Voltage Stability Assessment Method for the Korean Power System Based on Estimation of Thévenin Equivalent Impedance”, April 2019 MDPI Applied Science

[32] “Present Industry Practices with Cascading Outages," 2015 IEEE Power & Energy Society General Meeting, 2015, pp. 1-17, doi: 10.1109/PESGM.2015.7286023.

[33] R. Baldick et al., "Vulnerability Assessment for Cascading Failures in Electric Power Systems," 2009 IEEE/PES Power Systems Conference and Exposition, 2009, pp. 1-9, doi: 10.1109/PSCE.2009.4839939

[34] Xiaokang Xu, M. F. Kandlawala and Ming Wu, "NERC TPL-001-4 Transient Voltage Performance Compliance Study - Criteria Development, Study Methodology and Case Studies," 2016 IEEE Power and Energy Society General Meeting (PESGM), 2016, pp. 1-5, doi: 10.1109/PESGM.2016.7741072.

[35] Y. Zhu and D. Brown, "Expanding Transmission Planning Capabilities for NERC Standard TPL-001-2 Compliance," 2013 IEEE Power & Energy Society General Meeting, 2013, pp. 1-5, doi: 10.1109/PESMG.2013.6672385.

[36] J. Li, K. Yamashita, C. C. Liu, P. Zhang and M. Hofmann, “Identification of Cascaded Generator Over-Excitation Tripping Events,” 16th Power Systems Computation Conference 2008, Glasgow, Scotland.

[37] C. C. Liu, et al., Learning to Recognize the Vulnerable Patterns of Cascaded Events, EPRI Technical Report, 2007.

[38] N. Bhatt et al., "Assessing Vulnerability to Cascading Outages," 2009 IEEE/PES Power Systems Conference and Exposition, 2009, pp. 1-9, doi: 10.1109/PSCE.2009.4840032.

[39] U.S. Congress, Office of Technology Assessment, Physical Vulnerability of Electric Systems to Natural Disasters and Sabotage, June 1990. OTAE- 453, Washington D.C., June 1990

[40] IEEE Standard for Synchrophasor Measurements for Power Systems. In IEEE Std C37.118.1-2011 (Revision of IEEE Std C37.118-2005); IEEE: Piscataway, NJ, USA, 2011; pp. 1–61

[41] IEEE Standard for Synchrophasor Measurements for Power Systems—Amendment 1: Modification of Selected Performance Requirements. In IEEE Std C37.118.1a-2014 (Amendment to IEEE Std C37.118.1-2011); IEEE: Piscataway, NJ, USA, 2014; pp. 1–25

[42] North American Electric Reliability Corporation, “Phase Angle Monitoring”. Industry Experience Following the 2011 Pacific Southwest Outage Recommendation 27, Technical reference document, June 2016.

[43] Bose, A. Smart transmission grid applications and their supporting infrastructure. IEEE Trans. Smart Grid 2010, 1, 11–19

[44] A. Chandra, A. K. Pradhan and A. K. Sinha, "A Comparative Study of Voltage Stability Indices Used for Power System Operation," 2016 21st Century Energy Needs - Materials, Systems and Applications (ICTFCEN), 2016, pp. 1-4, doi: 10.1109/ICTFCEN.2016.8052703.

[45] F. A. Althowibi, M. W. Mustafa “Power System Voltage Stability: Indications, Allocations and Voltage Collapse Prediction” International Journal of Advanced Research in Electrical, Electronics and Instrumentation Engineering, Vol.2, Issue 7, July 2013, PP 3138-3152.

[46] S. Massucco, M. S. Grillo, A. Pitto and F. Silvestro “Evaluation of Some Indices for Voltage Stability Assessment” IEEE Bucharest Power Tech. Conference, June 28-July 2nd, Bucharest, Romania,2009, PP 1-8.

[47] F. Karbalaei, H. Soleymani and S. Afsharnia, “A Comparison of Voltage Collapse Proximity Indicators”, IPEC 2010 Conference Proceedings, 27-29 Oct. 2010, pp. 429-432

[48] S. K. N. Kumar and P. Renuga "FVSI Based Reactive Power Planning Using Evolutionary Programming" ICCCCT-10, 2010, PP 265-269.

[49] A.A. Fouad, Vijay Vittal, “Power System Transient Stability Analysis using the transient energy function method”, Department of Electrical Engineering, Iowa State University

[50] P.M. Anderson, A.A. Fouad, “Power System control and Stability”, A John Wiley & Sons, Inc., Publication, IEEE Power Engineering Society, Sponsor, Second Edition, 2003

[51] A. Michel, A. Fouad and V. Vittal, "Power system transient stability using individual machine energy functions," in IEEE Transactions on Circuits and Systems, vol. 30, no. 5, pp. 266-276, May 1983, doi: 10.1109/TCS.1983.1085360.

[52] Haes Alhelou, Hassan, Mohamad E. Hamedani-Golshan, Takawira C. Njenda, and Pierluigi Siano. 2019. "A Survey on Power System Blackout and Cascading Events: Research Motivations and Challenges" Energies 12, no. 4: 682.

[53] Peter W. Sauer, M.A. Pai, “Power System Dynamics and Stability”, Prentice Hall, Department of Electrical and Computer Engineering, University of Illinois at Urbana-Champaign, 1998.

[54] Noor Izzri Abdul Wahab, Azah Mohamed, "Area-Based COI-Referred Rotor Angle Index for Transient Stability Assessment and Control of Power Systems", Abstract and Applied Analysis, vol. 2012, Article ID 410461, 23 pages, 2012.

[55] Thierry Van Cutsem, Costas Vournas, “Voltage Stability of Electric Power System”, Springer US, 2008

[56] Atefeh Palizban, “Wide-Area Monitoring and Control Utilizing PMU Measurements for a System Protection Scheme”, Thesis for Master of Applied Science, Electrical and Computer Engineering, The University of British Columbia, 2015

[57] T. Aziz, T. K. Saha and N. Mithulananthan, "Distributed Generators Placement for Loadability Enhancement Based on Reactive Power Margin," 2010 Conference Proceedings IPEC, 2010, pp. 740-745, doi: 10.1109/IPECON.2010.5697023.

[58] Opiyo, Nicholas. (2018),” Droop Control Methods for PV-Based Mini Grids with Different Line Resistances and Impedances. Smart Grid and Renewable Energy”. 09. 101-112. 10.4236/sgre.2018.96007.

[59] B.M. Weedy, B.J. Cory, N. Jenkins, J.B. Ekanayake, G. Strbac, “Electric Power System”, Wiley, Fifth Edition, 2012

APPENDIX A

Simulating single machine infinite bus

For a system with fault clearing time (t_{clr}) equal the critical clearing time (t_{cct}) the plots below represent the trajectory for the region of attraction for a machine with different values of machine damping.

Case 1 - Region of attraction for $t_{clr} = t_{cct}$ when there is no damping in the machine

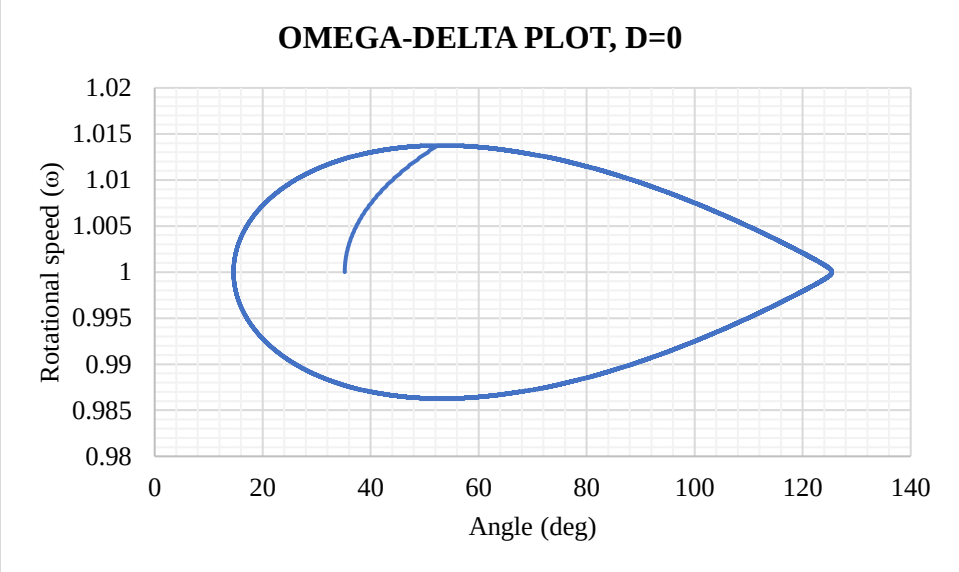

Machine swinging on a fault without damping

Case 2 - Region of attraction for $t_{clr} = t_{cct}$ when there is damping is added in the machine

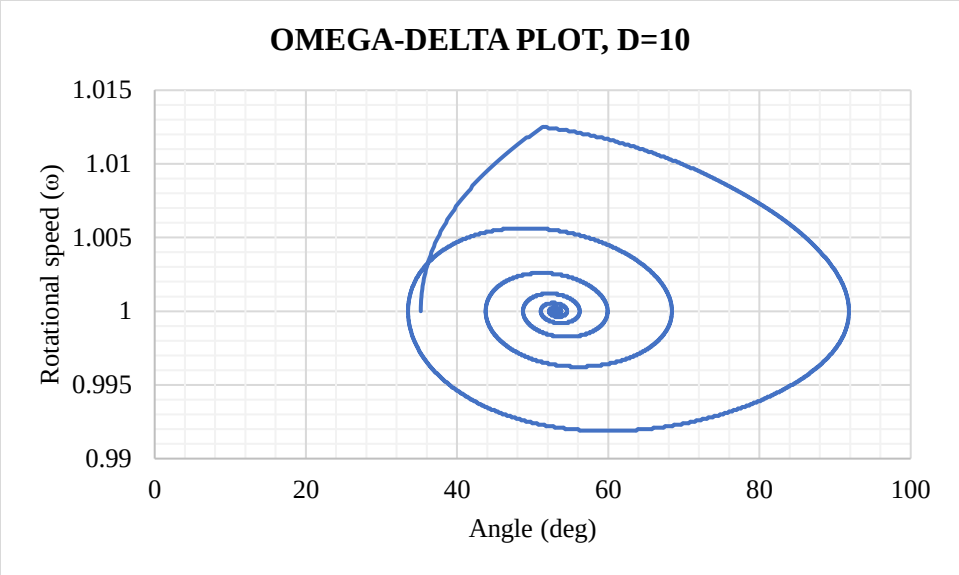

Machine swinging on a fault when damping is added

Simulating the Energy Function

The data from omega (angular velocity) and delta (rotor angle) have been extracted and used to see the energy function characteristics of the stable and unstable system.

The total energy of a system of the above model has been calculated from:

$$V_{(\delta,\omega)} = \frac{1}{2}M\omega^2 - P_m(\delta - \delta^s) - P_e\, max(\cos\delta - \cos\delta^s)$$

Where,

ω is not the actual rotational velocity but is the deviation in speed from pre-fault rotational speed.

P_m is the mechanical power input and $P_e max$ is the maximum electrical output of the system.

δ changes throughout the simulation time when a system is subjected to a disturbance and is dependent on power flow equation of pre fault, fault, post fault conditions as well as the fault clearing time.

δ^s is the angle at the stable equilibrium condition calculated from $\delta_s = \sin^{-1}\frac{P_m}{P_e max}$.

Critical energy V_{cr} is the potential energy calculated using the results of simulation and represented as:

$$V_{cr} = -P_m(\delta^{\mu} - \delta^{s}) - P_e\, max(\cos\delta^{\mu} - \cos\delta^{s})$$

This gives the boundary limit for system stability or region of attraction in the energy function. V_{cr} is obtained by setting $\omega = 0$ and $\delta = \delta^{u}$ in $V_{(\delta,\omega)}$ where δ^{u} is the unstable equilibrium point as suggested in section 2.6.2 energy function.

Initially, the value of fault clearing time is set at 0.310 s and gradually increased in steps of 0.001 s to obtain $V_{(\delta,\omega)} = V_{cr}$ on the faulted trajectory. Hence, the critical clearing time (t_{cct}) of closest match has been obtained as 0.315 s.

Case 1: When fault clearing time is less than critical clearing time $t_{clr} < t_{cct}$

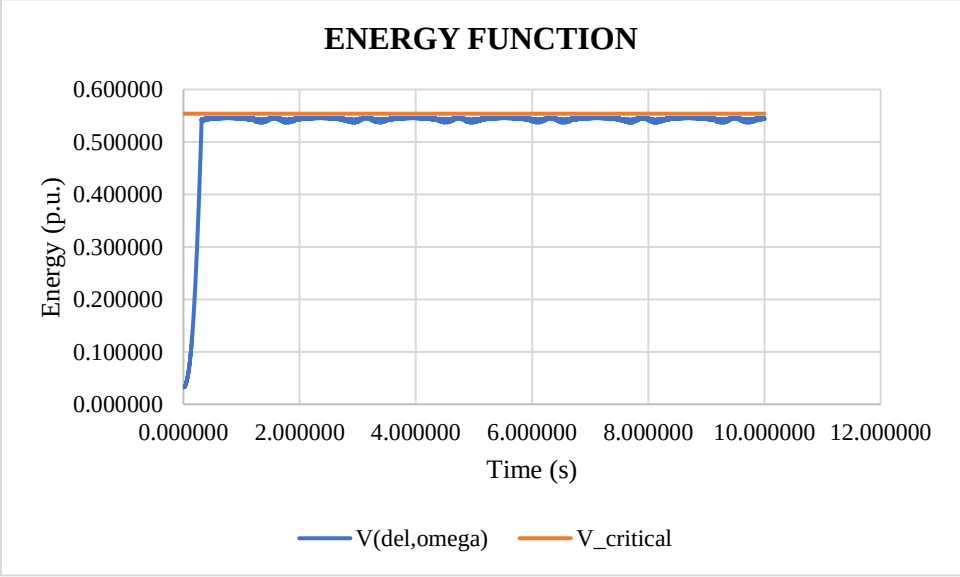

Energy function for fault clearing before critical clearing time

Above figure represent the plots where fault is cleared before critical clearing time. The horizontal line represents critical energy of system equal to 0.55393 and the energy function curve represents the trajectory of a faulted system during fault and post fault conditions. It can be seen that for fault clearing below the critical clearing time, the energy

function never exceeds the critical energy and thus proves the theory of region of attraction. This also satisfies the inequality of the type $V_{(\delta,\omega)} < V_{cr}$ so the system is stable.

Case 2: When fault clearing time is greater than critical clearing time $t_{clr} > t_{cct}$

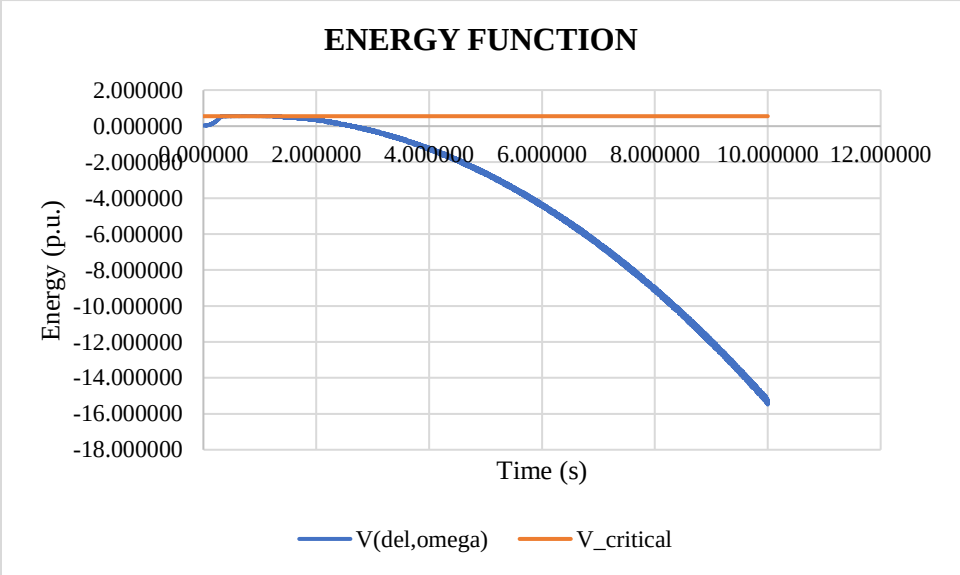

Energy function for fault clearing after critical clearing time

The above figure**Error! Reference source not found.** shows that when the fault clearing t ime is more than the critical clearing time, it crosses the critical energy boundary limit and becomes unstable.

Summary of Simulation Run

The summary of the simulation at different fault clearing time starting from 0.305s to 0.325s is shown in the table below**Error! Reference source not found.**.

Pm	1	pu
Pe max	1.5	pu
H	5	
Pre fault	2.1	
Fault	0.808	
Post fault	1.5	
Critical Clearing Time	0.315	s
dels	41.81	degree
dels	0.729722	rad
delu	2.41187	rad

delu 138.19 degree

Simulation result for different fault clearing time

t_{cl}	Angle at clearing	Speed at clearing	V(δ,ω) at clearing	t_{Max} Angle	Max angle	Speed at Max angle	V(δ,ω) at Max angle	V_{CR}	State
0.305	79.492	1.0132	0.51189	0.656	123.037	1.0	0.51813	0.55393	Stable
0.307	80.063	1.0132	0.51663	0.672	124.620	1.0	0.52493	0.55393	Stable
0.309	80.63	1.0133	0.52636	0.693	126.391	1.0	0.53176	0.55393	Stable
0.311	81.209	1.0133	0.53118	0.721	128.447	1.0	0.53862	0.55393	Stable
0.313	81.785	1.0134	0.54102	0.77	131.023	1.0	0.54522	0.55393	Stable
0.315	82.363	1.0134	0.54592	0.901	135.214	1.0	0.55245	0.55393	Stable
0.317	82.942	1.0134	0.55085	0.799	138.195	1.0017	0.55913	0.55393	Unstable
0.319	83.524	1.0135	0.56083	0.734	138.206	1.0026	0.56610	0.55393	Unstable
0.321	84.106	1.0135	0.56583	0.699	138.246	1.0032	0.57236	0.55393	Unstable
0.323	84.691	1.0135	0.57086	0.674	138.217	1.0037	0.57857	0.55393	Unstable
0.325	85.277	1.0136	0.58097	0.655	138.195	1.0042	0.58568	0.55393	Unstable

Implementing CoA and CASI in the IEEE 9-Bus system

The CoA was implemented as a test case on an interconnected power system by taking the IEEE 9-Bus and duplicating the same model but with some changes in loads and generators. A tie line was placed in between so that there was power flow.

The duplicated model is created having following changes in one of the systems:

1. The size of all three generators reduced by 20% of their MW capacity keeping the power factor fixed.
2. Load at all three buses is increased by 10% of its MW capacity keeping its power factor fixed.

A transient event was introduced by causing an increase in load at the duplicated IEEE 9-Bus system of about 50 MW.

The changes observed on centre of angle calculation is as follow:

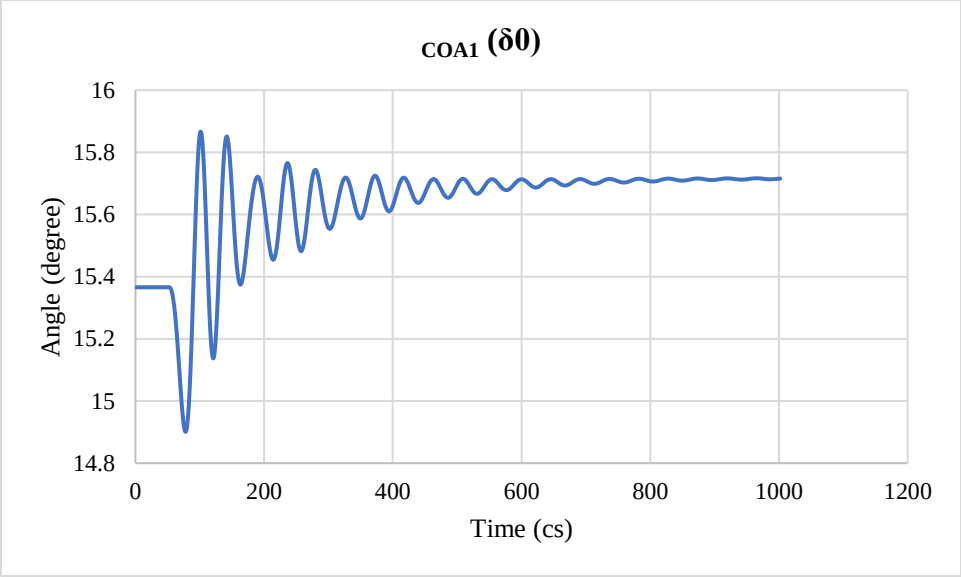

Centre of angle for Network 1

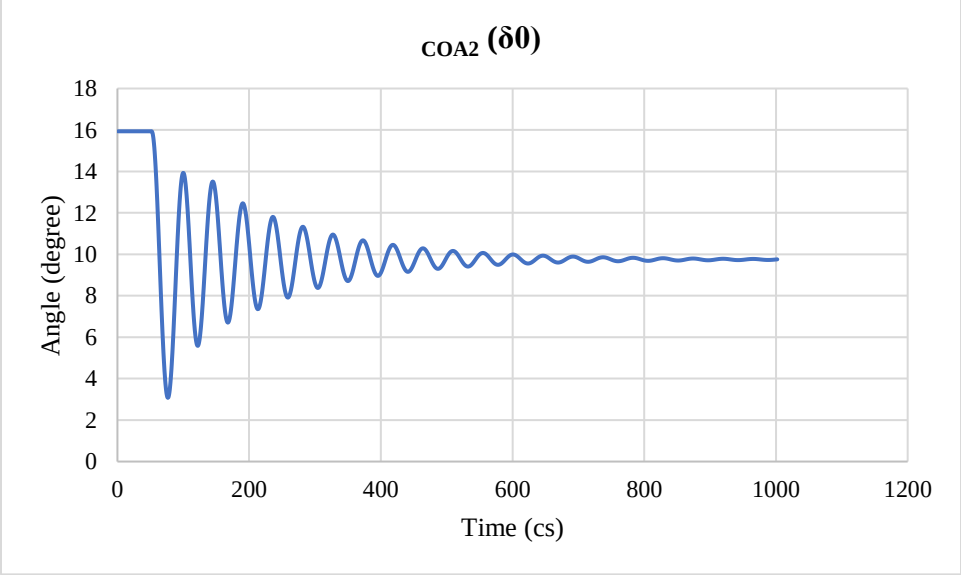

Centre of angle for Network 2

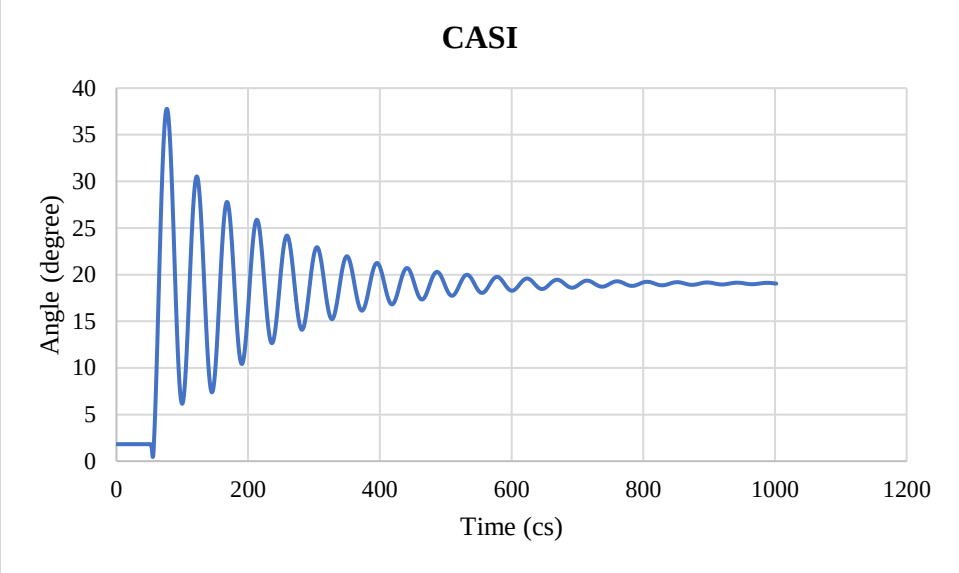

Centre of Angle Stability Index for combined network

For the flow of power from one power system to another, we observed the net difference of mechanical power of network 1 with network 2 is observed as:

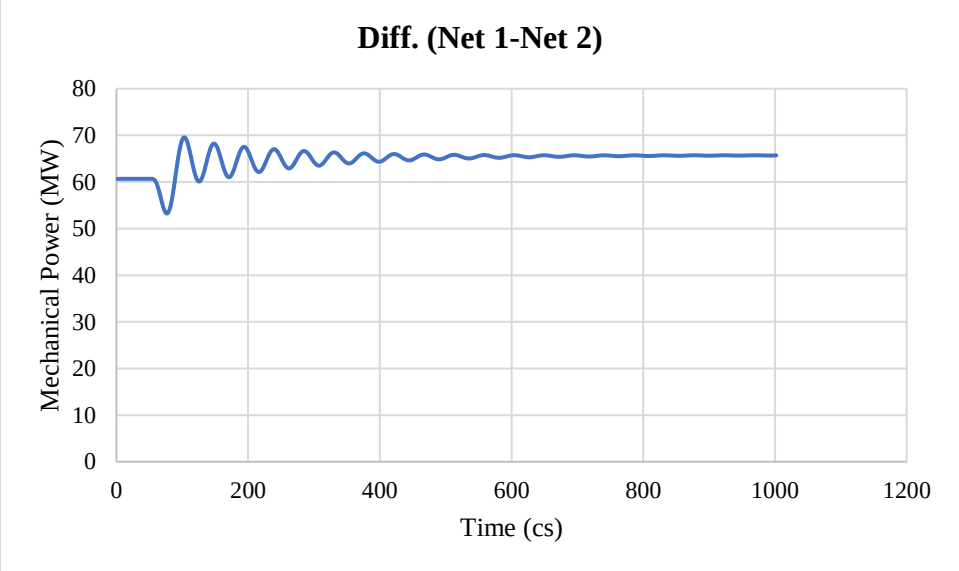

Mechanical power difference of Network 1 with Network 2

Discussion of Result

From numerous transient stability study, we observed that CASI always increased, and the [Psum 1 - Psum2] always increased in the same pattern. However, there is nothing that we could do in the two systems that would cause separation of the two systems according to the criteria we implicitly used.

Disturbance - Opening the Saint Thomas to Spring Garden line and tripping a Spring Garden Generator

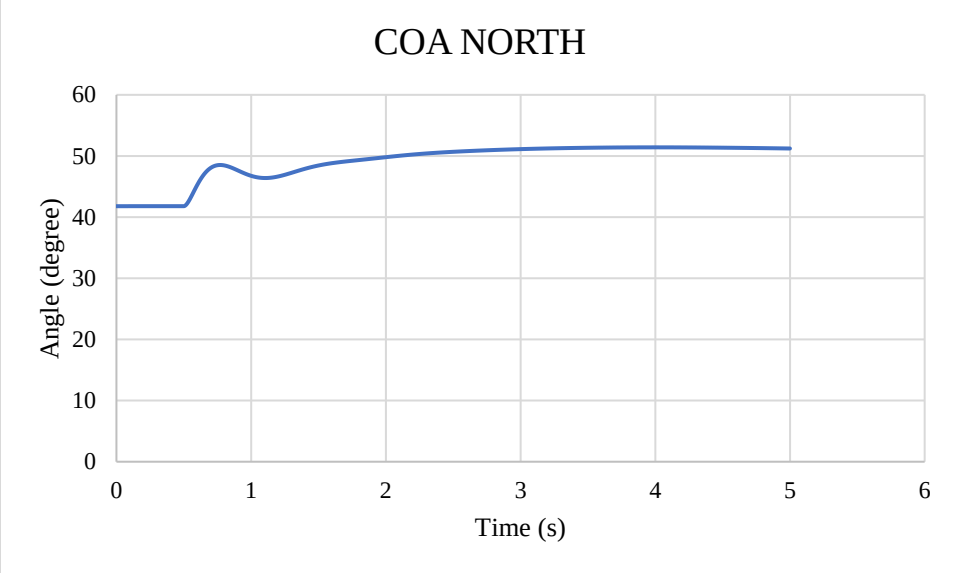

Centre of angle for northern microgrid on Disturbance

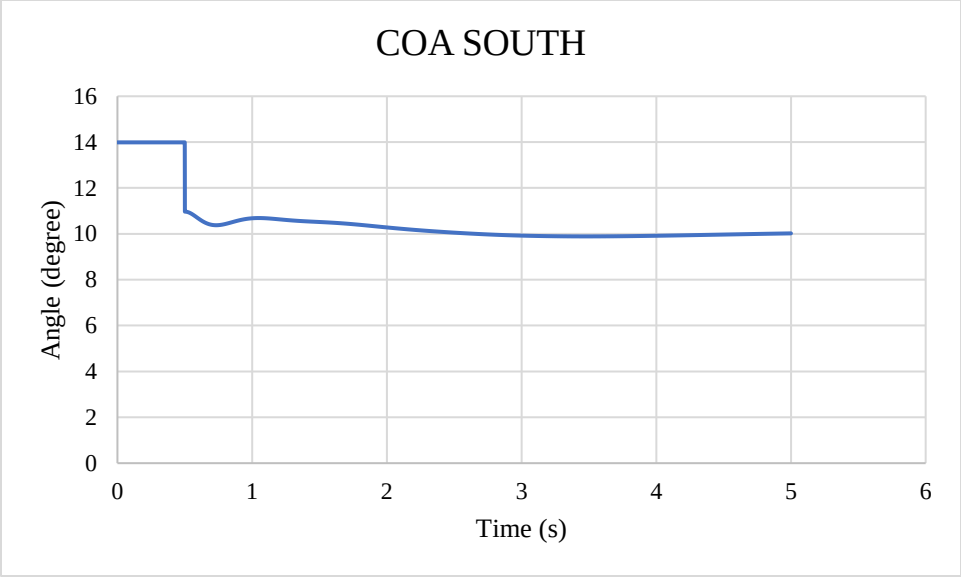

Centre of angle for southern microgrid on Disturbance

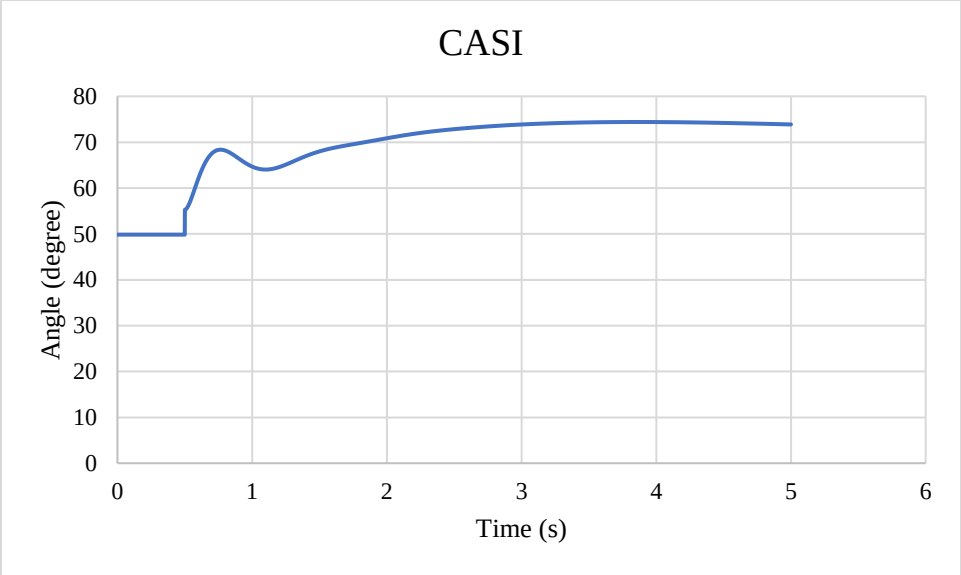

Centre of Angle Stability Index for Disturbance

APPENDIX B

Q-V characteristic for a lossless transmission system

$$Q_{required} = 0.5P + \frac{EV}{X}\left[\frac{V}{E} - \sqrt{1 - \left(\frac{PX}{EV}\right)^2}\right]$$

The equation for reactive power required to produce a desired voltage at a load bus in a lossless transmission has earlier been derived. It is:

The Q-V characteristics for the four "corner cases" of system voltage E (0.9 to 1.1 p.u.) and transmission reactance X (maximum and minimum for BLPC's buses on 30 MVA base) are shown. These characteristics have been plotted for four different load levels P at a constant load power factor of 0.90.

Strong source and strong transmission (E=1.1, X=0.03)

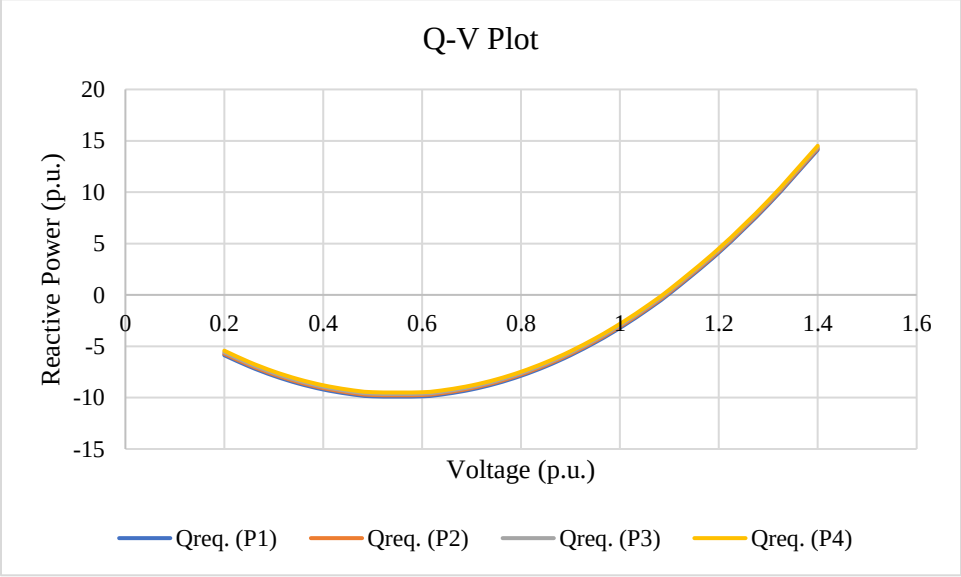

QV plot for a strong source and strong transmission system

Weak source and strong transmission (E=0.9, X=0.03)

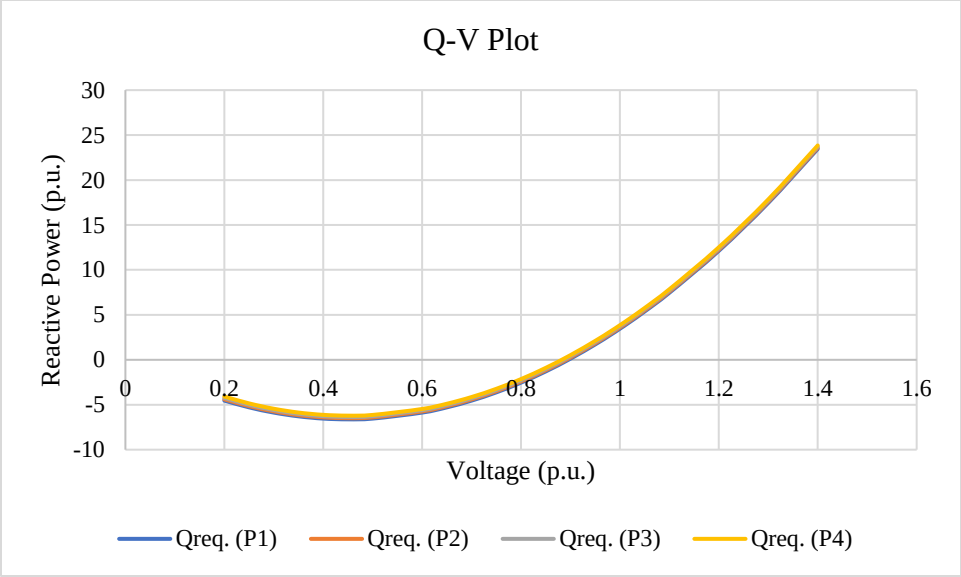

QV plot for a weak source and strong transmission system

Strong source and weak transmission (E=1.1, X=0.2)

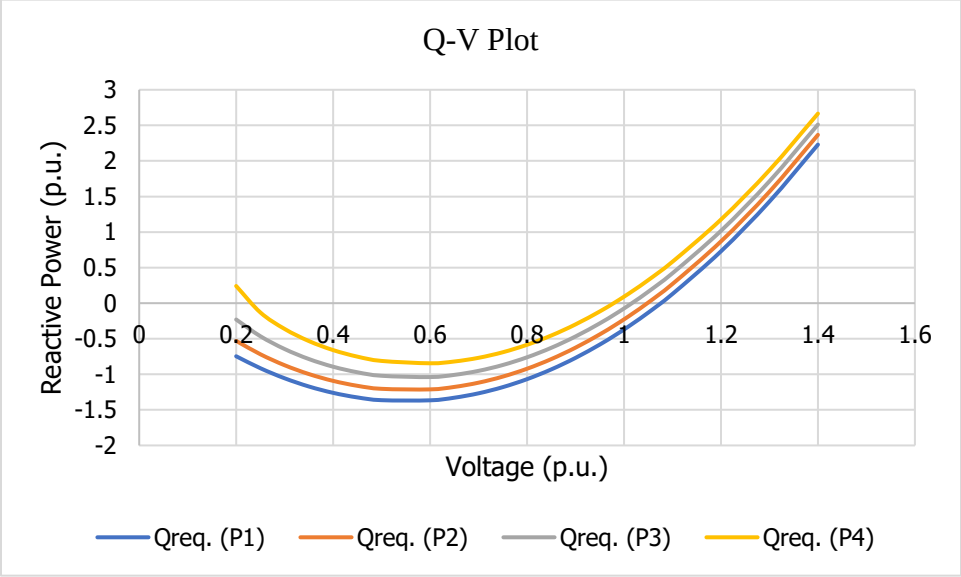

QV plot for a strong source and weak transmission system

Weak source and weak transmission (E=0.9, X=0.2)

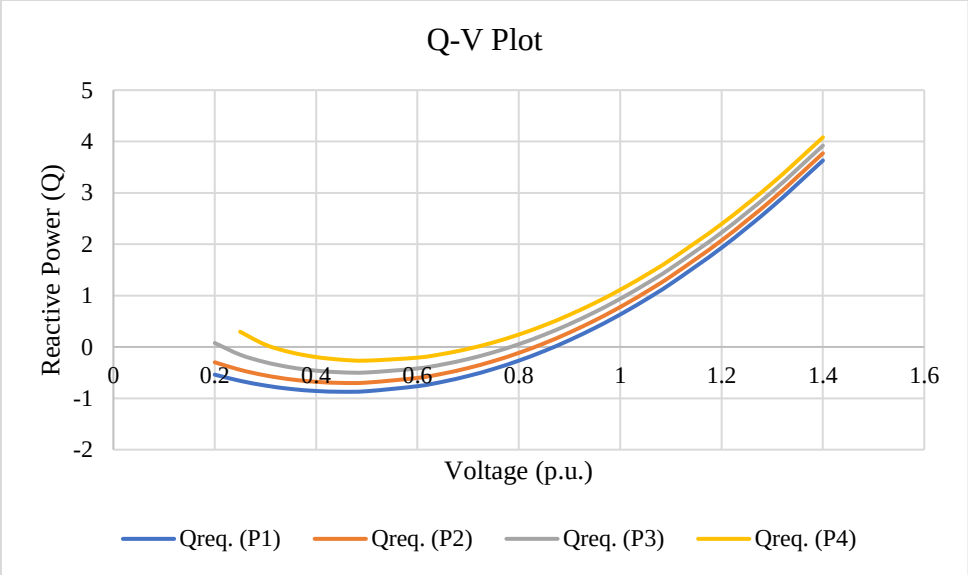

QV plot for a weak source and weak transmission system

These four characteristics are shown as reference case. However, it should be noted that it is the weak transmission line with X = 0.2 per unit which spreads out the Q-V graphs for different P values and makes them have a minimum at different values of load bus voltage.

Q-V characteristic for a lossy transmission system

For this illustration the supply voltage (E) is always equal to 1.0 p.u. Two different combinations of transmission line R and X have been used and the transmission line model. The following plots were observed.

Strong line (X=0.2, R=0.15)

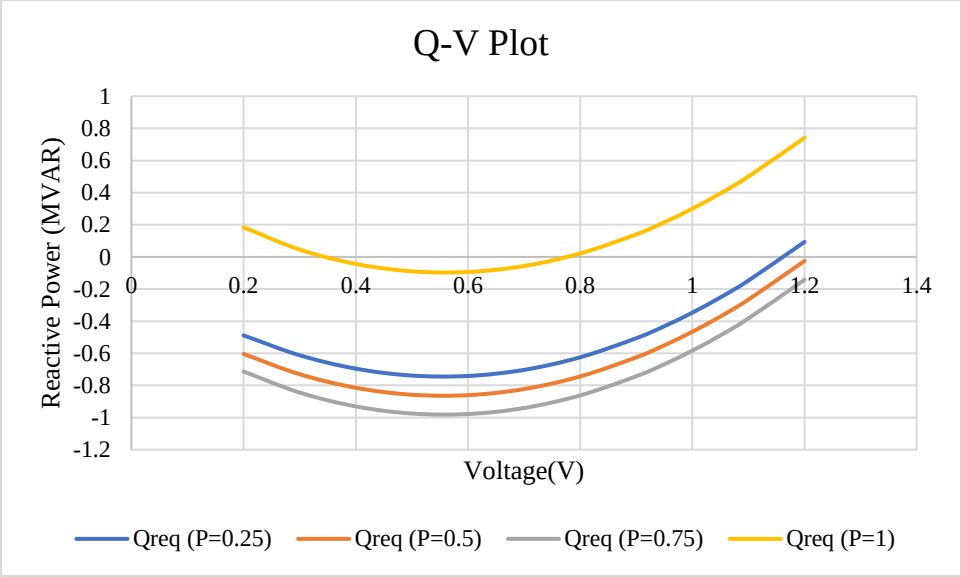

QV plot for a strong line in lossy system

Weak line (X=0.5, R=0.3)

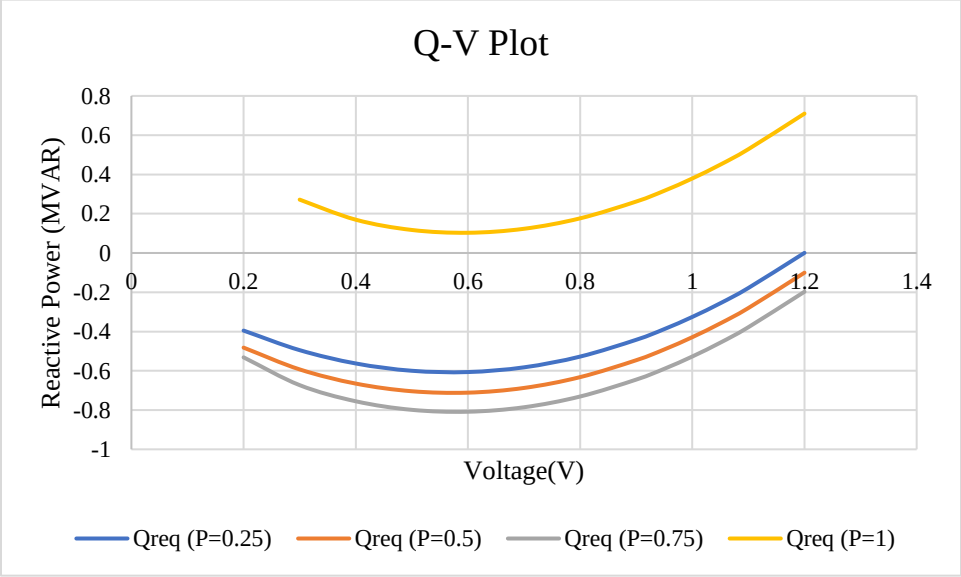

QV plot for a weak line in lossy system

For a low voltage transmission system, the X/R ratio is quite low (sometimes nearly equal to 1) resulting in different Q-V characteristics.

Analysing Q-V curves

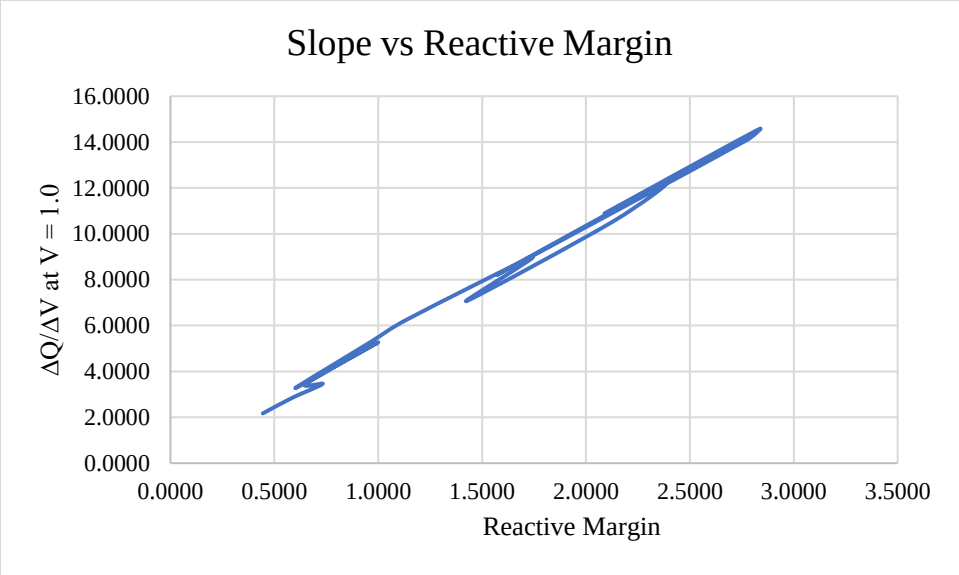

Slope at rated voltage versus Reactive Power Reserve margin for load buses

The slope of QV curve and reactive power reserve for all the buses are inter-related with each other and are directly proportional. This was also observed in their respective plots with the inverse of the Thevenin reactance.

Faults on adjacent bus voltage

3ϕ Fault at North 24.9 kV bus (North Weak Bus)

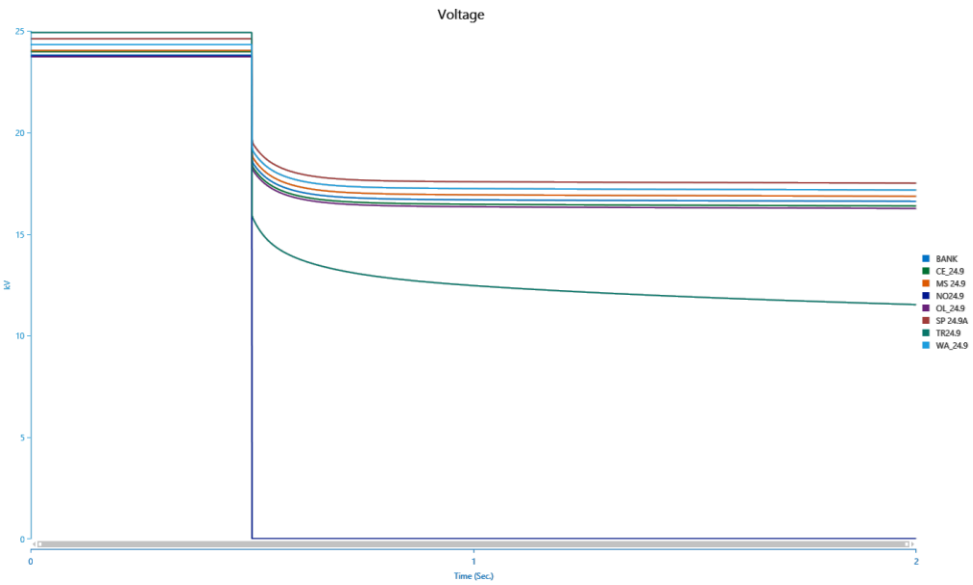

Effect of 3φ fault at North 24.9 kV bus

3ϕ Fault at Old Works 24.9 kV bus (South-east Weak Bus)

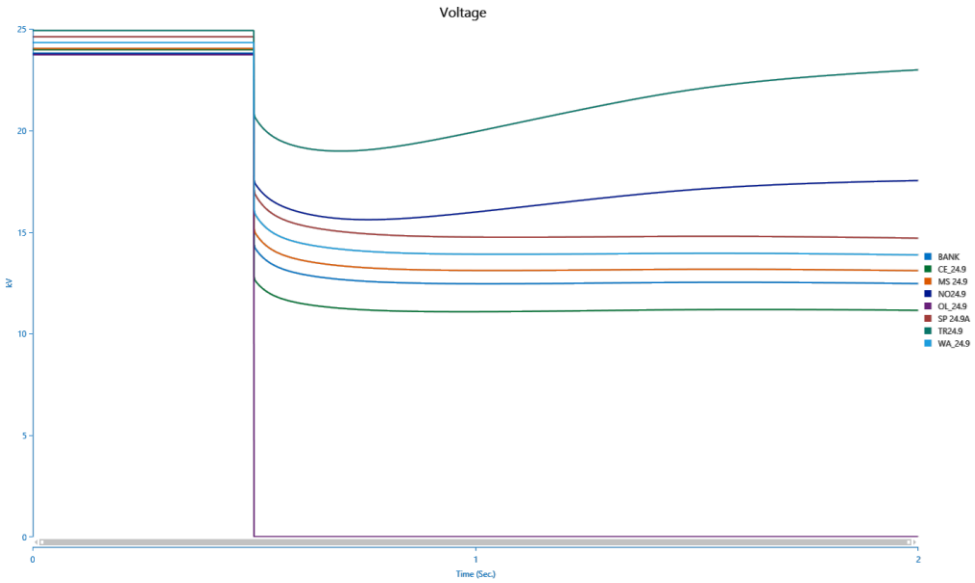

Effect of 3φ fault at Old Works 24.9 kV bus

3ϕ Fault at Banks 24.9 kV bus (South-west Moderate Bus)

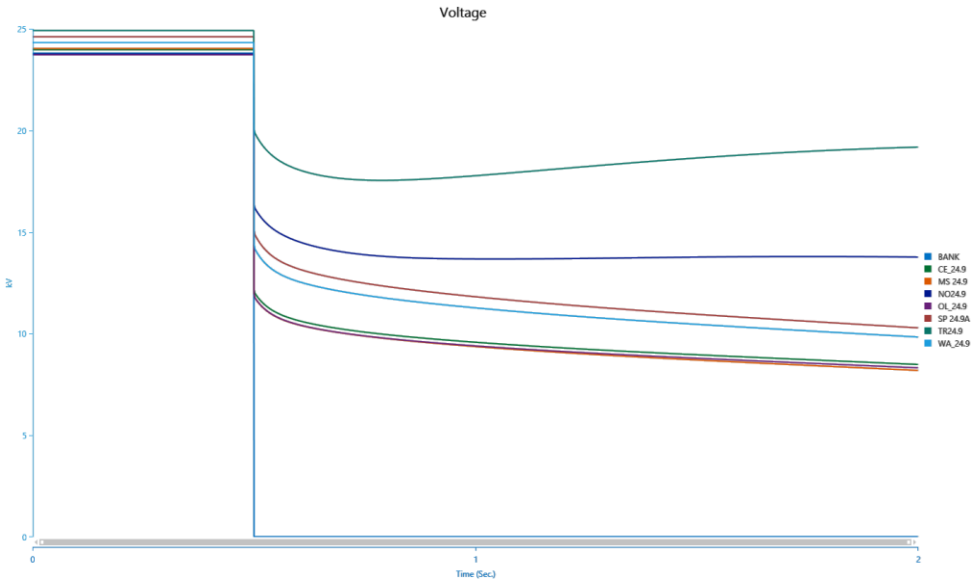

Effect of 3φ fault at Banks 24.9 kV bus

3ϕ Fault at Warren 24.9 kV bus (Central-west Moderate Bus)

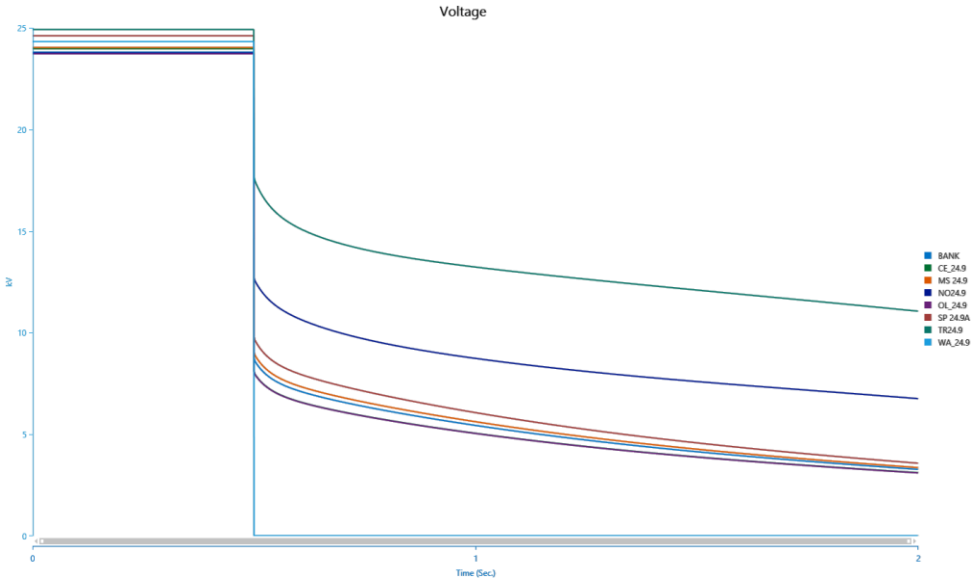

Effect of 3φ fault at Warren 24.9 kV bus

3ϕ Fault at Marhill Street 24.9 kV bus (South-west Strong Bus)

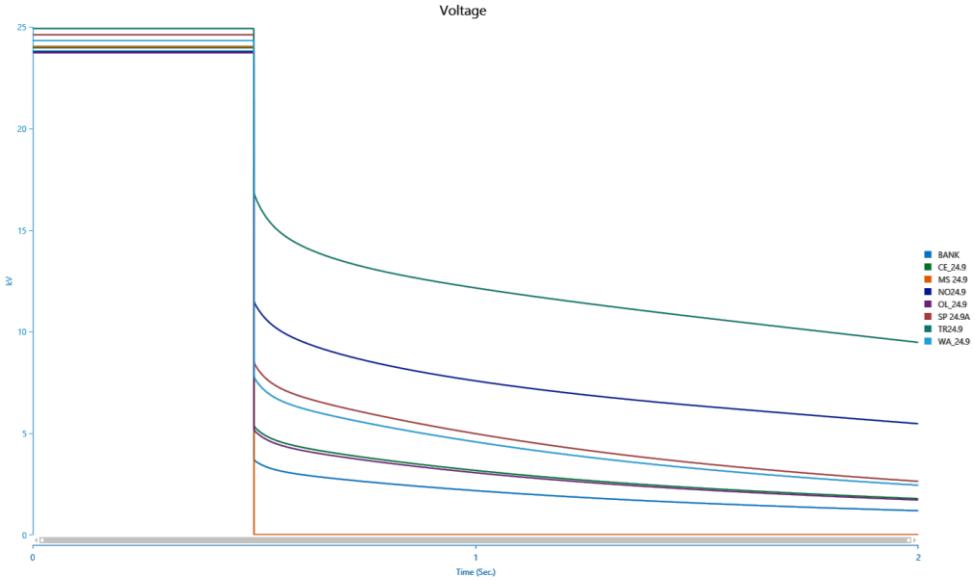

Effect of 3φ fault at Marhill Street 24.9 kV bus

3ϕ Fault at Central 24.9 kV bus (Central Strong Bus)

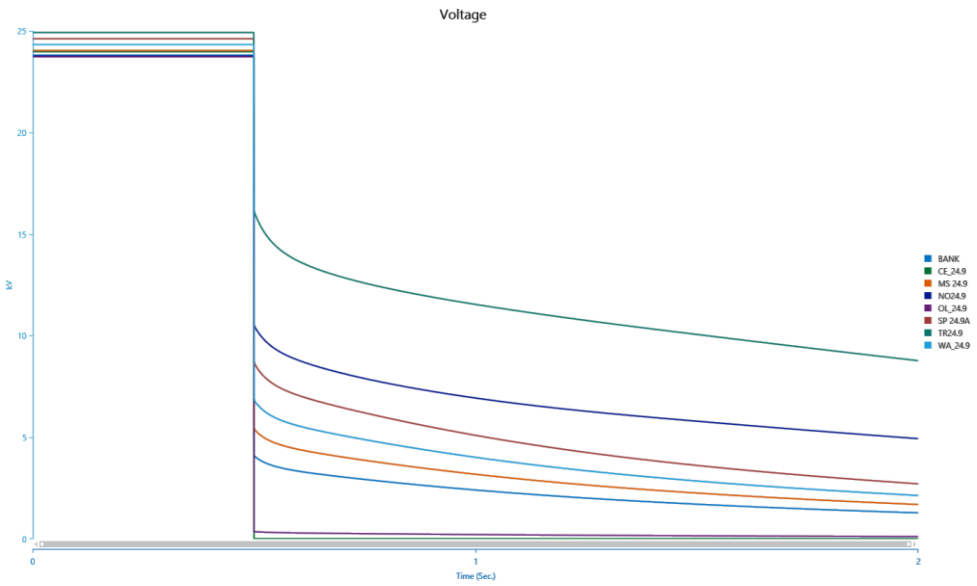

Effect of 3φ fault at Central 24.9 kV bus

QV for all BLPC buses

NORTH 24.9 kV

Adding a fictitious Generator with following parameters:		
Rated Voltage	24.9	kV
Capacity	500	MVA
Power Factor	0.01	%
Qmax	500	MVAR
Qmin	-500	MVAR

	Case 1	Case 2
Load Power (%)	25%	100%
Load Power (MW)	1.77	7.06
Initial Voltage (%)	97.27%	95.35%

Following results observed when reactive power required to maintain different voltage were done

S.N.	Operating Voltage (p.u.)	25% load	100% load
1	0.4	-0.46298	-0.4003
2	0.5	-0.49295	-0.4449
3	0.6	-0.48393	-0.44019
4	0.7	-0.43533	-0.39308
5	0.8	-0.34658	-0.30457
6	0.9	-0.17978	-0.13506
7	1	0.05173	0.09523
8	1.1	0.26786	0.31254
Reactive Power Reserve		-0.49295	-0.4449
ΔQ/ΔV @V=1.0		2.1613	2.1731
Qreq. for 1 pu Voltage		0.05173	0.09523
Voltage at slope=0		0.5	0.5
Change in Qreq. at 1.0 pu voltage			0.0435

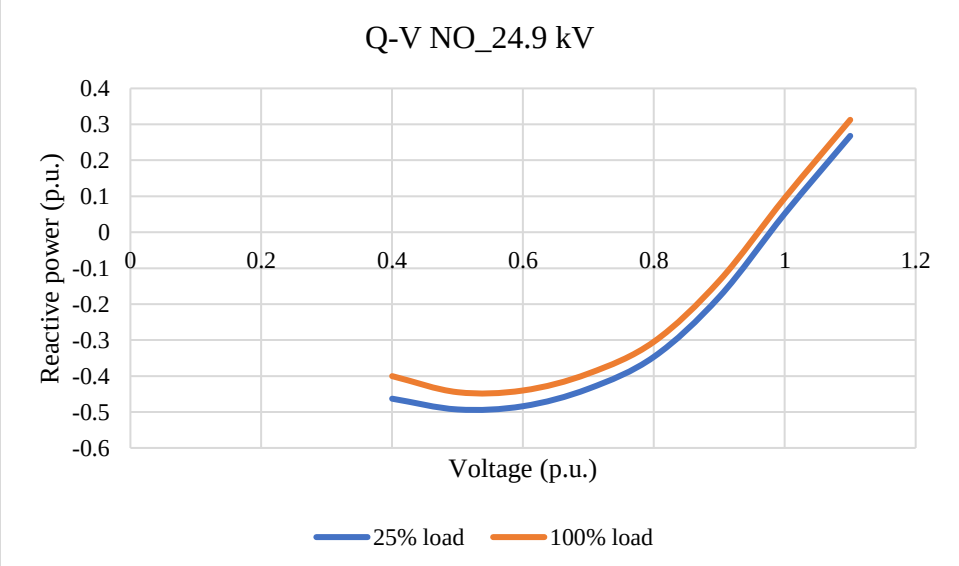

TRENT 24.9 kV

Adding a fictitious Generator with following parameters:		
Rated Voltage	24.9	kV
Capacity	500	MVA
Power Factor	0.01	%
Qmax	500	MVAR
Qmin	-500	MVAR
Load Power (%)	No load	
Load Power (MW)	0	
Initial Voltage (%)	100.00%	

Following results were observed when reactive power required to maintain different voltage were done

S.N.	Operating Voltage (p.u.)	No load
1	0.4	-0.26227
2	0.5	-0.31698
3	0.6	-0.32719
4	0.7	-0.29896
5	0.8	-0.23446
6	0.9	-0.13454
7	1	0.000526
8	1.1	0.1655
Reactive Power Reserve		-0.32719
ΔQ/ΔV @V=1.0		1.64974
Qreq. for 1 pu Voltage		0.000526
Voltage at slope=0		0.6

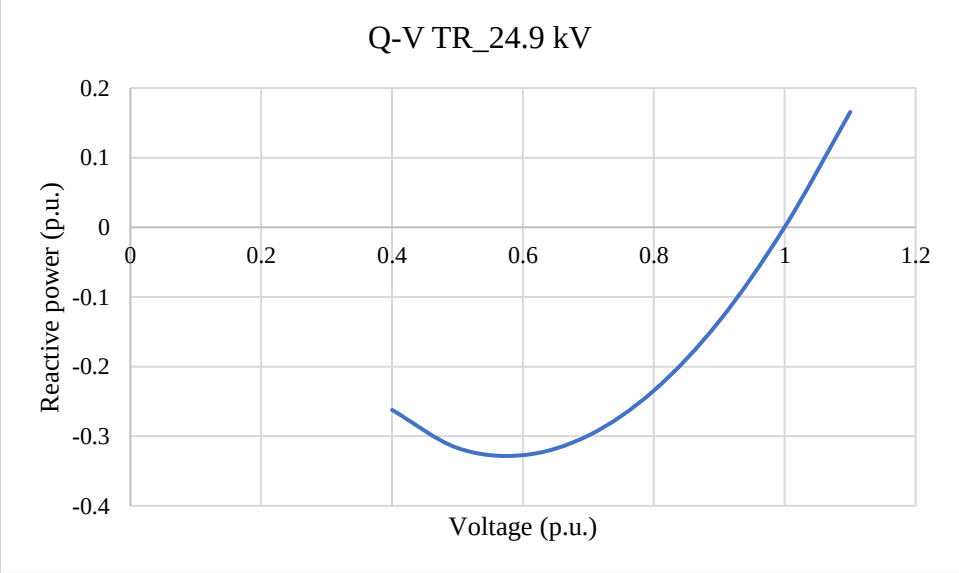

CARLTON 24.9 kV

Adding a fictitious Generator with following parameters:		
Rated Voltage	24.9	kV
Capacity	500	MVA
Power Factor	0.01	%
Qmax	500	MVAR
Qmin	-500	MVAR

	Case 1	Case 2
Load Power (%)	25%	100%
Load Power (MW)	0.875	3.5
Initial Voltage (%)	97.51%	96.71%

Following results observed when reactive power required to maintain different voltage were done

S.N.	Operating Voltage (p.u.)	25% load	100% load
1	0.4	-0.58555	
2	0.5	-0.63762	-0.58227
3	0.6	-0.63339	-0.5844
4	0.7	-0.57409	-0.52719
5	0.8	-0.45993	-0.41346
6	0.9	-0.28172	-0.23272
7	1	0.06172	0.10955
8	1.1	0.34402	0.39311
Reactive Power Reserve		-0.63762	-0.5844
ΔQ/ΔV @V=1.0		2.823	2.8356
Qreq. for 1 pu Voltage		0.06172	0.10955
Voltage at slope=0		0.5	0.6
Change in Qreq. at 1.0 pu voltage			0.04783

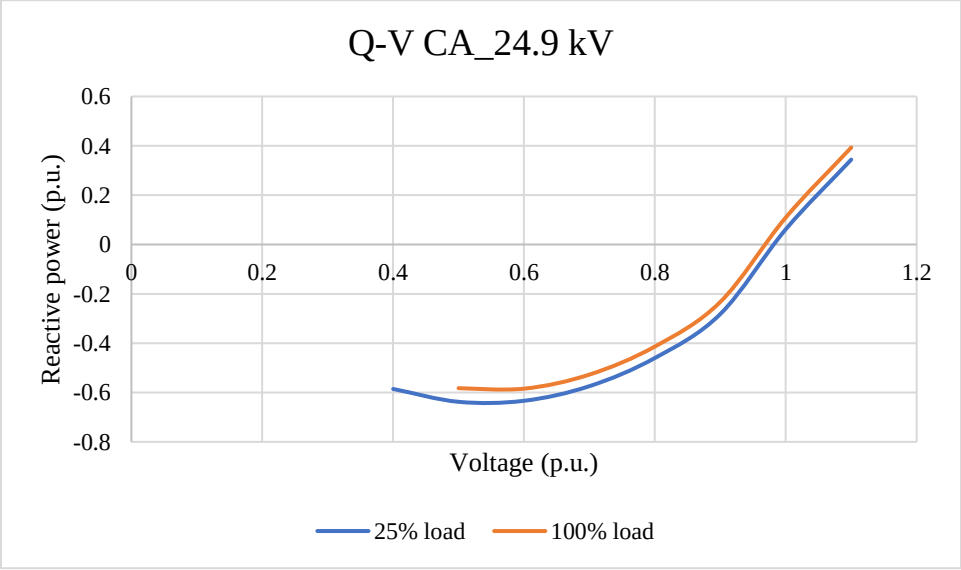

ST. THOMAS 24.9 kV

Adding a fictitious Generator with following parameters:		
Rated Voltage	24.9	kV
Capacity	500	MVA
Power Factor	0.01	%
Qmax	500	MVAR
Qmin	-500	MVAR
	Case 1	Case 2
Load Power (%)	25%	100%
Load Power (MW)	3.11	12.4
Initial Voltage (%)	98.62%	96.73%

Following results observed when reactive power required to maintain different voltage were done

S.N.	Operating Voltage (p.u.)	25% load	100% load
1	0.4	-0.6545	-0.60326
2	0.5	-0.76642	-0.71614
3	0.6	-0.78486	-0.73306
4	0.7	-0.72514	-0.67107
5	0.8	-0.59225	-0.53564
6	0.9	-0.38839	-0.32913
7	1	0.04201	0.10394
8	1.1	0.3855	0.45017
Reactive Power Reserve		-0.78486	-0.73306
ΔQ/ΔV @V=1.0		3.4349	3.4623
Qreq. for 1 pu Voltage		0.04201	0.10394
Voltage at slope=0		0.6	0.6
Change in Qreq. at 1.0 pu voltage			0.06193

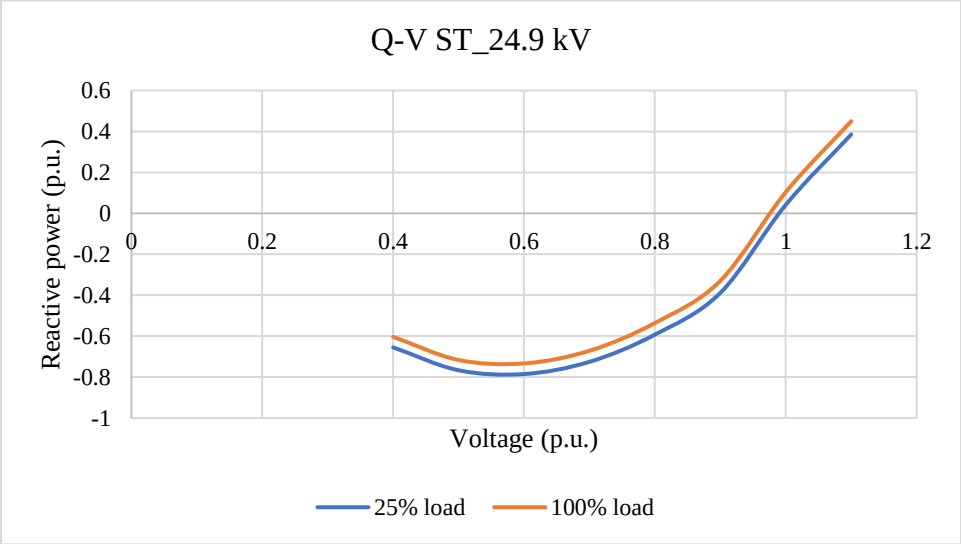

OLD WORKS 24.9 kV

Adding a fictitious Generator with following parameters:		
Rated Voltage	24.9	kV
Capacity	500	MVA
Power Factor	0.01	%
Qmax	500	MVAR
Qmin	-500	MVAR

	Case 1	Case 2
Load Power (%)	25%	100%
Load Power (MW)	1.43	5.72
Initial Voltage (%)	96.34%	95.16%

Following results observed when reactive power required to maintain different voltage were done

S.N.	Operating Voltage (p.u.)	25% load	100% load
1	0.4	-0.66292	-0.62304
2	0.5	-0.68711	-0.65218
3	0.6	-0.651	-0.6176
4	0.7	-0.55381	-0.52072
5	0.8	-0.39477	-0.36144
6	0.9	-0.17318	-0.13929
7	1	0.11054	0.14518
8	1.1	0.45489	0.49041
Reactive Power Reserve		-0.68711	-0.65218
ΔQ/ΔV @V=1.0		3.4435	3.4523
Qreq. for 1 pu Voltage		0.11054	0.14518
Voltage at slope=0		0.5	0.5
Change in Qreq. at 1.0 pu voltage			0.03464

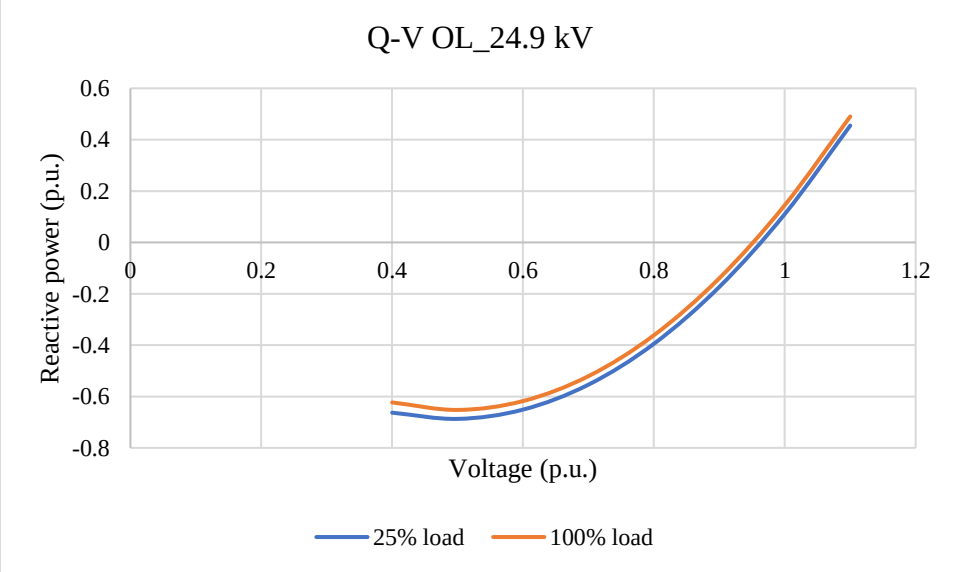

BANKS 24.9 kV

Adding a fictitious Generator with following parameters:		
Rated Voltage	24.9	kV
Capacity	500	MVA
Power Factor	0.01	%
Qmax	500	MVAR
Qmin	-500	MVAR

	Case 1	Case 2
Load Power (%)	25%	100%
Load Power (MW)	1.35	5.4
Initial Voltage (%)	96.77%	95.92%

Following results were observed when reactive power required to maintain different voltage were done

S.N.	Operating Voltage (p.u.)	25% load	100% load
1	0.4	-0.98971	-0.96255
2	0.5	-1.02989	-1.00115
3	0.6	-0.98146	-0.95106
4	0.7	-0.8419	-0.80975
5	0.8	-0.60864	-0.57465
6	0.9	-0.27899	-0.24307
7	1	0.1479	0.18573
8	1.1	0.67277	0.71273
Reactive Power Reserve		-1.02989	-1.00115
ΔQ/ΔV @V=1.0		5.2487	5.27
Qreq. for 1 pu Voltage		0.1479	0.18573
Voltage at slope=0		0.5	0.5
Change in Qreq. at 1.0 pu voltage			0.03783

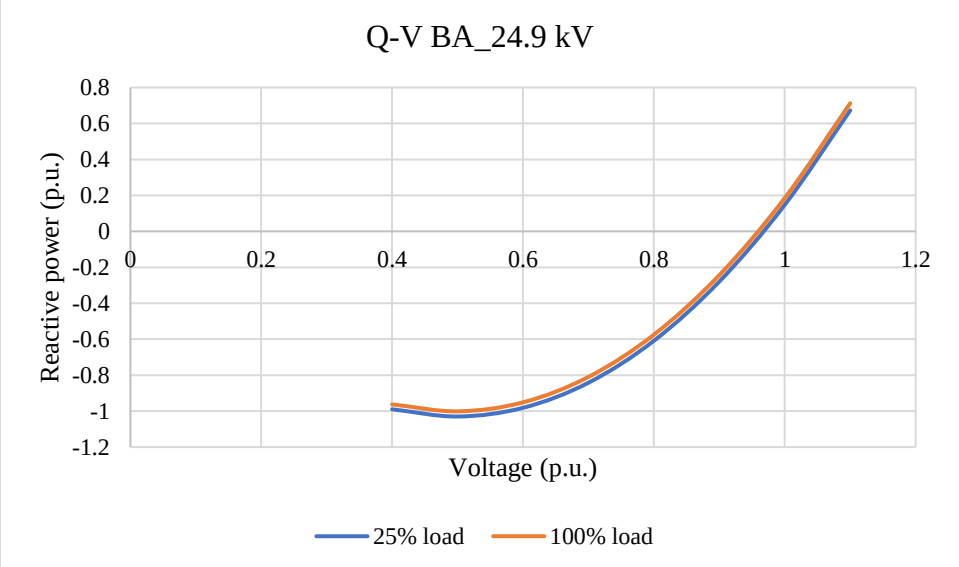

HAMPTON 24.9 kV

Adding a fictitious Generator with following parameters:		
Rated Voltage	24.9	kV
Capacity	500	MVA
Power Factor	0.01	%
Qmax	500	MVAR
Qmin	-500	MVAR

	Case 1	Case 2
Load Power (%)	25%	100%
Load Power (MW)	1.65	6.59
Initial Voltage (%)	96.10%	94.61%

Following results observed when reactive power required to maintain different voltage were done

S.N.	Operating Voltage (p.u.)	25% load	100% load
1	0.4	-0.61874	-0.5715
2	0.5	-0.64142	-0.60074
3	0.6	-0.60742	-0.56845
4	0.7	-0.51588	-0.47714
5	0.8	-0.36599	-0.3268
6	0.9	-0.15694	-0.11695
7	1	0.11095	0.15194
8	1.1	0.43678	0.47896
Reactive Power Reserve		-0.64142	-0.60074
ΔQ/ΔV @V=1.0		3.2583	3.2702
Qreq. for 1 pu Voltage		0.11095	0.15194
Voltage at slope=0		0.5	0.5
Change in Qreq. at 1.0 pu voltage			0.04099

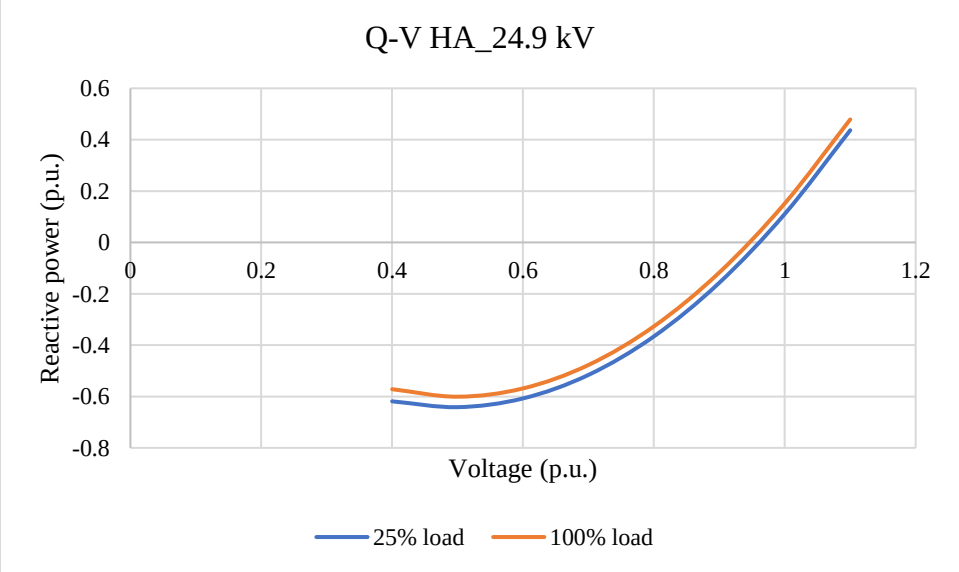

SEAWELL 24.9 kV

Adding a fictitious Generator with following parameters:		
Rated Voltage	24.9	kV
Capacity	500	MVA
Power Factor	0.01	%
Qmax	500	MVAR
Qmin	-500	MVAR

	Case 1	Case 2
Load Power (%)	25%	100%
Load Power (MW)	1.91	7.62
Initial Voltage (%)	95.81%	94.67%

Following results observed when reactive power required to maintain different voltage were done

S.N.	Operating Voltage (p.u.)	25% load	100% load
1	0.4	-0.96219	-0.91093
2	0.5	-1.00788	-0.96094
3	0.6	-0.95806	-0.91198
4	0.7	-0.81454	-0.76804
5	0.8	-0.57577	-0.52824
6	0.9	-0.24012	-0.19118
7	1	0.19091	0.24138
8	1.1	0.71599	0.76828
Reactive Power Reserve		-1.00788	-0.96094
ΔQ/ΔV @V=1.0		5.2508	5.269
Qreq. for 1 p.u. Voltage		0.19091	0.24138
Voltage at slope=0		0.5	0.5
Change in Qreq. at 1.0 p.u. voltage			0.05047

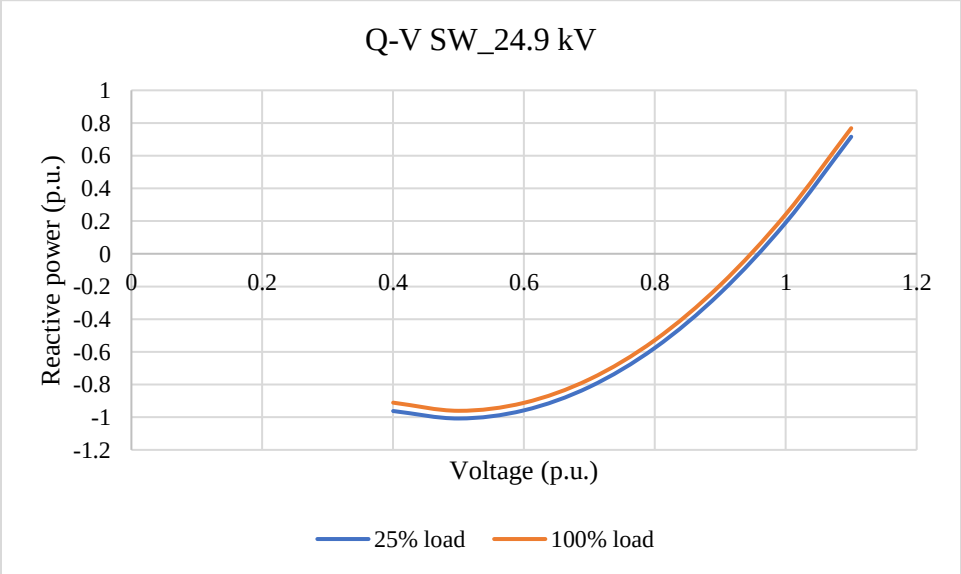

WOTTON 24.9 kV

Adding a fictitious Generator with following parameters:		
Rated Voltage	24.9	kV
Capacity	500	MVA
Power Factor	0.01	%
Qmax	500	MVAR
Qmin	-500	MVAR

	Case 1	Case 2
Load Power (%)	25%	100%
Load Power (MW)	2.38	9.53
Initial Voltage (%)	96.04%	94.80%

Following results observed when reactive power required to maintain different voltage were done

S.N.	Operating Voltage (p.u.)	25% load	100% load
1	0.4	-1.15664	-1.07366
2	0.5	-1.20946	-1.14221
3	0.6	-1.15209	-1.08884
4	0.7	-0.98166	-0.91933
5	0.8	-0.69785	-0.63501
6	0.9	-0.2984	-0.23427
7	1	0.21496	0.2807
8	1.1	0.84062	0.90848
Reactive Power Reserve		-1.20946	-1.14221
ΔQ/ΔV @V=1.0		6.2566	6.2778
Qreq. for 1 p.u. Voltage		0.21496	0.2807
Voltage at slope=0		0.5	0.5
Change in Qreq. at 1.0 p.u. voltage			0.06574

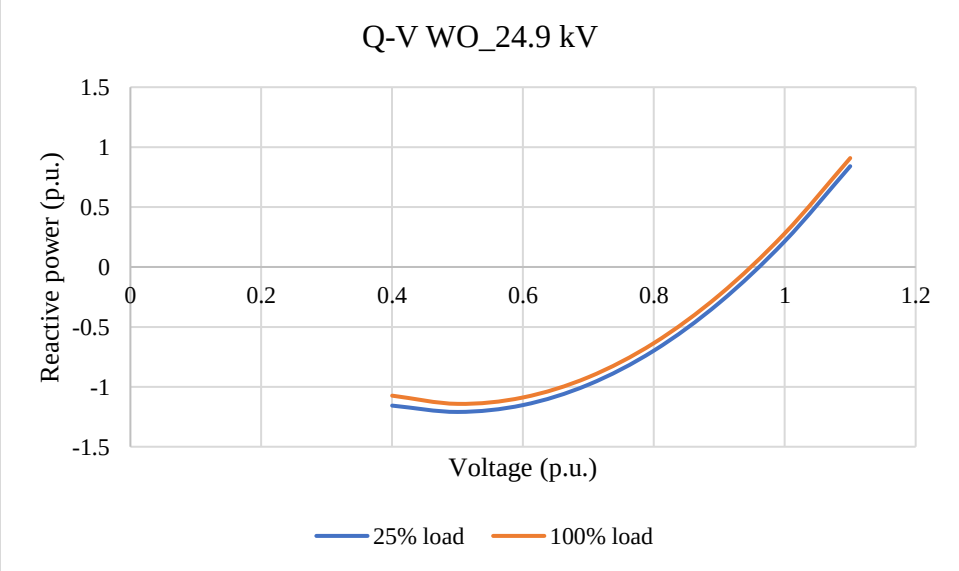

WILDEY 24.9 kV

Adding a fictitious Generator with following parameters:		
Rated Voltage	24.9	kV
Capacity	500	MVA
Power Factor	0.01	%
Qmax	500	MVAR
Qmin	-500	MVAR

	Case 1	Case 2
Load Power (%)	25%	100%
Load Power (MW)	1.63	6.53
Initial Voltage (%)	96.80%	96.26%

Following results were observed when reactive power required to maintain different voltage were done

S.N.	Operating Voltage (p.u.)	25% load	100% load
1	0.4	-1.69325	-1.66186
2	0.5	-1.77453	-1.74148
3	0.6	-1.70119	-1.6665
4	0.7	-1.46329	-1.42676
5	0.8	-1.05799	-1.01973
6	0.9	-0.4857	-0.44567
7	1	0.25064	0.29232
8	1.1	1.14686	1.19041
Reactive Power Reserve		-1.77453	-1.74148
ΔQ/ΔV @V=1.0		8.9622	8.9809
Qreq. for 1 pu Voltage		0.25064	0.29232
Voltage at slope=0		0.5	0.5
Change in Qreq. at 1.0 pu voltage			0.04168

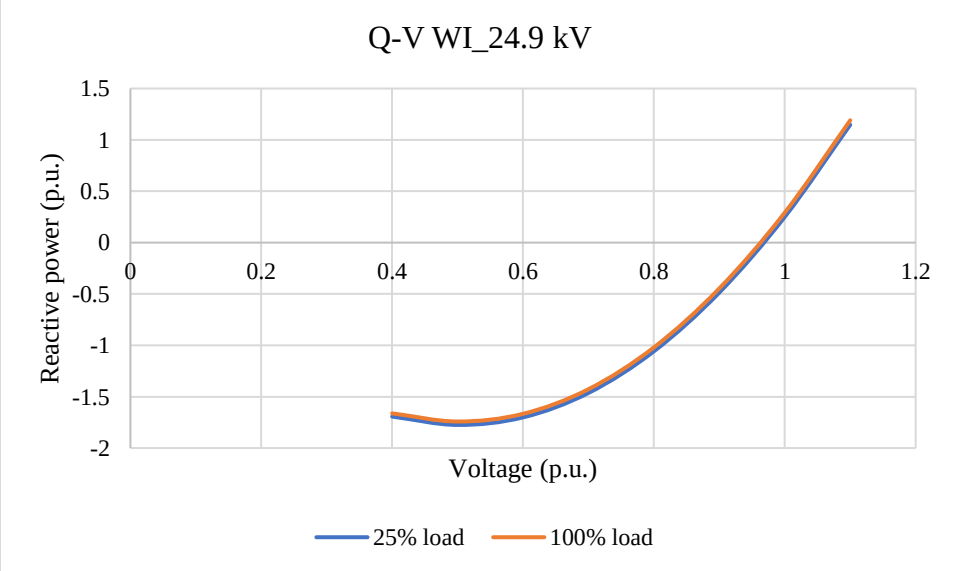

WARREN 24.9 kV

Adding a fictitious Generator with following parameters:		
Rated Voltage	24.9	kV
Capacity	500	MVA
Power Factor	0.01	%
Qmax	500	MVAR
Qmin	-500	MVAR

	Case 1	Case 2
Load Power (%)	25%	100%
Load Power (MW)	2.56	10.2
Initial Voltage (%)	98.60%	97.82%

Following results were observed when reactive power required to maintain different voltage were done

S.N.	Operating Voltage (p.u.)	25% load	100% load
1	0.4	-2.10024	
2	0.5	-2.20099	-2.13215
3	0.6	-2.12158	-2.05567
4	0.7	-1.85021	-1.78403
5	0.8	-1.38685	-1.31928
6	0.9	-0.72741	-0.65767
7	1	0.13057	0.20273
8	1.1	1.18207	1.25733
Reactive Power Reserve		-2.20099	-2.13215
ΔQ/ΔV @V=1.0		10.515	10.546
Qreq. for 1 pu Voltage		0.13057	0.20273
Voltage at slope=0		0.5	0.5
Change in Qreq. at 1.0 pu voltage			0.07216

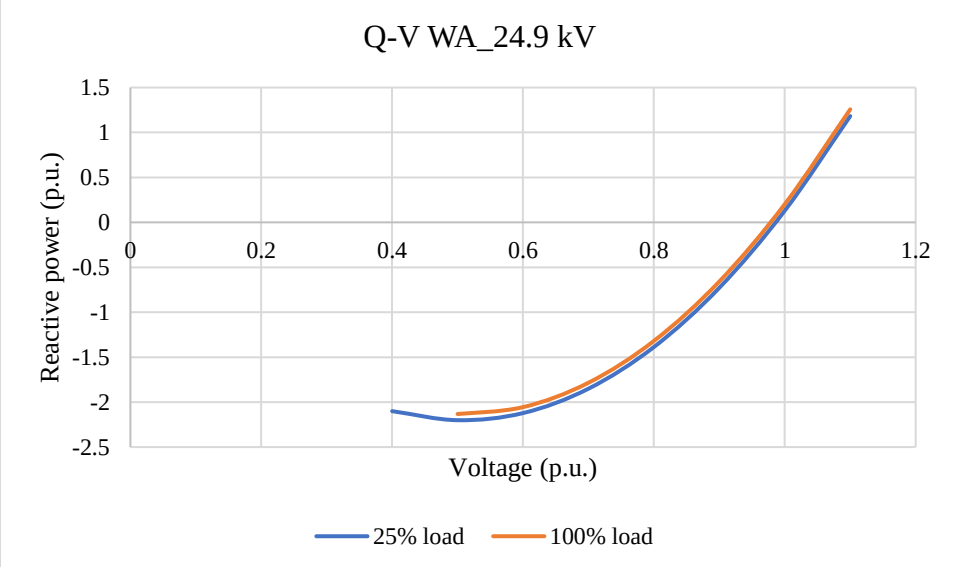

GARRISON 24.9 kV

Adding a fictitious Generator with following parameters:		
Rated Voltage	24.9	kV
Capacity	500	MVA
Power Factor	0.01	%
Qmax	500	MVAR
Qmin	-500	MVAR

	Case 1	Case 2
Load Power (%)	25%	100%
Load Power (MW)	3.165	11.4
Initial Voltage (%)	96.94%	95.60%

Following results were observed when reactive power required to maintain different voltage were done

S.N.	Operating Voltage (p.u.)	25% load	100% load
1	0.4		-1.36838
2	0.5	-1.30832	-1.42844
3	0.6	-1.27265	-1.3647
4	0.7	-1.08623	-1.16987
5	0.8	-0.76593	-0.84635
6	0.9	-0.31255	-0.3921
7	1	0.26951	0.18983
8	1.1	0.97821	0.89737
Reactive Power Reserve		-1.30832	-1.42844
ΔQ/ΔV @V=1.0		7.087	7.0754
Qreq. for 1 pu Voltage		0.26951	0.18983
Voltage at slope=0		0.5	0.5
Change in Qreq. at 1.0 pu voltage			-0.07968

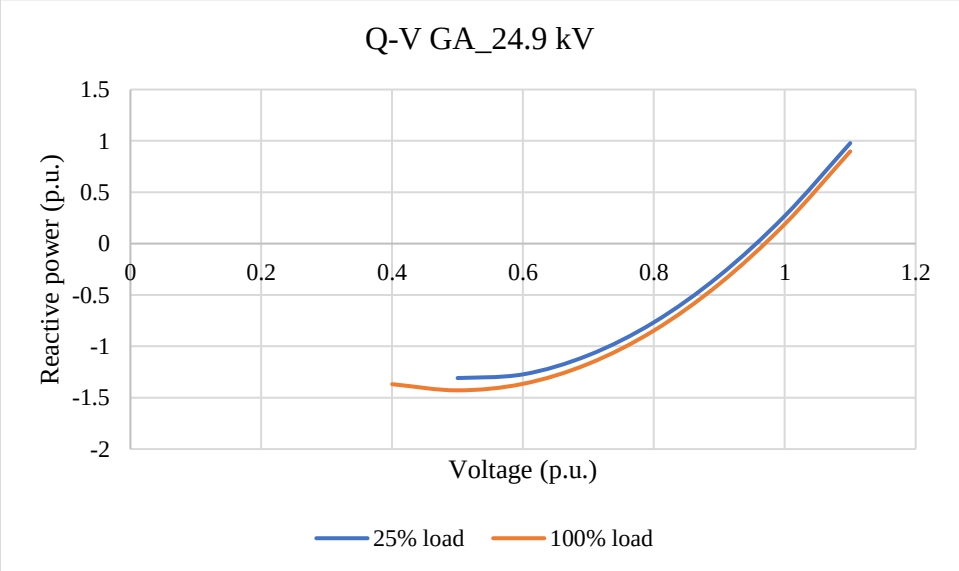

MARHILL STREET 24.9 kV

Adding a fictitious Generator with following parameters:		
Rated Voltage	24.9	kV
Capacity	500	MVA
Power Factor	0.01	%
Qmax	500	MVAR
Qmin	-500	MVAR

	Case 1	Case 2
Load Power (%)	25%	100%
Load Power (MW)	1.92	7.68
Initial Voltage (%)	97.28%	96.78%

Following results were observed when reactive power required to maintain different voltage were done

S.N.	Operating Voltage (p.u.)	25% load	100% load
1	0.4	-2.29556	-2.23156
2	0.5	-2.42145	-2.368
3	0.6	-2.33132	-2.28103
4	0.7	-2.02295	-1.97326
5	0.8	-1.47874	-1.42871
6	0.9	-0.70678	-0.65579
7	1	0.28971	0.34184
8	1.1	1.50254	1.5563
Reactive Power Reserve		-2.42145	-2.368
ΔQ/ΔV @V=1.0		12.1283	12.1446
Qreq. for 1 pu Voltage		0.28971	0.34184
Voltage at slope=0		0.5	0.5
Change in Qreq. at 1.0 pu voltage			0.05213

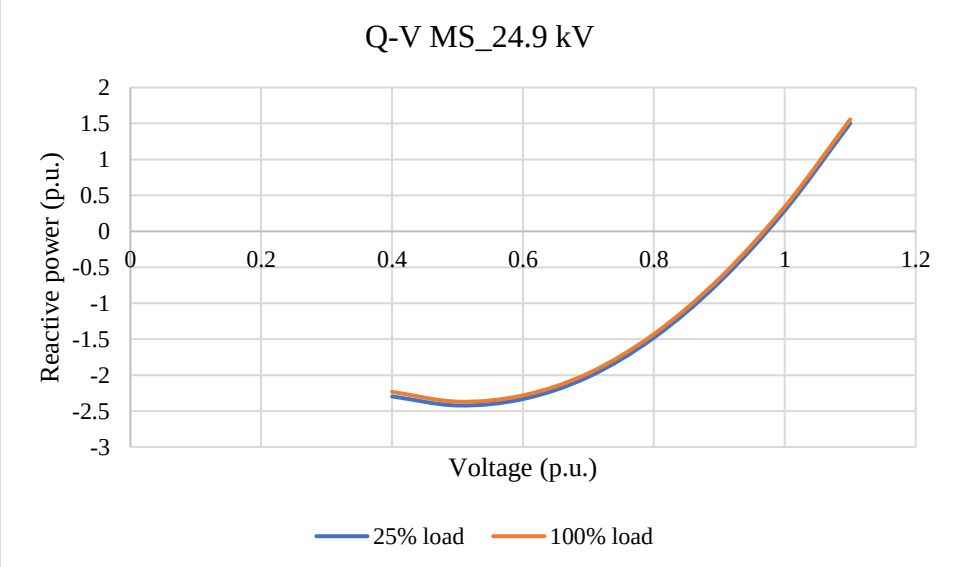

REGENCY PARK 24.9 kV

Adding a fictitious Generator with following parameters:		
Rated Voltage	24.9	kV
Capacity	500	MVA
Power Factor	0.01	%
Qmax	500	MVAR
Qmin	-500	MVAR

	Case 1	Case 2
Load Power (%)	25%	100%
Load Power (MW)	0.948	3.79
Initial Voltage (%)	96.40%	96.04%

Following results were observed when reactive power required to maintain different voltage were done

S.N.	Operating Voltage (p.u.)	25% load	100% load
1	0.4	-1.49612	-1.47209
2	0.5	-1.59511	-1.57225
3	0.6	-1.53409	-1.51156
4	0.7	-1.31973	-1.29689
5	0.8	-0.94652	-0.92318
6	0.9	-0.41899	-0.39499
7	1	0.25756	0.28222
8	1.1	1.07806	1.10357
Reactive Power Reserve		-1.59511	-1.57225
ΔQ/ΔV @V=1.0		8.205	8.2135
Qreq. for 1 pu Voltage		0.25756	0.28222
Voltage at slope=0		0.5	0.5
Change in Qreq. at 1.0 pu voltage			0.02466

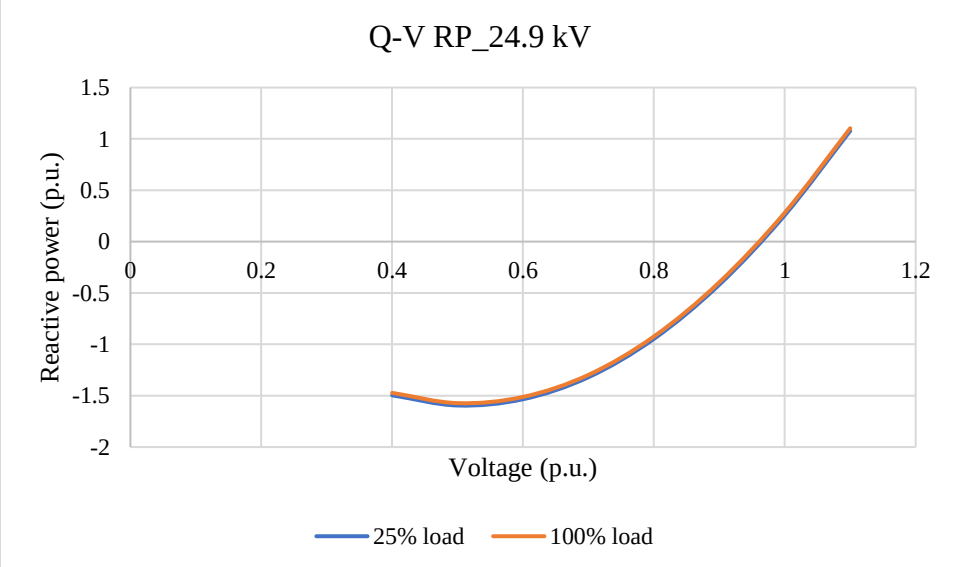

WHITEPARK 24.9 kV

Adding a fictitious Generator with following parameters:		
Rated Voltage	24.9	kV
Capacity	500	MVA
Power Factor	0.01	%
Qmax	500	MVAR
Qmin	-500	MVAR

	Case 1	Case 2
Load Power (%)	25%	100%
Load Power (MW)	2.36	9.43
Initial Voltage (%)	97.53%	97.03%

Following results were observed when reactive power required to maintain different voltage were done

S.N.	Operating Voltage (p.u.)	25% load	100% load
1	0.4		
2	0.5	-2.84697	-2.76983
3	0.6	-2.74669	-2.6802
4	0.7	-2.38888	-2.32635
5	0.8	-1.75728	-1.69599
6	0.9	-0.85519	-0.79409
7	1	0.30579	0.36721
8	1.1	1.71161	1.77403
Reactive Power Reserve		-2.84697	-2.76983
ΔQ/ΔV @V=1.0		14.0582	14.0682
Qreq. for 1 pu Voltage		0.30579	0.36721
Voltage at slope=0		0.5	0.5
Change in Qreq. at 1.0 pu voltage			0.06142

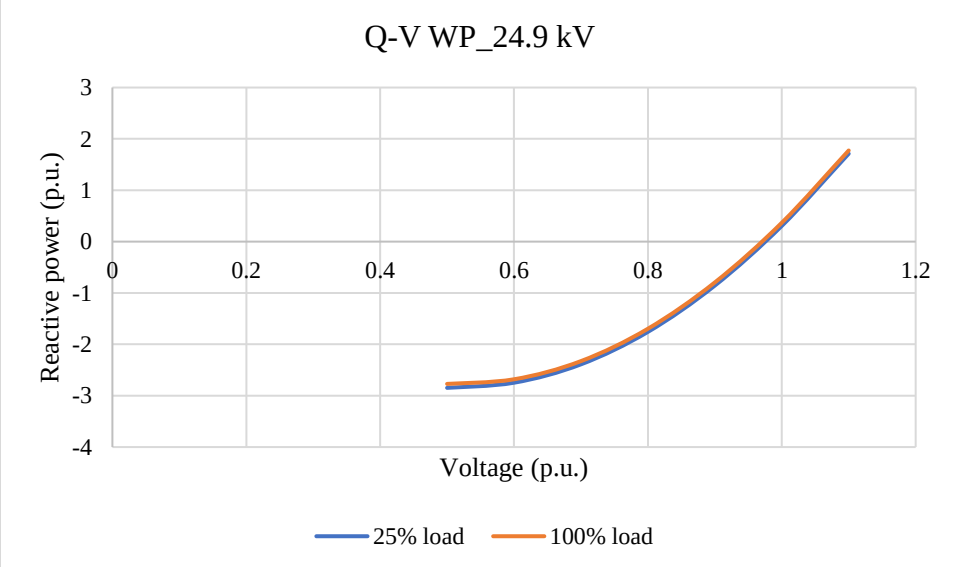

TEMPLE YARD 24.9 kV

Adding a fictitious Generator with following parameters:		
Rated Voltage	24.9	kV
Capacity	500	MVA
Power Factor	0.01	%
Qmax	500	MVAR
Qmin	-500	MVAR

	Case 1	Case 2
Load Power (%)	25%	100%
Load Power (MW)	2.66	10.6
Initial Voltage (%)	97.65%	97.08%

Following results were observed when reactive power required to maintain different voltage were done

S.N.	Operating Voltage (p.u.)	25% load	100% load
1	0.4	-2.76771	
2	0.5	-2.9431	-2.8402
3	0.6	-2.84453	-2.76473
4	0.7	-2.47923	-2.40554
5	0.8	-1.83067	-1.75871
6	0.9	-0.89971	-0.82796
7	1	0.30193	0.37414
8	1.1	1.75999	1.83358
Reactive Power Reserve		-2.9431	-2.8402
ΔQ/ΔV @V=1.0		14.5806	14.5944
Qreq. for 1 pu Voltage		0.30193	0.37414
Voltage at slope=0		0.5	0.5
Change in Qreq. at 1.0 pu voltage			0.07221

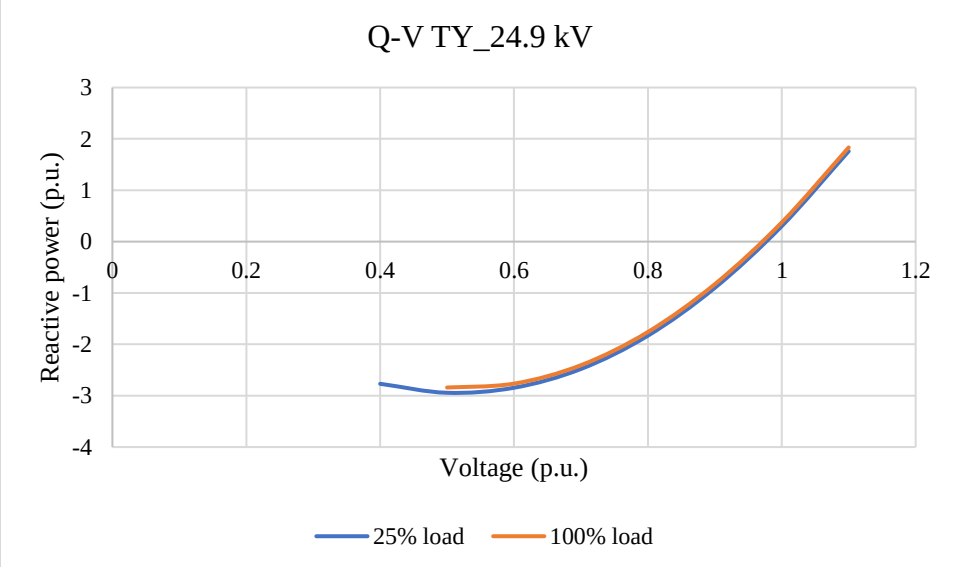

CENTRAL 24.9 kV

Adding a fictitious Generator with following parameters:		
Rated Voltage	24.9	kV
Capacity	500	MVA
Power Factor	0.01	%
Qmax	500	MVAR
Qmin	-500	MVAR

	Case 1	Case 2
Load Power (%)	25%	100%
Load Power (MW)	1.24	4.98
Initial Voltage (%)	96.44%	96.17%

Following results observed when reactive power required to maintain different voltage were done

S.N.	Operating Voltage (p.u.)	25% load	100% load
1	0.4		
2	0.5	-2.11085	-2.0888
3	0.6	-2.04822	-2.0252
4	0.7	-1.77488	-1.7509
5	0.8	-1.28559	-1.2608
6	0.9	-0.57109	-0.5454
7	1	0.33959	0.36599
8	1.1	1.42787	1.4551
Reactive Power Reserve		-2.11085	-2.0888
ΔQ/ΔV @V=1.0		10.8828	10.8911
Qreq. for 1 pu Voltage		0.33959	0.36599
Voltage at slope=0		0.5	0.5
Change in Qreq. at 1.0 pu voltage			0.0264

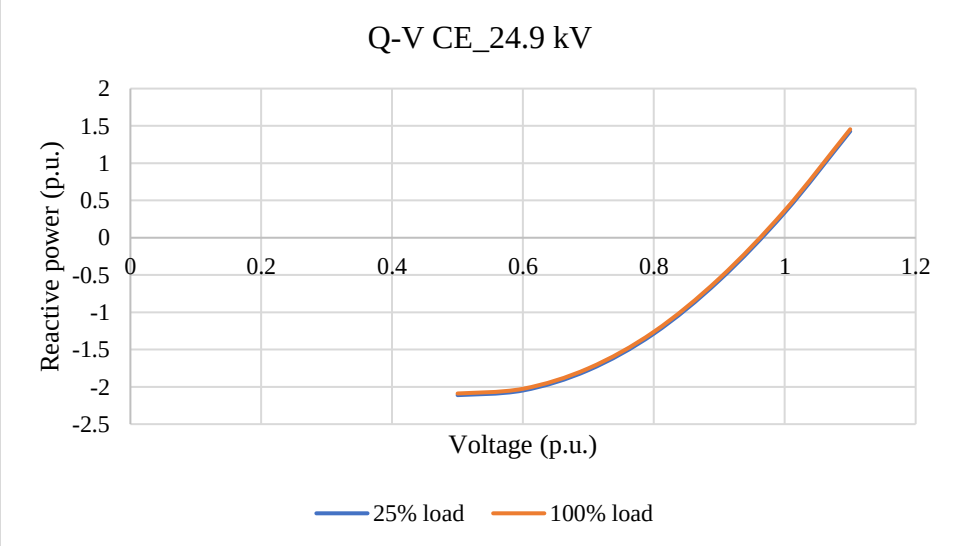

BELMONT 24.9 kV

Adding a fictitious Generator with following parameters:		
Rated Voltage	24.9	kV
Capacity	500	MVA
Power Factor	0.01	%
Qmax	500	MVAR
Qmin	-500	MVAR

	Case 1	Case 2
Load Power (%)	25%	100%
Load Power (MW)	0.373	1.49
Initial Voltage (%)	96.77%	96.70%

Following results were observed when reactive power required to maintain different voltage were done

S.N.	Operating Voltage (p.u.)	25% load	100% load
1	0.4		
2	0.5	-2.66212	-2.65483
3	0.6	-2.58879	-2.5813
4	0.7	-2.24661	-2.23891
5	0.8	-1.63395	-1.626
6	0.9	-0.74804	-0.73986
7	1	0.38784	0.39624
8	1.1	1.7574	1.76605
Reactive Power Reserve		-2.66212	-2.65483
ΔQ/ΔV @V=1.0		13.6956	13.6981
Qreq. for 1 pu Voltage		0.38784	0.39624
Voltage at slope=0		0.5	0.5
Change in Qreq. at 1.0 pu voltage			0.0084

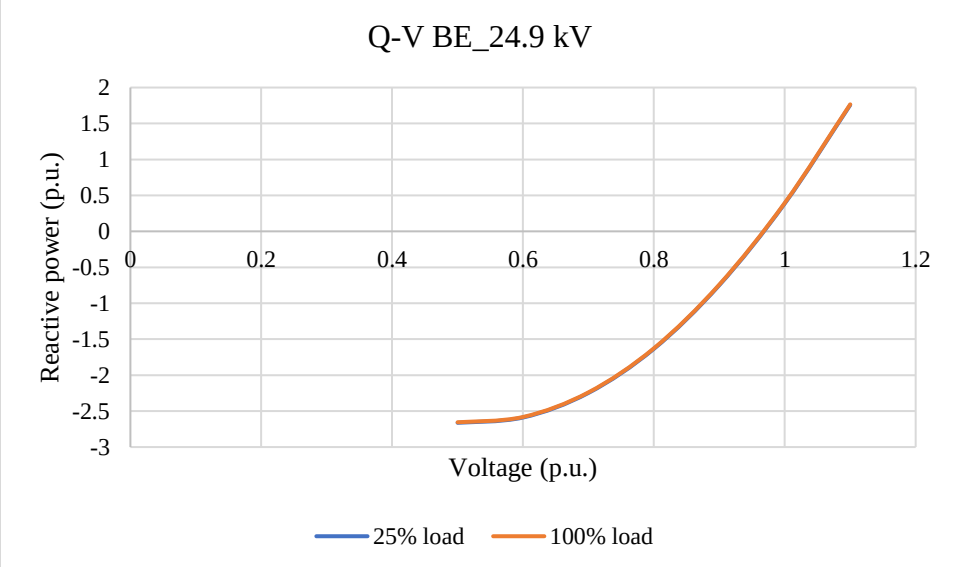

DESALINATION 24.9 kV

Adding a fictitious Generator with following parameters:		
Rated Voltage	24.9	kV
Capacity	1000	MVA
Power Factor	0.01	%
Qmax	1000	MVAR
Qmin	-1000	MVAR

	Case 1	Case 2
Load Power (%)	25%	100%
Load Power (MW)	0.167	0.668
Initial Voltage (%)	98.66%	98.65%

Following results were observed when reactive power required to maintain different voltage were done

S.N.	Operating Voltage (p.u.)	25% load	100% load
1	0.4	-5.86393	-5.86099
2	0.5	-6.19815	-6.19506
3	0.6	-5.98247	-5.97927
4	0.7	-5.23183	-5.22853
5	0.8	-3.94589	-3.94247
6	0.9	-2.0806	-2.07705
7	1	0.34864	0.35229
8	1.1	3.2615	3.26528
Reactive Power Reserve		-6.19815	-6.19506
ΔQ/ΔV @V=1.0		29.1286	29.1299
Qreq. for 1 pu Voltage		0.34864	0.35229
Voltage at slope=0		0.5	0.5
Change in Qreq. at 1.0 pu voltage			0.00365

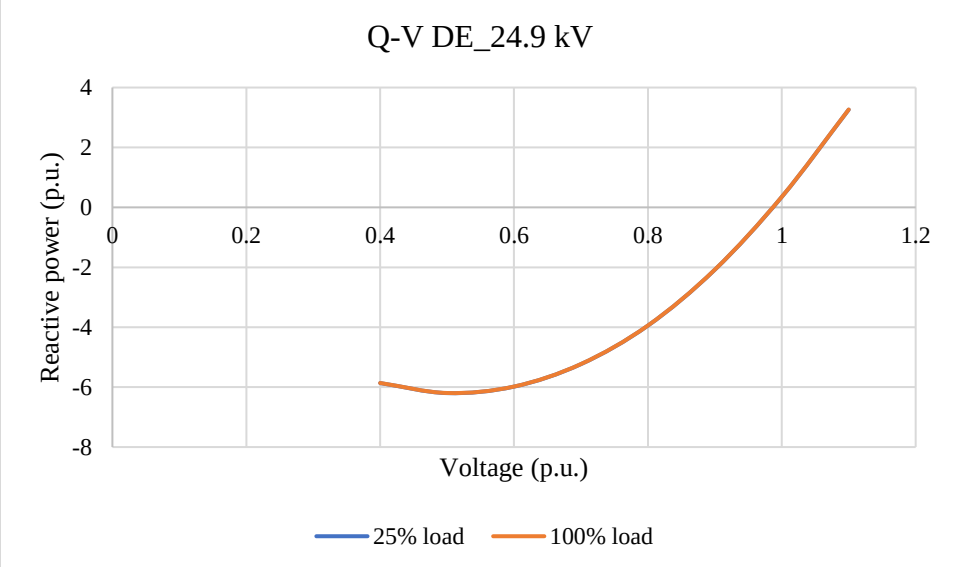

SPRING GARDEN 24.9 kV

Adding a fictitious Generator with following parameters:		
Rated Voltage	24.9	kV
Capacity	1000	MVA
Power Factor	0.01	%
Qmax	1000	MVAR
Qmin	-1000	MVAR

	Case 1	Case 2
Load Power (%)	25%	100%
Load Power (MW)	3.364	13.44
Initial Voltage (%)	99.02%	98.87%

Following results were observed when reactive power required to maintain different voltage were done

S.N.	Operating Voltage (p.u.)	25% load	100% load
1	0.4		
2	0.5		
3	0.6	-10	
4	0.7	-8.89524	-8.8235
5	0.8	-6.76939	-6.70111
6	0.9	-3.70757	-3.64126
7	1	0.4292	0.49439
8	1.1	5.30212	5.36676
Reactive Power Reserve		-10	-8.8235
ΔQ/ΔV @V=1.0		48.7292	48.7237
Qreq. for 1 pu Voltage		0.4292	0.49439
Voltage at slope=0		0.6	0.7
Change in Qreq. at 1.0 pu voltage			0.06519

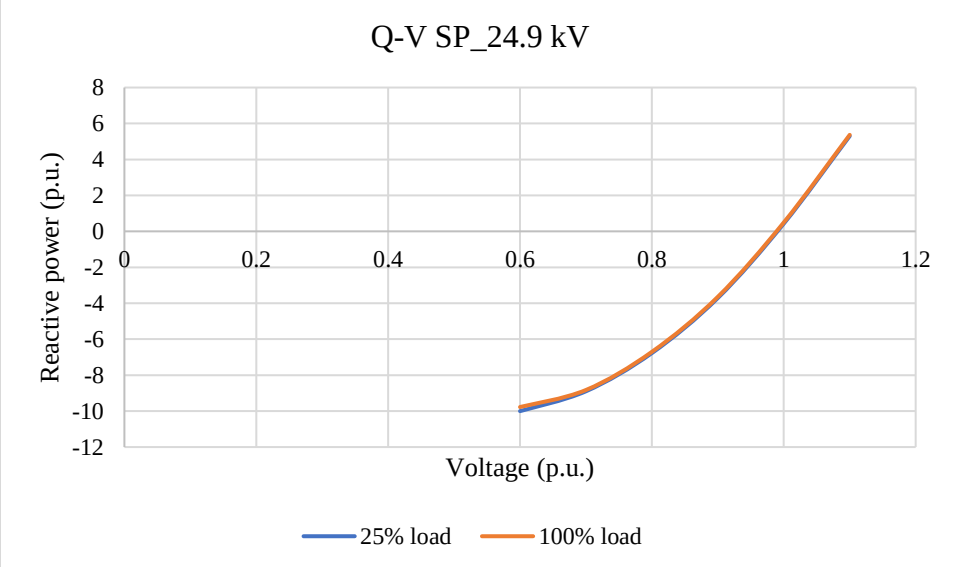

APPENDIX C

Effect of Cascading effect on system

With the simulation including tripping of generators, it is seen that the voltage and frequency drop down to zero immediately after the tripping of the generators.

Effect on Generation

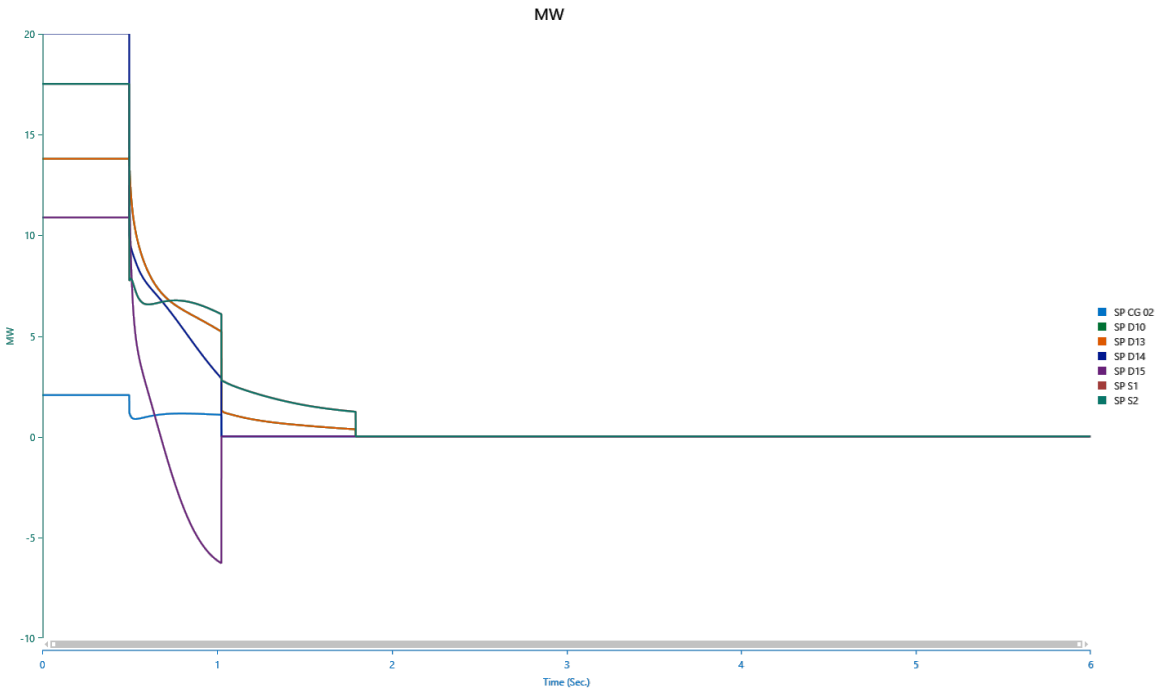

Effect of fault and generator tripping in generation

Effect on Bus Voltage

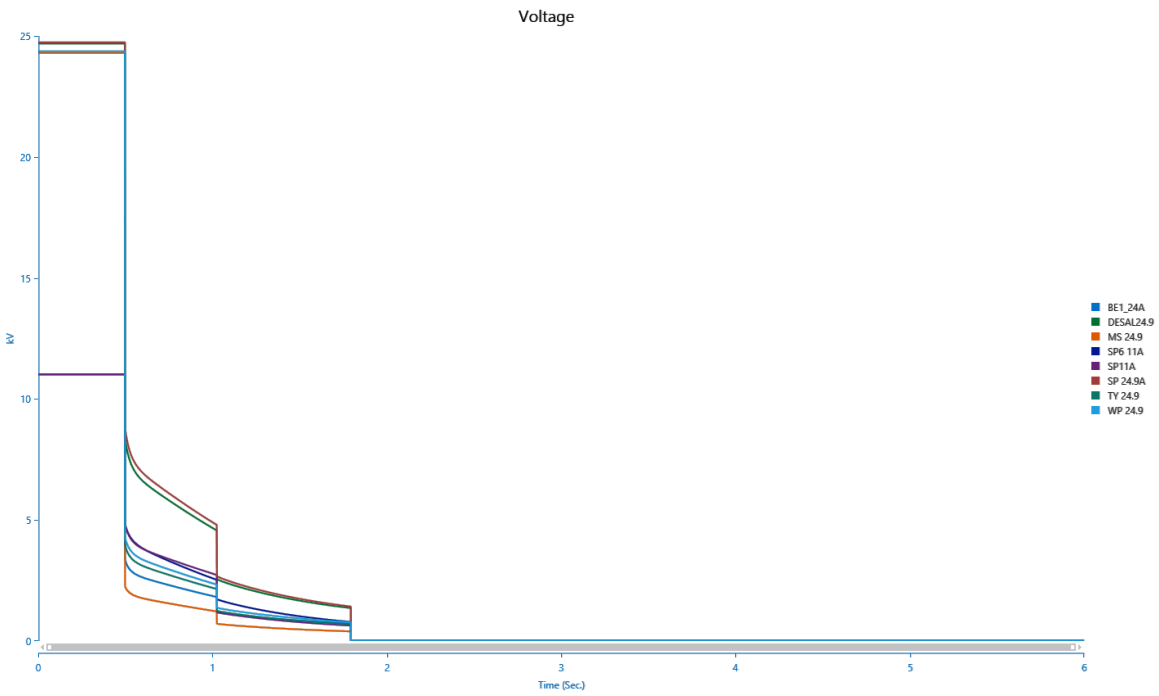

Effect of fault and generator tripping in nearby bus voltage

Effect on Bus Frequency

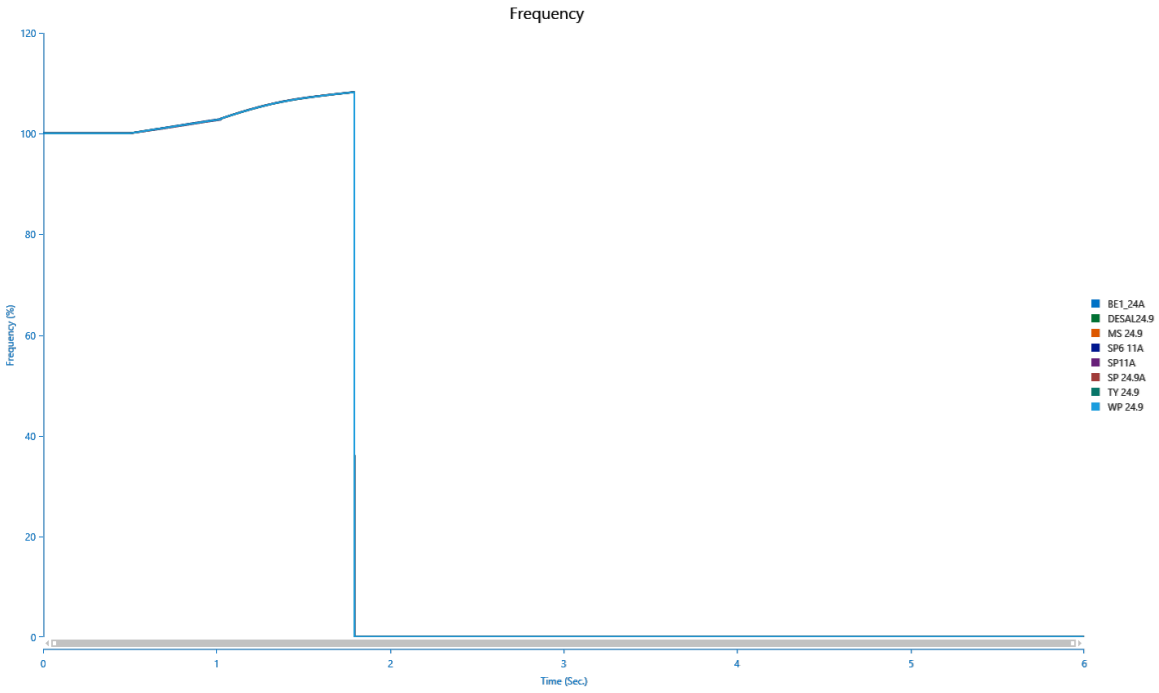

Effect of fault and generator tripping in nearby bus frequency

APPENDIX D

Plotting Q-B from derivation:

The derived equation relating reactive power required as a function of steady state stability limit B is shown in Chapter 2 as equation 2.18. It is quoted here.

$$Q_{required} = 0.5P + \frac{EV}{X}\left[\frac{V}{E} - \sqrt{1 - \left(\frac{PX}{EV}\right)^2}\right]$$

This ideal expression is plotted for power delivered to the load ranging from 0.25 p.u. to 1.25 p.u. and for different system voltage conditions represented by the ratio K = E/V

a. For K = E/V = 1.10

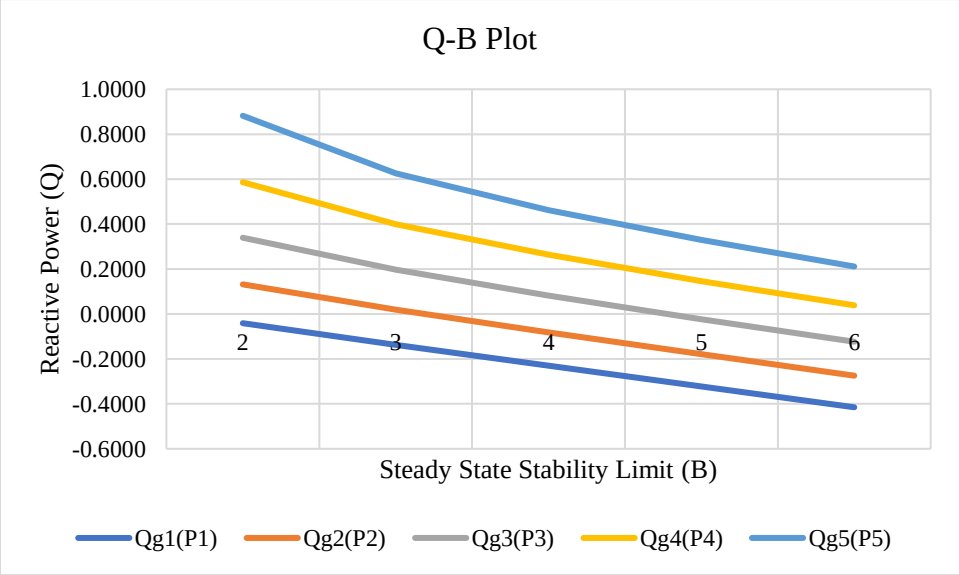

QB plot for range of load when supply voltage is 1.1 times the receiving voltage

b. For $K = E/V = 1.0$

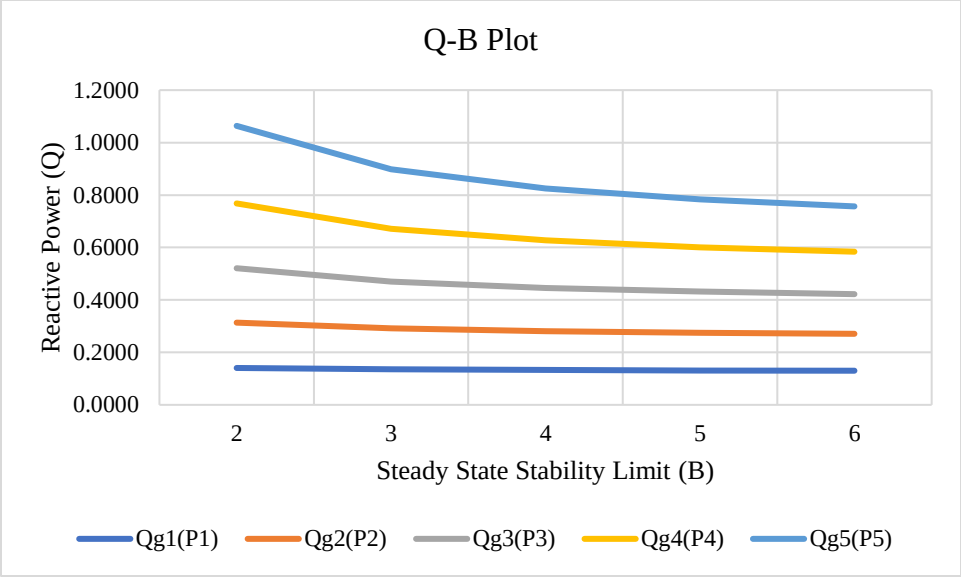

QB plot for range of load when supply voltage is same as receiving voltage

For K = E/V = 1, except for low values of B, the MVAR support required is totally independent of the steady state stability limit B.

c. $For\ K = E/V = 0.9$

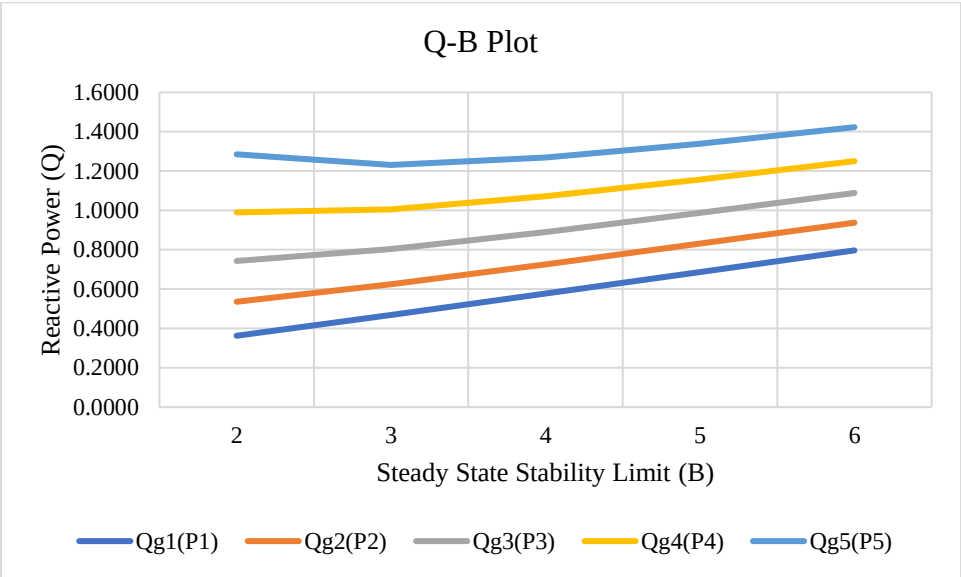

QB plot for range of load when supply voltage is 0.9 times the receiving voltage

For K = E/V less than 1, which could represent a poorly voltage regulated power system, the MVAR support required increases as the transmission strength increase as represented by a higher value of B.

CURRICULUM VITAE

Candidate: Birat Gyawali

University Attended: Kathmandu University, 2010-2014, Bachelor of Electrical and Electronics Engineering (Power & Control)